This work was exclusively supported by the Olivia Hendrickx Research Fund vzw

www.olivia.be

voor Jasmin en Flore

you can fight without ever winning

but never really win without a fight

from *Resist* of the album *Test for Echo* by *Rush* (1996)

Acknowledgements

This thesis is respectfully presented to Professor M. Waer, Rector of the Katholieke Universiteit Leuven, to Professor M. Casteels, Vice-Rector of the Group Biomedical Sciences and to Professor B. Himpens, Dean of the Faculty of Medicine. I want to emphasize here that this work is not solely my own merit but the result of joint efforts of many people to whom I wish to express my most sincere gratitude.

First of all, I want to thank the members of the jury, Professors E. Gilboa, B. Lambrecht, P. Proost and S. De Vleeschouwer. Thank you for the critical reviews of my work and for the helpful suggestions.

Ten tweede wil ik mijn oprechte dank betuigen aan mijn promotor en co-promotor. Professor Van Gool, het is ondertussen al 6 jaar geleden dat ik voor het eerst op uw bureau kwam. Toen als absolute leek in de tumorimmunologie, op zoek naar een interessant onderwerp voor mijn master thesis. Ondertussen bleek dit laatste een absoluut understatement. Het is voor mij een absolute eer geweest om al deze jaren met u te mogen werken in de tumorvaccinatiegroep. Ontelbare keren hebben we samen gezeten; op uw bureau, in het lab, in de auto of zelfs bij u thuis, steeds waren onze geanimeerde gesprekken – die niet altijd werkgerelateerd waren – heel erg verhelderend voor mij. Ik heb geleerd dat bij een doctoraatsonderzoek niet alleen het finale resultaat telt, maar dat het leerproces op zich met alle ups en downs op zijn minst even belangrijk is. Ik ben blij dat ik u hierbij aan mijn zijde heb gehad en heb mogen delen in uw enthousiasme en vastberadenheid. Uiteraard kijk ik uit naar onze verdere samenwerking.
Professor Ceuppens, bedankt om mij gedurende de afgelopen jaren in uw laboratorium te laten werken. Uw vermogen om de voor mij toch vaak complexe immunologische fenomenen glashelder te analyseren zijn voor mij erg waardevol geweest. Bedankt voor de vele kritische vragen en interessante discussies. Door in uw labo te hebben mogen werken heb ik geleerd dat onderzoek doen veel meer is dan alleen maar een manier van werken.

De wetenschappelijke en maatschappelijke relevantie van kankeronderzoek hoeft geen verdere uitleg. Het kostenplaatje hieraan verbonden is echter bijzonder hoog en de reguliere financieringskanalen zijn meer dan eens ontoereikend. Daarom wil ik mijn oprechte dank betuigen aan het Olivia Hendrickx Research Fonds (www.olivia.be) en in bijzonder aan voorzitster Mevrouw

Ilse De Reze. Hun onafgebroken financiële steun aan het tumorvaccinatieprogramma van Prof. Van Gool leidde niet alleen tot de verwezenlijking van deze thesis maar maakte het bovendien mogelijk dat reeds meer dan 150 gliomapatiënten konden behandeld worden met autologe DC vaccinatie.

De afgelopen jaren zijn niet alleen op het gebied van wetenschap heel intens geweest voor mij maar op zijn minst evenzeer dankzij de vele fijne mensen die ik heb mogen leren kennen. Aan de collega's van het Laboratorium voor Experimentele Immunologie: heel erg bedankt voor de fijne sfeer doorheen de jaren. Dominique, bedankt om mijn werk te bekijken vanuit jouw innovatieve invalshoeken en voor de vele leuke babbels daarnaast. Pascal, merci voor alle kritische wijsheden en voor de talloze hilarische discussies. Je weet me wel te vinden als je iemand nodig hebt om op jouw veestapel te passen. Kasran, ik heb jouw advies altijd ontzettend gewaardeerd en het spijt me dat ik het je vaak lastig heb gemaakt tijdens het squashen. Gaan we vanaf nu golfen ? Steven, het is ongelooflijk hoe snel de tijd voorbij gaat; ik herinner me nog de dag dat ik op het labo kwam als student en jij toen mijn begeleider was. Bedankt voor de solide basis die jij hebt gelegd voor de tumorvaccinatiegroep. Ik apprecieer enorm dat je ondanks jouw drukke klinische agenda de tijd kan vrijmaken om mijn onderzoek mee vooruit te helpen. Peter, bedankt voor de interessante suggesties en de leuke informele gesprekken. Het was altijd fijn je te ontmoeten. Veel succes ook met het verder uitbouwen van jouw onderzoeksgroep. Isabelle en Greet, ik heb steeds genoten van jullie aanwezigheid in het lab. Veel succes met jullie toekomstplannen ! Ina, Sonja en Valerie, ik vond het echt fijn met jullie erbij in maar zeker ook buiten het lab en we moeten zeker nog eens op stap gaan! Shen, thank you so much for the *v*ery *i*nteresting talks and drinks and good luck in your new job. An, heel veel succes met jouw verdere carrière en bedankt voor de fijne samenwerking. Tina, je bent ongetwijfeld een grote aanwinst voor het tumorvaccinatieteam. Ik hoop dat ik je toch een beetje wegwijs heb kunnen maken in de muis glioma wereld. Veel succes met jouw onderzoek ! Isabel, ik wens je veel geluk met jouw gezin en wil je bedanken voor alle hulp tijdens de afgelopen jaren. Succes in alles wat jullie ondernemen ! Li, I am always looking forward to more of your interesting data. Bedankt ook aan alle laboranten: Lieve, Kathleen, Ellen, Katja, Goedele en Vallentina. Clémentine, c'est vraiment super que tu as joint notre petite équipe ! Sandra, het is een echt plezier geweest om er een opgewekte en positief ingestelde collega als jou bij te hebben. Ook jouw diplomatieke talenten zijn méér dan eens van pas gekomen ! Georgina, chica loca, your latin spirit in the lab has always been really charming. Thank you so much for your assistance and kindness. I wish you all the best in Toronto ! Hilko, ik ben nog steeds geen fan van

de Hollandse eetgewoontes, maar samenwerken met jou was steeds een feest. Om nog niet te spreken van de partijtjes tennis(les), de introductie in de ornithologie, het verfijnen van de humane gedragswetenschappen of het rondtrekken in de Roemeense Karpaten. Bedankt en ik wens jou bij deze heel veel succes in alle op stapel staande uitdagingen ! Bert, sommige dingen in het leven zijn schaars. Goede vrienden behoren daar zeker toe. Ik ben heel erg dankbaar dat ik er in jou één gevonden heb. Bedankt voor de leuke jaren en heel veel succes in Boston. Ik kijk er al naar uit om weer op bezoek te komen!

Het is onmogelijk om iedereen uitvoerig te bedanken die mij heeft geholpen om dit werk tot stand te brengen. Speciale dank gaat uit naar Vik Van Duppen van Hematologie voor alle hulp bij de flowcytometrie en de leuke conversaties. Professor Debyser, Rik, Veerle, Jaan, Abdel en co. van Moleculaire Virologie en Gentherapie wil ik oprecht bedanken om mij te introduceren in de wondere wereld van de lentivirale vectortechnologie en optical imaging. Bedankt ook aan Peter Vermaelen van de MoSAIC. Louis, jouw uitstekende monoklonalen waren onmisbaar bij mijn werk. Heel veel respect en dank ook voor het uitstekende werk van Karin en Inez van het animalium. Ook Ruth (VIB), Liesbet en Els (Vesalius Research Centrum), Professor Frank Claessens (Moleculaire Endocrinologie), Professor Kris Thielemans en Carlo Heirman (VUB) , Jos L (Legendo) en An, Omer en Lien (Transplantatie) wil ik langs deze weg bedanken. Bedankt ook aan alle studenten die hun steentje hebben bijdragen aan dit project.

Door de jaren heen is Leuven een echte thuis geworden en heb ik het geluk gehad om enkele heel fijne mensen te leren kennen die ondertussen goede vrienden zijn geworden. Bedankt allemaal voor de leuke weekends, feestjes, (poker)avonden in bruine kroegen, sportieve uitspattingen, het lunchen op vrijdagmiddag, poolen, babysitten, … en dit alles geldt evenzeer voor de Tiensevesters, Gentenaars en vrienden uit Harelbeke en daarbuiten.

Ik wil ook van deze gelegenheid gebruik maken om iedereen van mijn familie, en in bijzonder mijn grootouders, ouders en Liesbeth en Didier van ganser harte te bedanken voor alle mogelijkheden en steun die ik altijd van jullie gekregen heb en nog steeds krijg.

Jasmin, als ik zou proberen neer te schrijven wat jij voor mij betekent dan had dit boek ontelbaar veel pagina’s … bedankt schat om steeds onvoorwaardelijk in mij te blijven geloven en om alles

positief te bekijken. Ik weet zeker dat onze kleine Flore nu al beseft dat ze een mama uit de duizend heeft !

Table of Contents

List of Abbreviations

AP	alkaline phosphatase
APC	antigen presenting cell(s)
Arg1	arginase 1
ATCC	American Type Culture Collection
BBB	blood-brain barrier
BLI	bioluminescent imaging
BM	bone-marrow
b-ME	beta-mercaptoethanol
CCL	CC chemokine ligand
CCR	CC chemokine receptor
CD40-L	CD40-ligand
cFLIP	IL-1β-converting enzyme inhibitory protein
COX-2	cyclooxygenase-2
cpm	counts per minute
cRNA	complementary RNA
CTL	cytotoxic T lymphocyte
CTLA-4	cytotoxic T lymphocyte antigen-4
DC	dendritic cell(s)
DCi	immature DC
DCm	mature DC
dLN	draining lymph node(s)
DMEM	Dulbecco's modified essential medium
DTH	delayed-type hypersensitivity
EDTA	ethylene diamine tetra-acetic acid
eGFP	enhanced green fluorescent protein
EGFR	epidermal growth factor receptor
FCS	fetal calf serum
Fluc	Firefly luciferase
FOV	field of view
FoxP3	Forkhead box P3
FSC-SSC	forward-side scatter
Gal-1	galectin-1
GAR:FITC	fluorescein isothiocyanate-conjugated goat anti-rabbit antibody
GBM	glioblastoma multiforme
GITR	glucocorticoid-induced TNF-receptor related protein
GM-CSF	granulocyte-colony stimulating factor
GMP	good manufacturing practice
gp	glycoprotein
HE	hematoxylin-eosin
HGG	high-grade glioma
HIV	human immunodeficient virus
ICAM-1	intercellular adhesion molecule 1
IDO	indoleamine 2,3-dioxygenase
IFN-α/β/γ	interferon-alpha/beta/gamma
IgG	immunoglobulin class G

IL-4	interleukin-4
iNOS	inducible nitric oxide synthase
LFA-1	leukocyte function antigen-1
LLC	Lewis lung carcinoma
LPS	lipopolysaccharide
mAb	monoclonal antibody
MAGE	melanoma antigen
MDSC	myeloid-derived suppressor cells
MHC	major histocompatibility complex
MLR	mixed lymphocyte reaction
MTT	3-(4,5-dimethylthiazol-2-yl)-2,5-diphenyltetrazolium bromide
NK	natural killer
PBMC	peripheral blood mononuclear cells
PBS	phosphate-buffered saline
PCR	polymerase chain reaction
pDC	plasmacytoid DC
PD-L1	programmed death ligand-1
PE	phycoerythrin
PerCP	peridinin-chlorophyll protein
PGE_2	prostaglandin E_2
PHA	phytohemagglutinin
PI	propidium iodide
rhu	recombinant human
ROS	reactive oxygen species
RPMI	Roswell Park Memorial Institute
SEM	standard error of the mean
STAT-3	signal transducer and activator of transcription-3
TAA	tumor-associated antigen
TAM	tumor-associated macrophages
TCR	T cell receptor
TGF-β	transforming-growth factor beta
Th	helper T cells
TIL	tumor-infiltrating lymphocyte(s)
TLR	toll-like receptor
TNF-α	tumor necrosis factor alpha
Treg	regulatory T cell
VEGF	vascular-endothelial growth factor
wt	wild-type

Chapter 1. Introduction

1.1. Cancer from a historical perspective

Already in the Egyptian era, there are written reports on malignancy, but it was Hippocrates who first introduced the term 'cancer'. The growth pattern of a tumor reminded him of a moving crab, which led to the terms 'carcinos' (a tumor). According to Hippocrates, tumors were caused by an imbalance between the four body fluids: blood, phlegm, yellow bile and black bile. Already in antiquity, cancer treatment was associated with the stage of the disease and like nowadays, largely depended on a staging system, a concept put forward by Cornealius Celsus (1,2). Going one step back, Claudius Galen put forward the fluidics theory again as originally suggested by Hippocrates. His rigid theories and dominant reasoning reigned medicine in the medieval European world for longer than a millennium, during which no real progress in cancer treatment was made. Medicine entered a new era in the 16th century's Renaissance with the emergence of the innovative scientific spirit that was roaming the world. Since autopsies were no longer forbidden, the knowledge of the human anatomy increased rapidly and led to the discovery of the lymphatic system by Gaspard Aselli (3,4). The knowledge of cancer was further broadened by clinical observations of different types of malignancy and case reports. 0nly rationalism and empiricism, the true foundations of the Enlightenment, allowed a new revival of science, including medicine. Pioneer experimental research was carried out by Bernard Peyrilhe who withdrew fluid from a breast cancer lesion and injected it into a dog's peritoneal cavity. Further advances were made by skilled surgeons as John Hunter and his student, Astley Paston Cooper. They were the first ones to incorporate the idea of predisposition to cancer on the basis of genetics, age and environmental factors. The discovery of radiation by Pierre and Marie Curie at the end of the 19th century resulted in the first non-surgical cancer treatment. From then on, oncology became a multidisciplinary discipline and experimental cancer research since has led us to a better understanding of this disease (5). At present, cancer is still a leading cause of death worldwide, accounting for 13 percent of all deaths (7.9 million deaths in 2007) (6,7). To illustrate the vast amount of research effort dedicated to cancer, the PubMed Entrez query 'cancer' yielded over two million entries at the time this work was written.

1.2. Glioma

1.2.1. Classification, epidemiology and molecular pathology

The term 'glioma' refers to all tumors of glial cell origin, including astrocytic tumors, oligodendrogliomas, ependymomas and mixed gliomas. Gliomas account for approximately 75 percent of primary malignant brain tumors. Within the astrocytic tumors, glioblastoma multiforme (GBM) is not only the most frequent brain tumor in adults but represents also the most malignant one and is assigned grade IV by the World Health Organisation. Together with grade III anaplastic astrocytoma, GBM are categorized as high-grade glioma (HGG). This grading is associated with cytologically malignant, mitotically active, necrosis-prone neoplasms with pre- and postoperative disease evolution and fatal outcome (8,9). Despite state-of-the-art oncological treatment, prognosis remains dismal for GBM patients with a median survival of only 14 months. Relapse is universal and at the time of relapse, prognosis is even worse and virtually all patients are dead within 18 months (10-12). The five-year survival rate is less than three percent. The incidence of GBM is approximately three to four patients per 100,000 per year, which makes it an orphan disease (13). Like for most types of cancer, the incidence of central nervous system (CNS) tumors increases with age with a peak incidence for high-grade GBM between 60 and 65 years (14).

When it comes to risk factors for GBM, both environmental and genetic factors must be taken into account. The only firmly established exogenous environmental cause of GBM is exposure to high-dose radiation (15,16). Reports on a causative relationship between exposure to electromagnetic fields and brain tumor incidence are lacking, although recent meta-analysis draws particular attention to mobile phone use (17). The plausibility of neurocarcinogenicity by a myriad of endogenous and exogenous chemical compounds has been described but remains inconsistent. However, it would be too premature to conclude that those environmental risks do not contribute to gliomagenesis (18). Inherited syndromes such as neurofibromatosis and Li-Fraumeni syndrome have been associated with an increased risk for GBM and other types of primary brain tumors (19,20). Mechanisms important for DNA repair and thus for maintenance of genomic integrity represent another category of processes that are investigated in the context of malignancy (21-24).

During the last years, research has been focused on the molecular pathology of cancer, including GBM. This is actually the prelude to a new era in both diagnostic and therapeutic medicine,

moving away from broad pathologic diagnoses and relatively non-specific therapies to predictive individualized care (25,26). The chromosomal alterations that are most regularly observed in GBM are linked with several tumor suppressor genes and oncogenes, although many genes in these regions have yet to be examined. It is now accepted that two molecular pathways can lead to GBM; one pathway results from tumor progression of low grade astrocytoma (secondary GBM), whereas the second pathway does not involve a clinically evident precursor (primary or *de novo* GBM). Extensive molecular data on gene mutations, polymorphisms, chromosomal alterations, global patterns of methylation, acetylation, splicing and protein networks become available nowadays. Incorporating these data into clinical treatment decisions remains a considerable challenge but will undoubtedly be of high benefit for brain tumor patients (27).

1.2.2. State-of-the-art therapy for GBM

The current treatment pillars for patients diagnosed with GBM consist of maximal safe resection of the tumor mass followed by (toxic) chemotherapy and/or radiotherapy. The superiority of the combination of radiotherapy and temozolomide over radiotherapy alone was clearly demonstrated in a phase III trial by Stupp *et al.* (28). The striking two-year survival of 27 *versus* 10 percent of patients represents the most important breakthrough in GBM therapy for the last decade (29). Together with age and Karnofsky Performance Score, the extent of resection was found to be a significant prognostic factor. Hence, fluorescence-guided tumor resection with aminolevulinic acid, resulting in a higher probability of complete resections, was of clear benefit to GBM patients (30).

1.2.3. Innovative treatment strategies in the fight against GBM

During the last decades, new approaches have been investigated for their potential usefulness in GBM treatment. We hereby distinguish three main categories, being immunotherapy, gene and stem cell therapy and targeted therapy. GBM immunotherapy is discussed separately in paragraph 1.3.

1.2.3.1. Gene and stem cell therapy

Since non-viral gene therapy with liposomes and plasmid DNA has been abandoned due to their limited transfection efficacy, the focus has shifted to the use of powerful viral vectors to deliver genes into or exert a cytotoxic effect upon GBM target cells. The transgenes delivered by non-replicating adenoviral vectors and vectors derived from herpes simplex virus are either based on direct tumor cell killing, inhibition of angiogenesis or stimulation of the antitumor immune response. Although most cells in the CNS are either non- or slowly dividing cells compared with tumor cells and are hence less prone to be infected by the viral vector, safety is a major concern in viral gene therapy. A lot of effort has been put in increasing both the safety and tumor-specificity of the replication-competent vectors (31,32).

In- and outside cancer therapy, stem cells and their potential applications have drawn a huge amount of attention over the last years. Due to their inherent tumor-tropic properties, they can be exploited to deliver anticancer genes to invasive and even metastatic tumors. Apart from pro-drug activating enzymes, an array of interleukins, interferons, metalloproteinases and apoptosis-promoting genes is under investigation in the context of experimental stem cell therapy. It is expected that these concepts will soon be introduced in clinical trials for GBM patients (33).

1.2.3.2. Targeted therapy

The concept of 'oncogene addiction' is central to strategies for selecting patients who are most likely to benefit from targeted molecular therapy. It is the persistence of these signals, promoting tumor growth and invasion that makes them potentially vulnerable to targeted attack by small molecular inhibitors. In comprehensive recent reviews, Omuro *et al.* and Mason summarized the main oncogenetic signaling pathways for which single and multitargeted drugs are being developed (29,34). Many of these drugs are under investigation for GBM. It is beyond the scope of this work to provide a complete listing of inhibitors currently in trials. Therefore, we only highlight gefitinib and erlotinib as inhibitors of epidermal growth factor receptor (EGFR) tyrosine kinase. Although EGFR is overexpressed in 60 percent of GBM and gefitinib and erlotinib are well tolerated, overall efficacy in unselected patients is minimal compared with historical controls. The combination of bevacizumab, an anti-VEGF antibody and the cytotoxic agent irinotecan was recently described to have significant antitumor activity against recurrent grade III-IV HGG, albeit with significant toxicity (35). Unfortunately, the first molecular targeted therapy phase II clinical

trials in malignant glioma have not translated into significant changes in current clinical practice, and to date, no new molecule seems to be promising enough to justify a large phase III trial. Therefore, the focus now lies on multitarget compounds or combinations of single-target drugs (36).

1.3. Immunotherapy for GBM

Lack of surveillance by the immune system has now been accepted as an important hallmark of cancer (37). Basically, immunotherapy tries to restore or improve antitumor immunity. Although artificial, in this paragraph, we uncouple the antitumor immune response from the reciprocal effect of the tumor on the immune system. The latter will be discussed in paragraph 1.4. For an outstanding comprehensive review on cancer immunology in general, we refer to the recent work by Finn (38).

1.3.1. GBM immunotherapy at a glance

The relative absence of lymphatic vessels and the presence of the blood-brain barrier (BBB) make the brain an immunologically 'privileged' site. However, the current perception is that immune reactions do occur within the CNS, although qualitatively and quantitatively different from those in other anatomical locations. This is demonstrated by the presence of tumor-infiltrating lymphocytes (TIL) and by systemic antitumor immunity (39,40). Most likely, this immune privileged state is due to the fact that the blood-brain barrier (BBB) may still be intact in early tumor lesions, whereas tumor progression goes along with BBB disruption. Moreover, several groups have shown the drainage of interstitial fluid from the brain into deep cervical lymph nodes (LN), providing an access path for the systemic immune system to the tumor. Despite lack of constitutive expression of major histocompatibility complex (MHC-) molecules on CNS cells, immune responses can be primed in the brain by microglia and capillary pericytes that can act as antigen presenting cells (APC) (41).

In the context of GBM, 'immunotherapy' encompasses different strategies, classified as passive serologic treatment, adoptive cell transfer, cytokine therapy, and active cell-mediated immunotherapy, the latter being discussed in chapter 1.3.2. *Passive serologic immunotherapy* implies the administration of a monoclonal Ab (mAb) that recognizes a cell-surface epitope

exclusively expressed on GBM cells and conjugated to a toxic payload. Key limitations for this approach are the difficulty of identifying a prominent cell surface protein that is ubiquitously expressed on GBM cells (but not on normal brain cells) and the stability of its expression. Tenascin, glycoprotein-240 (gp240) and EGFR, both wild-type (wt) and a mutated form designated as EGFRvIII, have been clinically targeted in this manner (42,43). *Adoptive immunotherapy* is based on the transfer of tumoricidal T cell populations into GBM-bearing hosts. Both allogeneic and autologous lymphocytes have been used, *ex vivo* stimulated either in a specific or non-specific manner. The latter category comprises lymphokine-activated killer cells that caused serious adverse effects. Systemic or intratumoral delivery of TIL or other specifically activated effector cells has been well tolerated in pilot studies and the results justify further study. *Cytokine therapy* consists of the systemic or local administration of cytokines such as interleukin-2 (IL-2) and interferon-gamma (IFN-γ) to enhance immunity in a non-specific manner (44). Taken together, the above mentioned immunotherapeutic strategies have not yielded a clear-cut benefit for patients, despite some cases with radiologic response. Hence, more powerful treatment options are required (39).

1.3.2. Dendritic cell-based cancer vaccines: general overview and current issues

1.3.2.1. Introduction

It is far beyond the scope of this work to provide a complete review of the many experimental and clinical cancer settings in which dendritic cells (DC) have been applied. This kind of immunotherapy is often referred to as 'DC tumor vaccination'. It is imperative that the term 'vaccination' in this context should not be considered in a stringent sense, but instead points to the administration of autologous immune cells to patients with the aim to induce or boost an antitumor immune response. Over the past decades, DC have proven to be the ideal cellular tools to break immunological tolerance against tumors by initiating a T cell mediated antitumor immune response through induction of effector T cells and by allowing this response to persist through memory T cells. DC do not only bridge innate and adaptive immunity but have also a pivotal role in most aspects of adaptive immunity (45-48). Immature DC (DCi) which reside in virtually every organ and tissue at the interface of potential pathogen entry sites, continuously sample antigens. If danger signals (such as the presence of pathogens, tissue damage or signs of inflammation) are detected, DCi undergo maturation and become genuine APC. By upregulation

of chemokine receptors such as CC chemokine receptor 7 (CCR7), mature DC (DCm) are guided to the T cell areas of draining LN (dLN) of the tumor, where they initiate primary T cell responses. DC are often termed professional APC because of their high expression of MHC-, adhesion and costimulatory molecules and their specific cytokine secretion profile. Depending on their nature, antigens are processed through the endogenous or exogenous pathway of antigen processing, resulting in antigen presentation in an MHC class I or class II context respectively. Since the MHC class II pathway is leaky, DC are able to 'cross-present' exogenous antigens on MHC class I molecules (49). Thereby, they can prime CD8+ and CD4+ T cells, both necessary for the optimal induction and persistence of a T cell-mediated antitumor immune response (50). Antigen-selected T cells undergo extensive expansion but are also subject to silencing or tolerance by tolerogenic DC that can eliminate (delete) or block (suppress) T cells. If deletion is avoided, the T cell clone is allowed to differentiate and to display an array of potential killer, helper or even suppressive activities. The complete picture of interactions between DC and the other types of immune cells has become extremely complex. DC-based cancer vaccines mainly aim at the induction of effector CD8+ T cells which function as cytotoxic T lymphocytes (CTL) (51,52). Efficient T cell priming requires three consecutive signals from APC; *(i)* the link between MHC-presented antigenic epitopes and the T cell receptor (TCR), *(ii)* the interaction between costimulatory signals CD80 and CD86 on APC and CD28 on T cells and *(iii)* reciprocal signaling between CD40 on APC and CD40-L on activated CD4+ T cells (53,54).

DC and their potency to initiate and modulate antitumor immune responses against HGG are under investigation by many research groups, including ours (55,56). In brief, preliminary *in vitro* research rapidly led to a clinical feasibility study. Currently, promising results are obtained from a phase I/II cohort comparison trial, providing a rationale to proceed to a randomized controlled clinical trial (57-62). Since the development of DC-based cancer immunotherapy is a multi-facet process, one should proceed very carefully through each of these steps, keeping in mind that substantial optimization is not only feasible but required. Below, the most important issues on DC immunotherapy in general and on GBM-directed DC vaccination in particular are discussed.

1.3.2.2. Clinical condition before vaccination

It is evident that the selection of cancer patients that are eligible for DC immunotherapy is of crucial importance, not only with regard to their general immune status (affecting the quality of the cell population from which DC are derived), but also to disease stage that might have a severe

impact on the outcome of DC vaccination (63). For immunotherapy against HGG, the extent of resection, the age of the patient and the histological subtype of HGG are important variables that should be taken into account in this context (Figure 1, box 1).

1.3.2.3. DC differentiation

Different lineages and subsets of DC have been identified and have mainly been categorized in CD11c+ myeloid DC and CD11c- plasmacytoid DC (Figure 1, box 2). The myeloid pathway displays a pronounced plasticity depending on the cytokines the monocyte precursor encounters and generates Langerhans cells that are found in tissues with stratified epithelia such as the skin, and interstitial DC that are found in all other tissues. Plasmacytoid DC (pDC) secrete large amounts of type I interferons in response to viral infection. Most clinical studies to date have been carried out with *ex vivo*-generated DC derived from peripheral blood mononuclear cells (PBMC), resembling myeloid interstitial DC. Apart from these, clinical-grade DC can also be generated *ex vivo* from CD34+ hematopoietic stem cells or they can be isolated directly from fresh human blood, in which they only represent a marginal fraction (less than 0.5 percent) of the white blood cells (45,52). None of these DC subtypes has proven to be superior in comparative clinical trials and subtype preferences are mainly based on preclinical observations and early clinical experience. DC and their progenitor cells display a remarkable degree of plasticity; different cytokines skew the *in vitro* differentiation process of monocytes into DC with different phenotypes and functions and hence distinct types of immune responses (48). Up to now, there are no standardized criteria on requirements of DC phenotype and purity. Virtually all reported analyses on DC quality consist of cytokine measurements upon different kinds of DC triggering and the capacity to stimulate allogeneic T cells in a mixed lymphocyte reaction (MLR) (63).

1.3.2.4. Loading of DC with tumor antigen(s) and maturation

A vast body of literature has been dedicated to one of the most critical issues in DC-based cancer immunotherapy, namely the loading of DC with tumor antigens (Figure 1, box 3). Roughly, we can distinguish whole tumor cell approaches and tumor-associated antigen (TAA) specific approaches. Choosing between either whole tumor cell preparations or rather (sets of) defined tumor antigens is mostly inherent to the type of tumor. For tumors with well characterized TAA profiles (such as melanoma), there are many trials published and ongoing using defined TAA or even the dominant

epitopes thereof. On the contrary, for cancer types with no universally expressed TAA that is crucial for tumor cell survival (such as GBM), investigators often rely on the use of whole tumor cell preparations. Working with defined TAA has the disadvantage of potentially selecting tumor escape variants, whereas autoimmune problems might arise by targeting the whole cellular antigen pool (55,64). TAA can be classified as either unique tumor antigens (resulting from point mutations in genes that are ubiquitously expressed such as β-catenin) or shared tumor antigens. Shared antigens, present on many independent tumors, can be further divided into three groups; *(i)* cancer-germline genes that are frequently expressed in many tumors but not in normal tissues (except for testis and placenta) such as the melanoma antigens (MAGE), *(ii)* differentiation antigens which are present in tumor cells and their normal counterparts such as tyrosinase and *(iii)* over-expressed antigens which are present at higher levels in tumor cells than in normal cells such as Her-2/neu. Viral antigens, resulting from infection with oncogenic viruses, complete this picture. Although their expression is not consistently found in all patients, relevant TAA for GBM include EGFRvIII, gp100 and gp240, tenascin, survivin, the alpha-chain of the IL-13 receptor, tyrosinase, tyrosinase related proteins 1 and 2, MAGE-1 and -3, and others (65,66). Most of the above TAA are not strictly tumor-specific but are rather (abnormal) self-antigens. Hence, breaking of immunological tolerance to these antigens is not only very difficult to establish but implies the risk of inducing harmful autoimmunity.

For specific TAA-approaches, DC can be pulsed with synthetic peptides that can easily be produced in good manufacturing practice (GMP) grade. Alternatively, genetic approaches with either defined mRNA or viral vectors containing the TAA genes can be applied (53,64,67). Aiming at an enhanced CD4+ T cell stimulation, cytoplasmic antigens have been redirected to the MHC class II presentation pathway by coupling endosomal or lysosomal targeting signals to the antigen (68). Loading of DC with specific TAA is dependent on the knowledge of the patients' MHC haplotype and the identification of defined TAA epitopes. Loading purified whole TAA proteins onto DC allows for the simultaneous processing of multiple epitopes, theoretically resulting in both CD4+ and CD8+ T cell priming. Many research groups – including ours – have used the complete protein content of the tumor cell. These methods encompass loading of DC with tumor lysate, amplified mRNA or total tumor RNA, necrotic and apoptotic tumor cell remnants and so-called fusions of DC and tumor cells (63). By using this strategy, major concerns have been raised on the risk of inducing autoimmune phenomena, the lack of detailed immunomonitoring and the large amounts of tumor material needed. Recently, small natural membrane vesicles, called

exosomes, released by a wide variety of cell types (including DC), are under investigation as antigen delivery tools (69).

Concerning the amount of tumor antigen that has to be loaded on DC, several studies have shown that more is not necessarily better. There seems to be a discrepancy between the amount of antigen expressed by DC or processed in the MHC class I pathway and the stimulatory capacity of DC *in vivo* (53).

Another topic of debate in DC immunotherapy is the maturation status of the cells and maturation signals applied to force DCi to become DCm. Since antigen uptake and the machinery governing antigen processing is severely halted in mature DC, it is desirable to load DC with antigens when the cells are in an immature state. Several methods to mature both human and mouse DC have been described and include the use of a classical pro-inflammatory cytokine mixture of tumor necrosis factor alpha (TNF-α), IL-1β, IL-6 together with prostaglandin E2 (PGE_2); CpG motifs; bacterial lipopolysaccharides (LPS); viral double-stranded RNA; poly I:C and CD40-ligand (CD40-L). Each of these products or combinations thereof mimics an *in vivo* inflammatory environment and represent the danger signal required for DC to become fully activated (70).

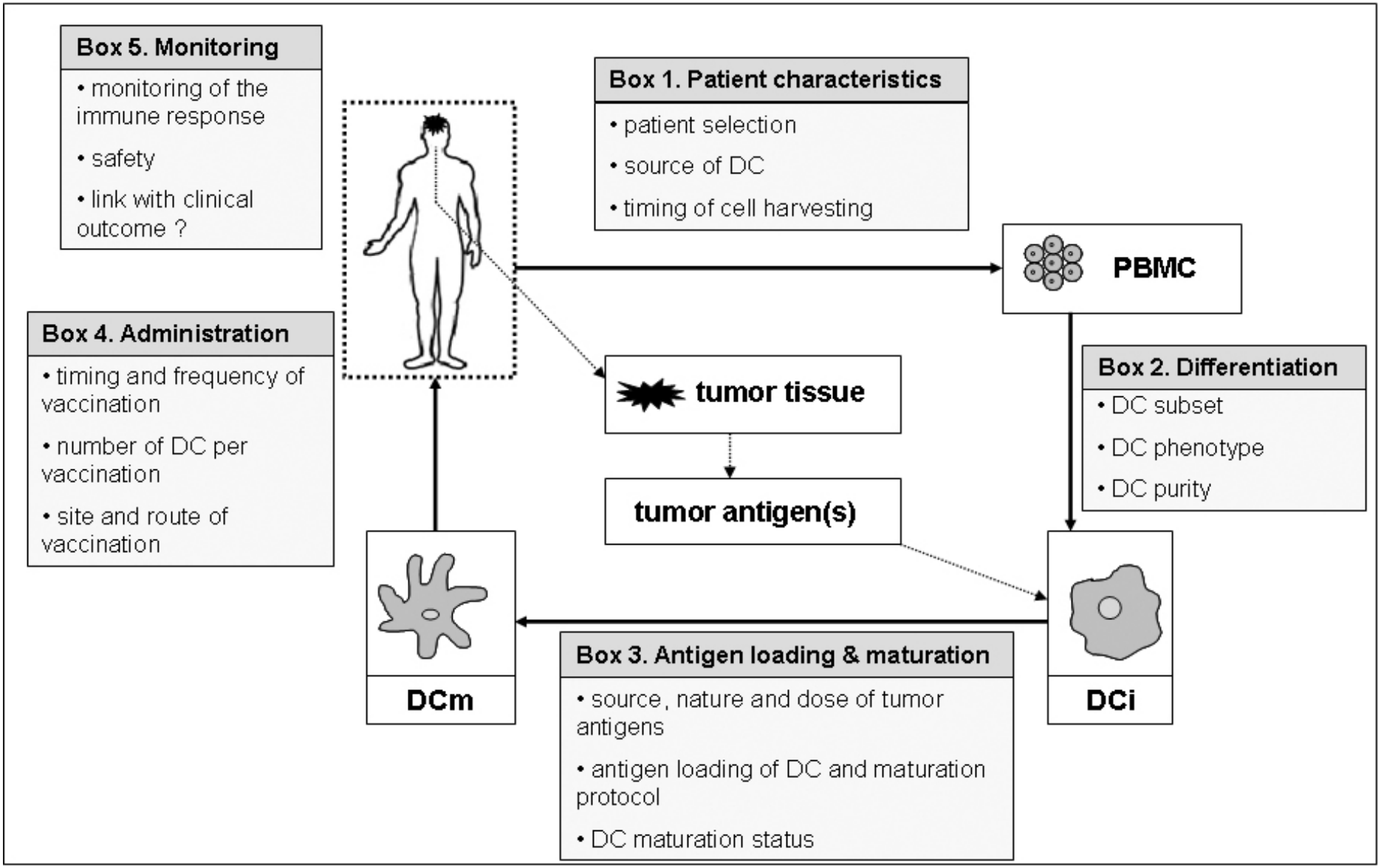

Figure 1. DC-based tumor vaccination: basic concept and main issues.

1.3.2.5. Administration of antigen-loaded DC

Finally, the *ex vivo* generated, antigen-loaded and fully mature DC have to be administered to the patient. Basic questions regarding timing and frequency of vaccination, the number of DC per vaccine and the site and route of vaccination are still open (Figure 1, box 4). These prove to be very critical since a patients' immune system needs to (at least partially) recover from earlier toxic anticancer chemotherapy before it can build an effective antitumor response. Although empirically, it was initially believed that the more frequently a DC vaccine was given, the more potent the induced immune response would be. However, reports are now emerging that even myeloid DC can also expand regulatory T cells (Treg), which are able to decrease or even completely shutdown immune responses, both in humans and mice (see 1.4.2.) (71). Clear-cut data on the optimal number of DC that should be injected per vaccination are not available. Since the immune system seems to function as an on-or-off system, the main criterion for DC immunotherapy with regard to the number of vaccinated DC is an arbitrary minimal amount (roughly five million cells in humans and one million in mice) rather than an amount defined upon a classic dose-response relationship.

A major concern related to *ex vivo* generated DC is how to establish an effective *in vivo* migration to the T cell areas towards the tumor-dLN. It has been well documented that only a small fraction of intradermally injected DC are actually homing towards the secondary lymphoid organs (72). Attempts to enhance migration of *ex vivo* generated DC by preconditioning with inflammatory cytokines or a toll-like receptor (TLR) agonist (such as imiquimod, binding TLR-7) are currently under investigation. Combining multiple routes of DC administration within one patient might be highly beneficial to induce true systemic immunity able to attack tumor lesions at different locations in the body (73). Targeting tumor antigens selectively to DC *in situ* might circumvent this problem and relies on the intrinsic and optimal mechanisms governing DC migration from the periphery towards the secondary lymphoid organs (47,74).

1.3.2.6. Immune monitoring

Once a cancer patient has been treated with DC-immunotherapy, it is of crucial importance to evaluate the immunologic effects in the broadest manner possible. Monitoring the immune response and linking these data to the clinical outcome represents one of the most difficult obstacles in the field of cancer immunotherapy (Figure 1, box 5). Robust, reliable, reproducible

and quantitative assays to evaluate vaccine-induced immune responses in each clinical DC trial are mandatory. A detailed overview of all monitoring tools that were used in the many clinical studies so far is beyond the scope of this work. Obviously, the way in which immune monitoring is organized is directly related to the vaccine design itself. When specific TAA are targeted, detection of the corresponding immune responses is much more straightforward compared with strategies using the entire (and undefined) set of tumor antigens. When measuring immune responses in the context of DC immunotherapy, one has to keep in mind that during the course of tumor progression, spontaneous antitumor immune responses might develop. These spontaneous responses are often prone to tumor-induced immune suppression but might interfere with the assessment of vaccine efficacy (74,75).

1.3.3. Tackling GBM with RNA-loaded DC: rationale

The potency of tumor vaccination with RNA-loaded DC has been well documented both *in vitro* and *in vivo* (76,77). The amount of tissue available for extraction of tumor antigens is often the limiting factor for GBM immunotherapy. Since tumor-derived RNA can be amplified *in vitro*, a virtually unlimited source of tumor antigens becomes available (77). Other advantages of loading DC with RNA include the reported high transfection efficiency combined with low toxicity and safety risks. Moreover, RNA-molecules are translated into proteins by the DC themselves and those proteins are subsequently processed in the endogenous pathway of antigen processing, resulting in optimal priming of CD8+ T cells. Researchers have dedicated a lot of effort to the improvement of RNA transfection methods. Three techniques have been investigated: lipid-mediated transfection, electroporation and passive transfection (78,79). By now, electroporation has proven to be the method of choice for the introduction of exogenous RNA-molecules into DC. It does not require additional reagents and is compatible with clinical use (80). Unfortunately, up to now, a standardized DC electroporation protocol is lacking (81-83). It is clear that we are far from optimized RNA-loaded DC vaccines. Already validated in several experimental studies, improving the intrinsic characteristics of DC such as cytokine, chemokine and co-stimulator expression through transfection with additional mRNA species seems very promising (74). Combining this with downregulation of mechanisms within the DC that are inhibitory to immunity might lead to an artificial but extremely powerful APC.

1.3.4. Dendritic cell vaccination in GBM patients

Several groups worldwide have initiated clinical trials in which several hundreds of GBM patients were included up to now (63). These publications deal with safety and feasibility and both immunological and clinical outcomes have been documented. Although pronounced immunological responses are often observed, there is rarely a strong correlation with the clinical outcome as reported by Wheeler *et al.* (84). However, the conventional response criteria used in oncology, originally developed to monitor effects of radio- and chemotherapy, might not be fully appropriate to measure the beneficial effect of active immunotherapy (85).

1.4. The balance between antitumor immunity and GBM-induced immune suppression

Tumors mostly escape immunosurveillance, resulting in tumor progression and ultimately death by disease. Many tumor-induced but also homeostatic mechanisms are in fact counteracting an efficient antitumor immune response. In this paragraph, the most relevant obstacles for the induction of immunity against GBM are highlighted (86). The immune privileged status of the CNS has already been discussed in paragraph 1.2.1.

1.4.1. Intrinsic mechanisms of GBM tolerance

Although under normal physiological conditions, the immune system has a wide range of mechanisms for immune surveillance, cancer is an extremely prevalent disease (37). Immunological tolerance to cancer is, at least in part, mediated by the expression and presentation of (abnormal) self-antigens by neoplastic cells. The endogenous mechanisms designed to prevent autoimmunity also protect tumors from rejection. Central tolerance is induced by macrophages, DC and epithelial cells of the thymus that all participate in the processing and display of self-antigens to immature T cells within the thymus. Thymic negative selection assures that T cells that otherwise would react towards self-proteins in the periphery and thereby potentially cause autoimmunity, are clonally eliminated. However, negative selection is leaky, so backup mechanisms in the periphery must come into play.

Outside the thymus, at least four different peripheral mechanisms determine whether a thymic emigrant T cell becomes activated; *(i)* the level and persistence of antigen, *(ii)* the activation status

of the involved APC, *(iii)* the ability of T cells to recognize an antigen and *(iv)* the influence of suppressive regulatory cells (87). Transient antigen exposure activates T cells to eliminate antigen-bearing cells and to differentiate into memory T cells capable of mediating a secondary immune response upon antigen re-exposure. However, persistent exposure to low or high levels of antigen results in tolerance by T cell deletion, a process in which T cells are removed by apoptosis or activation-induced cell death. Moreover, due to lack of costimulatory signals, T cells can become anergic, which renders them functionally inactive. Finally, self-reactive T cells may also be spatially compartmentalized away from their antigen and physically unable to detect it (88).

1.4.2. Regulatory T cells

Defined as a T cell population that functionally suppresses an immune response by influencing the activity of other T cells, Treg have emerged as very important cells involved in the prevention of autoimmunity and in the controlled downregulation of undesired immune responses. However, these cells are also potent suppressors of endogenous and induced antitumor immune responses. Treg represent 5 to 10 percent of the peripheral CD4+ T cell pool in humans and mice. There are two main subsets of Treg, which differ in terms of induction and effector mechanisms. One subset develops during the normal process of T cell maturation in the thymus and is referred to as 'naturally occurring' (89). Sakaguchi *et al.* showed in 1995 that the expression of the IL-2 receptor alpha chain (CD25) could serve as phenotypic marker for these CD4+ Treg, although CD25-expression is not restricted to Treg (90). Other markers include glucocorticoid-induced TNF-receptor related protein (GITR) and CTLA-4 (91,92). The identification of the unique Treg transcription factor Forkhead box P3 (FoxP3) lead to a revival and rapid evolvement of the Treg field. *In vitro*, these cells act on a cell-cell contact basis, whereas multiple modes of action have been described *in vivo*. The second subset of 'adaptive' Treg develops as a consequence of peripheral T cell activation under particular conditions of suboptimal antigen exposure and/or costimulation. The latter subcategory includes CD4+IL-10+FoxP3- Treg (termed 'Tr1') mainly acting through IL-10, and CD4+TGF-β+ Treg mainly acting through transforming-growth factor beta (TGF-β) (termed 'Th3') (93,94). In mice, the role of Treg in tumor immunopathogenesis has largely been defined using reagents that target Treg *in vivo*, albeit in a non-specific way. These approaches include treatment with monoclonal antibodies (mAb) against CD25, GITR and CTLA-4 (95-99). Different sources of Treg have been identified in the tumor microenvironment: *(i)* Treg from the thymus, LN, bone marrow and peripheral blood can traffic to the tumor site. This trafficking is

facilitated by the expression of CCR2 and CCR4 on Treg and abundant expression of CC chemokine ligands (CCL), such as CCL2 and CCL22 in the tumor microenvironment (100). *(ii)* The tumor microenvironment can suppress APC differentiation and function (through IL-10, TGF-β and VEGF) and these dysfunctional APC can subsequently promote Treg differentiation. *(iii)* DCi in the tumor microenvironment and dLN can induce Treg expansion. *(iv)* Normal T cells can be converted into Treg by TGF-β, often present at high concentration in the tumor milieu. The suppressive mechanisms of Treg have been investigated in many *in vitro* and *in vivo* models. Multiple mechanisms, acting simultaneously, rather than a single mode of action are proposed. *(i)* Treg can induce B7-H4 expression in APC and these B7-H4+ APC induce T cell cycle arrest. *(ii)* When activated, Treg are able to directly kill T cell and APC targets through perforin-granzyme B dependent pathways. *(iii)* Treg expressing CTLA-4 induce indoleamine 2,3-dioxygenase (IDO) expression in APC which in turn suppress T cell activation by reducing tryptophan availability. *(iv)* The release of IL-10 and TGF-β by Treg directly inhibits T cell activation and the expression of MHC-molecules, CD80, CD86 and IL-12 by APC. *(v)* Competitive consumption of IL-2 by Treg represents an alternative suppressive mechanism (86,88).

The antigen-specificity of Treg is still poorly understood. Many TAA are self-antigens and since Treg are specific for self-antigens, it is possible that Treg recognize at least a subset of TAA. Treg can also have TAA specificity because they were induced in dLN and/or the tumor microenvironment. Some data suggest that differentiation, expansion and activation of Treg are driven in an antigen-specific manner, whilst activated Treg display suppressor activity in a non antigen-specific way (88). Most likely, this suppressive activity is interfering with both TAA-specific priming and effector functions of effector T cells (101).

1.4.3. Innate immune cells counteracting antitumor immunity

The interaction between tumor cells and the innate arm of the immune system is increasingly recognized to play a decisive role in the outcome of immunosurveillance throughout the multiple stages of carcinogenesis. Although undoubtedly contributing to tumor rejection initially, in a setting of unresolved inflammation, tumor cells and stromal elements subvert host innate immune mechanisms to promote disease progression (86,102).

1.4.3.1. Tumor-associated macrophages

Macrophages are a prominent component of the cellular response to tumors, mediating diverse functions. TLR-dependent activation of macrophages results in the production of reactive oxygen species (ROS) and the secretion of inflammatory cytokines. Galarneau *et al.* recently showed in a murine GBM model that tumor growth is more rapid in mice depleted of macrophages (103). In contrast to these beneficial activities, tumor-associated macrophages (TAM) play major roles in tumor progression. Mirroring the obsolete Th1/2 paradigm, many refer to polarized macrophages as M1 and M2 cells. In general, M1 cells have an IL-12^{hi}, IL-23^{hi}, IL-10^{lo} phenotype, are efficient producers of effector molecules such as ROS and nitrogen intermediates and inflammatory cytokines (IL-1β, TNF), participate as inducer and effector cells in polarized Th1 responses and mediate resistance against intracellular parasites and tumors. In contrast, M2 cells participate in polarized Th2 reactions, promote killing and encapsulation of parasites, are present in established tumors and promote progression, tissue repair and remodeling and have immunomodulatory functions. Similar to the Th1/Th2 nomenclature, the M1/M2 dichotomy is not sufficient to completely cover the entire macrophage spectrum. It is currently accepted that TAM represent a skewed M2 population. Circulating blood monocytes are actively recruited to the tumor site by tumor-derived chemotactic factors such as CCL2, macrophage-colony stimulating factor and VEGF. In the tumor microenvironment, monocytes differentiate into TAM that establish a symbiotic relationship with tumor cells; tumor-derived factors positively modulate TAM survival and TAM-derived factors promote tumor cell proliferation, survival, matrix deposition, tissue remodeling and neoangiogenesis. TAM produce cytokines that negatively modify the outcome of a potential antitumor response. IL-10, IL-6, VEGF and TGF-β inhibit the maturation and activation of tumor-associated DC. IL-10 and TGF-β promote Th2 cells and Treg which inhibit a T cell mediated antitumor response. Since TAM contribute to tumor progression to such a high extent, they represent relevant targets for therapy. TAM activation, recruitment, survival, effects on angiogenesis and matrix remodeling and effector molecules are all currently under investigation (104-107).

1.4.3.2. Myeloid-derived suppressor cells

Tumor progression in patients and experimental animals with cancer is frequently associated with the expansion of a cell population of myeloid origin. Under normal conditions, CD31+CD11b+Gr1+ myeloid precursors differentiate into DC, macrophages or granulocytes. The presence of tumor and tumor-derived factors blocks this differentiation pathway and leads to the accumulation of immature CD11b+Gr1+ myeloid cells, termed myeloid-derived suppressor cells (MDSC) (108). To exert their function, these cells require cell-cell contact and compromise both innate and adaptive immunity. Innate immunity is inhibited by suppressing natural killer (NK) cell-mediated lysis and by polarizing macrophages towards the TAM subtype. Adaptive immunity is inhibited by suppressing the activation and proliferation of T cells and antibody production by B cells. MDSC also limit the availability of mature and functional DC, facilitate the development of FoxP3+ Treg and favor tumor angiogenesis. It has recently been proposed that MDSC represent the true link between inflammation and cancer. Chronic inflammation causes an increase in MDSC that inhibits immune surveillance and antitumor immunity, thereby facilitating malignant cell transformation and proliferation (109-111).

1.4.4. GBM immune evasion

The genetic instability of GBM and the repeated exposure to immune selective pressures increase the potential for selection of tumor cell variants with an enhanced capacity to evade immune attack. Many studies have demonstrated that tumor cells simultaneously utilize multiple immune evasion strategies (86,109).

1.4.4.1. Secreted immunosuppressive factors

PGE2. Cyclooxygenase-2 (COX-2) derived PGE_2 has an extremely wide range of action, both under physiological circumstances and in cancer. PGE_2 promotes tumor cell invasion, motility and angiogenesis and induces immunosuppression by downregulating the production of Th1 cytokines (IL-2, IFN-γ and TNF-α) and upregulating Th2 cytokines (IL-4 and IL-10). PGE_2 inhibits T cell activation and suppresses the antitumor activity of NK cells and macrophages. Moreover, PGE_2 induces MDSC and has a direct effect on Treg by inducing FoxP3 expression in non-Treg cells and

by increasing Treg activity. Finally, COX-2 overexpressing tumor cells induce IL-10 expression in mature DC, thus promoting Treg induction (112,113).

TGF-β. The three closely related isoforms of TGF-β (TGF-β1, 2 and 3) are involved in the regulation of inflammation, angiogenesis and cell proliferation. TGF-β inhibits T cell activation and proliferation, as well as the maturation and function of APC. Recent *in vitro* data even show that TGF-β1 expression in glioma cells was upregulated by conditioned medium from CD3-activated T cells, suggesting secretion of this cytokine in response to immunity (114). The synthesis of cytotoxic molecules including perforin, granzymes A and B, IFN-γ and Fas-L is impaired by TGF-β in CTL. It might also facilitate the conversion of naïve T cells to Treg and recruitment of Treg towards the tumor site (115,116). The accumulation and functionality of Treg in experimental glioma has been very well documented by Grauer *et al.* and Fecci *et al*. (96,98).

IL-10. The function of IL-10 in cancer is complex: depending on the model used, it can display immunosuppressive or immunostimulating activities and is therefore often termed immunomodulatory. IL-10 can act on both tumor cells and immune cells to inhibit antitumor immune responses. It has been documented that IL-10 is involved in the inhibition of IL-2 induced T cell proliferation, DC and macrophage T cell activation and downregulation of MHC class II molecules on APC (117).

VEGF. In addition to promoting angiogenesis, VEGF downregulates antitumor immunity, both by inhibiting the activation of nuclear factor-κB in DC, thereby preventing DC maturation, and by suppressing the activation of T cells. VEGF also promotes the generation of MDSC (118).

1.4.4.2. Evading tumor-effector cell interactions

Extracellular matrix proteins. Efficient lysis of tumor cells is dependent on proper binding of effector cells to the target cell surface. T cell proliferation and cytokine production is inhibited by tenascin-C and it has been documented that GBM cells produce thick glycosaminoglycan coats which protect them from CTL activity (109).

Intercellular adhesion molecule-1 (ICAM-1, CD54). ICAM-1 functions as a cell surface receptor for leukocyte function antigen-1 (LFA-1) that is present on CTL and NK cells. This interaction facilitates T cell recognition of TAA presented in MHC class I context on APC and target cells. Disruption of the LFA-1/ICAM-1 interaction inhibits target cell lysis and hence constitutes one mechanism of T and NK cell immune evasion (119).

MHC class I defects. Displaying aberrant MHC class I molecules by tumor cells may allow them to evade T cell detection. Several types of abnormal MHC class I expressions have been documented: *(i)* complete MHC class I loss, *(ii)* MHC class I allelic loss and *(iii)* loss of MHC class I haplotype. Very low expression of MHC class I molecules has been observed in glial tumors as well (120).

1.4.4.3. MHC class I deficient tumors escape NK cell killing

NK cells represent one of the core elements of the innate immune system, lysing target cells. Unlike T cells, NK cells preferentially target tumor cells lacking MHC class I molecules. In fact, in normal tissues, NK cell tolerance is maintained by the expression of inhibitory killer immunoglobulin-like receptors on NK cells reacting with MHC class I molecules. MHC class I-low or -deficient GBM tumors can escape NK cell lysis by the ectopic expression of human leukocyte antigen-G, that has a role in the protection of the fetus from allorejection by maternal T and NK cells (121).

1.4.4.4. The Fas-Fas-L pathway of apoptosis

Binding of Fas receptor and its ligand, Fas-L, initiates a signaling cascade resulting in apoptosis of Fas-expressing cells. Tumor cells can disrupt this apoptotic pathway at different levels; Fas surface expression can be downregulated or a soluble decoy receptor can be secreted. Inhibition of caspase-8 activation by expression of Fas-associated death domain-like IL-1β-converting enzyme inhibitory protein (cFLIP) has also been documented. Strikingly, Fas-L-expressing tumor cells can in turn attack activated Fas+ T cells (109).

1.4.4.5. Other immunosuppressive mechanisms

B7-H1. Programmed death ligand-1 (PD-L1), alternatively termed 'B7-H1', has a strong immunomodulatory activity and has been described on both normal tissues and tumors. Microglial-associated B7-H1 expression plays a role in controlling autoimmune disease, but in the context of malignancy, it helps to create an immunosuppressive network in the tumor microenvironment (122). Reverse signaling through PD-L1 and PD-L2 into DC might result in a suppressive DC phenotype (123).

Galectin-1. The expression of galectin-1 (Gal-1), a β-galactoside-binding protein, has been well documented on a wide range of tissues and in particular on malignant lesions and the associated stromal cells. Gal-1 has diverse functions in several aspects of cancer biology, including the regulation of tumor transformation, cell cycle regulation and apoptosis. Futhermore, this glycan-binding protein may also contribute to tumor metastasis by modulating cell adhesion, migration and invasiveness. In addition, Gal-1 acts as a negative regulator of T cell immunity and contributes to tumor cell evasion of T cell responses (124).

Signal transducer and activator of transcription-3 (STAT-3). STAT-3 is commonly constitutively activated in diverse cancers (including GBM), through different signaling pathways such as the PI3K-AKT-mTor pathway. Constitutive STAT-3 activity in tumors negatively regulates inflammation, DC activity and T cell immunity (125). In particular, the release of pro-inflammatory cytokines and chemokines is suppressed. In addition, STAT-3 positively regulates the expression of anti-apoptotic proteins such as Bcl-2, Bcl-XL, Mcl-1, survivin and cFLIP in GBM cells (126).

Indoleamine 2,3-dioxygenase. IDO is one member of the enzyme-pair that degrades the essential amino acid tryptophan in mammals. In cancer, IDO is overexpressed in both tumor cells and stromal immune cells where it promotes the establishment of tolerance to tumor antigens. In conditions of tryptophan shortage, T cells undergo cell cycle arrest. IDO is also upregulated in APC upon Treg induced CTLA-4/B7-dependent cell-cell signaling and these IDO+ 'regulatory' DC can easily expand Treg (127,128).

The L-arginine metabolism. In higher organisms, the control of amino acid metabolism is emerging as an evolutionarily preserved strategy for limiting the expansion of actively proliferating cells – including antigen-activated T lymphocytes – and tumor cells have adopted this concept to avoid or restrain attack by the immune system. Interference with the L-arginine metabolism is also a major mechanism of action of MDSC. The latter cells use two enzymes involved in the L-arginine metabolism to control T-cell responses: inducible nitric oxide synthase (iNOS), which generates nitric oxide and arginase 1 (Arg1), which depletes the milieu of arginine. Th1 cytokines induce iNOS, whereas Th2 cytokines upregulate Arg1. Induction of either enzyme alone results in a reversible blockade in T-cell proliferation. When both enzymes are induced together, peroxynitrites, generated by iNOS under conditions of limited arginine, cause activated T lymphocytes to undergo apoptosis (129-131).

1.5. Towards an optimal cancer vaccine: are we there yet ?

Although a negative answer to the question above seems disappointing at first, it is clear that we are only starting to get a glimpse of the complex mechanisms controlling antitumor immunity and counteracting immune suppression. The true unraveling of these processes and their interplay provide tumor immunologists with a continuously growing number of potential targets. In immunotherapy for cancer – including malignant glioma – researchers and clinicians are leaving the obsolete frameworks of therapies based on single strategies. It is now accepted that in the majority of patients and tumors, the establishment of immunological control of malignancy will not be reached by boosting the effector arm of the immune response only. At least transient downregulation of the counteracting natural and/or tumor-induced immunosuppressive mechanisms may be equally relevant, if not more (132).

When optimization is applied in a strict way to DC vaccination, tremendous opportunities still lie in generation of the most appropriate DC subset, DC maturation, nature and source of tumor antigens, DC loading method, route, dose and frequency of vaccination. Biological safety was one of the main questions to be addressed initially. In most studies, toxicity is limited to mild local reactions at the injection sites, although febrile reactions and tumor pain have been reported (59). Major autoimmune side effects were anticipated as most tumor antigens are self-antigens but were not or only rarely observed (133). Between 1996 and 2004, more than sixty clinical trials have been completed using tumor antigen-loaded DC and many more are in progress or scheduled (74). All of them apply different methods of DC-generation, nature and source of antigens and loading techniques, which makes it at this stage extremely hard to draw even preliminary conclusions. Efforts are undertaken to make *ex vivo* generated DC more responsive to chemotactic cues (thereby improving DC homing to secondary lymphoid organs), to increase the expression of costimulatory molecules (to make them even better APC) or to force the cells to obtain a more activated phenotype with e.g. TLR ligands. Obviously, the gold standard in DC cancer therapy has yet to be defined (74). Up to now, there is no or only limited evidence that DC vaccines represent a means of inducing protective immunity in cancer patients that is superior to other immunotherapeutic strategies. Often half or even less of the treated patients exhibit immune responses against the vaccinated antigen(s). Despite occasional correlations between immunological and clinical responses in this kind of single-arm trials, it is not yet clear whether the modest clinical responses were caused by the vaccination, or whether they reflect the

selection of patients with better prognoses and capable of mounting efficient immune responses (53).

We are now at the beginning of the era in which immunotherapy is claiming its place in the multimodal treatment of cancer. Removal of bulky tumor by surgical resection remains crucial and the extent of resection often represents a predictor for final outcome. Immunological control of minimal residual disease is conceptually more feasible to establish, even if the remaining tumor cells are actively spreading. Potential synergies between conventional chemotherapy and radiotherapy on one hand and immunotherapy on the other hand, have recently drawn special interest. It has been noted that chemotherapy can cause DC activation through enhanced cross-presentation of tumor antigens if chemotherapy induced apoptosis leads to a pro-inflammatory environment at the site of tumor cell death. Moreover, chemotherapy mediated reduction of immunosuppressive leukocytes can act synergistically with DC vaccination or adoptive T cell transfer (134). The other way round, DC vaccines might sensitize GBM cells to chemotherapy (135). Similarly, it has been documented that radiotherapy might preferentially remove suppressor T cells, permitting a more efficient effector T cell activity. The combined use of DC vaccines with administration of mAb such as anti-CD134 or anti-angiogenesis therapy in an adjuvant setting might even yield a more efficient immune response (136-138).

1.6. Experimental rodent models for malignant glioma

Over the last 4 decades, thousands of *in vitro* and *in vivo* reports in both rat and mouse GBM models have been published (Table 1). It is highly important to highlight a few but fundamental differences between those models. A first distinction is to be made between spontaneous oncogenesis in genetically engineered mice and engrafted (i.e. the implantation of primary tumor cells or tumor cell lines) tumor models. Although spontaneous tumor models are mimicing the clinical situation of gliomagenesis much more closely than the engrafted models, the main drawbacks are the poor reproducibility, low tumor penetrance, prolonged latency for tumor formation and the need for advanced *in vivo* imaging techniques. On the other hand, since engrafted models lack the stepwise genetic changes occurring during tumor progression, many of them remain well circumscribed, lack characteristic histological vascularization and rarely recapitulate the tumor-of-origin phenotype. Nevertheless, based on their fairly good

reproducibility, engrafted models are best suited for evaluating preclinical therapies such as DC immunotherapy (139,140).

Below, we briefly summarize the most relevant reports in the murine GL261 glioma model, since this model has been used in our studies as well. Ni *et al.* underscored the immunogenicity of the GL261 tumor cells by treating mice with an intracranial glioma with tumor extract-pulsed cloned DC. Cured animals showed increased DTH responses to GL261 cells and long-term tumor protection was observed (141). Aoki *et al.* showed that pulsing DC with a complex of tumor extract with cationic liposomes induces an antitumor immune response against intracerebral glioma in which CD8+ T cells are involved (142). Protective immunity against intracranial glioma growth obtained through immunization with either lysate- or RNA-loaded DC was reported by Insug *et al*. Adding recombinant IL-12 to the vaccine regimen further improved its efficacy (143). The survival benefit of combining vaccination with lysate-pulsed DC and IFN-β gene therapy was demonstrated by Saito *et al.* (144). Similarly, the group of Tsugawa *et al*. reported that the sequential intratumoral delivery of an IFN-α encoding adenoviral vector and DC induced long-term survival and specific CTL activity (145). The same group moreover showed that intratumoral administration of DC, genetically engineered to secrete IFN-α, enhances the efficacy of systemic vaccines with cytokine-gene transduced tumor cells (146). Kjaergaard *et al.* observed complete tumor regression of established intracranial tumors with infiltration of both CD4+ and CD8+ T cells using vaccines created through electrofusion of DC and irradiated tumor cells (147). Survivin, a member of the inhibitor of apoptosis family of proteins, has been the GL261 TAA of choice for Ciesielski *et al*. In particular, the authors exploited the xenogeneic differences between human and murine surviving sequences to develop a more immunogenic tumor vaccine (148). The efficacy of systemic immunotherapy with DC loaded with GL261 antigens was confirmed by Pellegatta *et al*., but the authors moreover introduced the concept of cancer stem cells in this model. They reported that DC-targeting of cancer stem cells within the GL261 tumor cell pool provides a higher level of protection against GL261 glioma (149,150). Recently, Grauer *et al.* illustrated the pronounced impact of FoxP3+ Treg in this model and stated that Treg elimination is even a prerequisite for successful eradication of established glioma using tumor lysate-pulsed DC (98,99).

Species	Strain	Tumor	Type of tumor	Origin of tumor	Immunogenic	Number of publications (*in vitro/total in vivo/orthotopic in vivo*)
Mouse	C57BL/6	GL261	Glioma	Syngeneic (methylcholantrene induced)	+	(56/35/27)
	athymic nude, SCID or other immuno-deficient mice[1]	U251	Glioma	Human	+	(47/79/50)
		U87	Glioblastoma	Human	+	(124/101/53)
Rat	Lewis	CNS-1	Glioma	Syngeneic (methylnitrosurea induced)	+	(7/7/6)
	Wistar (outbred)	C6	Glioma	Syngeneic (methylnitrosurea induced)	+	(2381/517/371)
		A15A5	Glioma	Syngeneic (ethylnitrosurea induced)	+	(7/5/3)
	Fischer	F98	Glioma	Syngeneic (ethylnitrosurea induced)	(weak)	(113/45/40)
		RG2 (D74)	Glioma	Syngeneic (ethylnitrosurea induced)	-	(59/31/22)
		RT2	Glioma	Syngeneic (methylnitrosurea induced)	+	(5/12/10)
		9L (T9)	Gliosarcoma	Syngeneic (methylnitrosurea induced)	+	(436/223/173)

Table 1. Experimental rodent glioma models.

Entrez pubmed queries used were respectively: [(species) (tumor) glioma (*in vivo*)] for #[total in vivo]; [(species) (tumor) glioma (in vivo in brain)] for #['orthotopic in vivo] and [(species) (tumor) glioma] minus [(species) (tumor) glioma (in vivo)] for #[in vitro]. [(1)] Immunological studies in immunodeficient hosts for human glioma xenografts require 'humanisation', *i.e.* repopulation of the host with functional human immune cells (often CD34 progenitor cells with additional transfer of effector cells or additional immunization with APC such as DC).

Chapter 2. Aims of the study and experimental approach

2.1. General aim

For GBM, no curative breakthroughs have been obtained in any therapeutic field during the last decades. Hence the prognosis for these patients remains dismal and a further search for better therapy is undoubtedly required (29). A defective immunological surveillance has been recognized as a hallmark of cancer (including GBM) allowing malignancy to progress with often fatal consequences (37). In this context, innovative immunotherapeutic treatments aiming to restore or even improve antitumor immunity are now emerging as promising anti-GBM strategies. Active immunotherapy – also termed tumor vaccination – consisting of treatment with autologous, tumor antigen-loaded DC, is believed to be the most powerful tool for the induction of efficient T cell mediated antitumor immune responses (47,53). This kind of immunotherapy is being explored for many types of cancer with often spectacular results in experimental models. So far, objective clinical responses in humans are limited, although many cancer patients treated with DC exhibit pronounced immune responses. However, these antitumor immune responses are often counteracted by the tumor via a wide array of immunosuppressive mechanisms, finally leading to tumor cell escape from immunosurveillance (38,46). A better understanding of the balance between antitumor immunity and immunosuppression will be essential to shed light on new treatment modalities that simultaneously boost the effector arm of the immune response and reduce the harmful tumor-induced immunosuppression.

Our research group has previously established that DC-based immunotherapy is a promising tool in the fight against GBM. In parallel with the experimental data presented here, a phase I/II clinical trial for GBM patients is conducted by our research group. Briefly, autologous DC from a GBM patient are differentiated *ex vivo* from PBMC and are subsequently pulsed with autologous GBM tumor antigens obtained from a tumor lysate. Mature, antigen-loaded DC are then administered to the patient in the form of a cellular vaccine. The basic concept of this methodology is that the vaccinated DC migrate to the secondary lymphoid organs where they can prime or boost T cell mediated antitumor immunity. For GBM patients, DC immunotherapy is undoubtedly promising and warrants further investigation (59,63). At the same time, many questions regarding GBM immunotherapy are still open and require further exploration. In this work, we try to address some of these issues in a more standardized setting both *in vitro* and in an experimental mouse

model. The overall aims of this study are *(i)* to optimize DC immunotherapy for GBM and *(ii)* to unravel the cellular mechanisms governing antitumor immunity and immune suppression. We hope that insights in the immunological mechanisms explored in this work might generate new hypotheses for being tested in the clinical setting as part of the cohort comparison clinical trial HGG-IMMUNO-2003.

2.2. Specific aims and methodology

2.2.1. Immunotherapy against glioma with RNA-loaded DC: proof of concept

It has been shown by our group that GBM immunotherapy with DC, targeting the entire repertoire of tumor antigens provided by tumor lysates, is a valuable approach (58,59). However, in GBM patients, the amount of tumor tissue available for lysate preparation is often a limiting factor. Using total tumor RNA instead of tumor lysate for DC loading could offer a virtually unlimited source of tumor antigens, since mRNA can be amplified *in vitro* (151). Others have shown that transfection of DC with tumor-derived RNA is highly efficient with minimal safety risks (76-79,151,152). Therefore, we first validate the concept of DC loading with RNA-molecules **(4.3.)** and subsequently perform functional assessment of DC loaded with total glioma-derived RNA in a murine *in vitro* system **(4.4)**. Secondly, the therapeutic efficacy of RNA-loaded DC is explored in an experimental glioma model in which mice are prophylactically vaccinated with DC and subsequently undergo orthotopic tumor challenge with GL261 glioma cells **(4.5)**. Finally, we also explore the specificity of the DC induced immune response in the experimental glioma model **(4.6.)**.

2.2.2. Implementation of bioluminescent imaging in an experimental mouse model for DC immunotherapy against glioma

Despite their clinical relevance, a major disadvantage of orthotopic tumor models is that animals need to be sacrificed to assess tumor growth. To evaluate glioma growth in our experimental setting and in particular the effect of DC immunotherapy, we implement *in vivo* bioluminescent imaging (BLI) in this model **(Chapter 5)**. Native GL261 glioma cells are therefore lentivirally transduced with Firefly luciferase (Fluc), allowing *in vivo* visualisation of Fluc-expressing GL261

cells through BLI. This type of optical imaging allows non-invasive, rapid, reproducible assessment of intracranial tumor load in a semiquantative way (153). The implementation of BLI in our model will not only lead to a reduction in the number of mice needed, but will further enable us to monitor any therapeutic effect in real-time.

2.2.3. Study of the balance between antitumor immunity and immune suppression in experimental murine glioma

Despite the promising potential of DC immunotherapy, the vaccine-induced antitumor immunity, mainly T cell driven, is in most cases not sufficient to completely eradicate an established tumor and thus to provide long-term immunological protection. Other interventions, such as (temporarily) lowering of the many immunosuppressive mechanisms could facilitate the development of a more potent effector immune response (154). The experimental mouse model used in this study offers an outstanding stage to explore in depth the involvement of specific cell populations and to study immune reactions within the brain itself. In particular, we investigate the role of CD8+ effector T lymphocytes, since it is established that cytotoxic CD8+ T cells are key players in antitumor DC vaccination (155,156). We therefore deplete CD8α+ cells *in vivo* through administration of a CD8α-depleting mAb **(6.3)**. A major role in GBM tumor immunology has been attributed to Treg, a subset of CD4+ T cells that prevent autoimmunity under normal physiological conditions but are also potent suppressors of antitumor immune responses (88). We aim to boost antitumor immunity by eliminating Treg *in vivo* by administration of an anti-CD25 mAb **(6.4)**. Since persistent immunological control of glioma formation is necessary to prevent tumor relapse, we address this by subjecting mice that are long-term survivors from initial tumor challenge, to intracranial re-challenge with glioma cells **(6.5)**. Virtually impossible to accomplish in humans, our experimental glioma model allows detailed monitoring of local immunological processes within the brain. In a series of experiments, we explore these immune events in tumor challenged mice that were either treated with DC vaccination, received anti-CD25 treatment or received combined treatment. In an attempt to cover both innate and adaptive immunity, we study brain infiltrating lymphocytes as well as myeloid cells **(6.6)**.

Chapter 3. Materials and methods

3.1. Animals, cell lines and culture media

3.1.1. Mice

Female adult (10 weeks old) C57BL/6J and BALB/C mice were purchased from Harlan (Horst, The Netherlands). C57BL/6J-*Tyrc*$^{-2J/J}$ mice were purchased from Jackson Laboratories (ME, USA). The animals were housed in filtertop cages, bedded with saw dust and had free access to food and water. All animal experiments were approved by the bioethics committee of the Katholieke Universiteit Leuven that follows international guidelines.

3.1.2. Tumor cell cultures

Methylcholantrene-induced murine C57BL/6J syngeneic GL261 glioma cells were kindly provided by Dr. Eyüpoglu from the University of Erlangen (Germany). GL261 tumor cells were maintained in Dulbecco's modified essential medium (DMEM) supplemented with 10 % heat-inactivated fetal calf serum (FCS), 2 mM L-glutamine, 100 U/ml penicillin, 100 µg/ml streptomycin and 100 µg/ml gentamycin sulfate (all from Lonza, Verviers, Belgium). MC17-51 fibrosarcoma (ATCC clone CRL-2799) and Lewis lung carcinoma (LLC) tumor cells, kindly provided by Prof. Conway from the Katholieke Universiteit Leuven (Belgium), were maintained in RPMI with the same supplements as mentioned for the GL261 cells. Cells were cultured in a humidified atmosphere containing 5 % CO_2 at 37 °C.

3.1.3. Lentiviral transduction of GL261 cells with Firefly luciferase

Construction and production of the lentiviral vector pCHMWS-Fluc-IRES-Puro was performed as for previously described constructs (157). The day before transduction, GL261 cells were seeded in a 96-well plate at 15,000 cells per well. On the day of transduction, medium was replaced by DMEM containing vector (5 x 10^4 pg/ml p24, multiplicity of infection < 1) and incubated for 5 h. After transduction, medium was replaced, and 48 h later, the cells were assayed for luciferase activity. Transduced cells were splitted twice per week. Puromycin (Sigma-Aldrich, Bornem,

Belgium) was used at 1 µg/ml once a week to select for stably transduced cells. Transduction was performed under L2 containment and before release of transduced GL261 cells to L1 containment, cell cultures were tested for absence of recombinant vectors in a rescue assay and p24 protein concentration was measured by an ELISA (HIV-1 p24 core profile ELISA, DuPont, Dreiech, Germany).

3.1.4. Primary cell cultures

Splenocytes, lymph node cells and brain-infiltrating lymphocytes were cultured in RPMI supplemented with 10 % heat-inactivated FCS, 2 mM L-glutamine, 100 U/ml penicillin, 100 µg/ml streptomycin, 1x non-essential amino acids (Lonza) and 50 µM beta-mercaptoethanol (b-ME, Sigma-Aldrich, Bornem, Belgium). DC medium consisted of RMPI-1640 supplemented with 10 % heat-inactivated fetal calf serum, 2 mM L-glutamine, 100 U/ml penicillin, 100 µg/ml streptomycin and 50 µM β-ME. Digestion medium consisted of RPMI 1640 with 10 % heat-inactivated serum, 2.5 mg/ml of collagenase D (Roche) and 5 U/ml of DNase I (Invitrogen). Cells were cultured in a humidified atmosphere containing 5 % CO_2 at 37 °C.

3.2. Generation of murine DC and loading with RNA-molecules

3.2.1. DC culture

DC were derived from bone marrow (BM) progenitor cells as described (158,159). Recombinant murine GM-CSF (20 ng/ml) was kindly provided by Prof. Dr. Kris Thielemans (Vrije Universiteit Brussel, Brussel, Belgium). Medium was refreshed on day 3 and 5 of culture. Immature DC (DCi) were harvested on day 7 of culture by vigorous pipetting and washed with phosphate buffered saline (PBS, Lonza).

3.2.2. Electroporation of DC with RNA

For DC loading with total RNA (from GL261, LLC, MC17-51 tumor cell lines or splenocytes), DCi were transfected with 15 µg of total RNA per million DCi through exponential decay electroporation (300 V and 150 µF) with a GenePulser electroporator (Bio-Rad, Nazareth,

Belgium). RNA extraction was performed with the RNeasy Midi Kit (Qiagen, Venlo, The Netherlands) and quality controlled with an Agilent 2100 Bioanalyzer (Santa Clara, CA, USA). Cells were resuspended in OptiMEM medium (Gibco, Invitrogen, Merelbeke, Belgium) at 20 x 10^6 per ml and 4 x 10^6 DCi were used per electroporation cuvette. The mRNA load for enhanced green fluorescent protein (eGFP) and Fluc reporter genes was 1 µg per million DCi. For lysate-loading (DCm-GL261-L), DCi were co-incubated with GL261 lysate at 100 µg per million DCi per ml OptiMEM medium for 30 min at 37 °C. Lysates were generated by exposing GL261 cells to 6 consecutive freeze/thaw cycles (3 min in liquid nitrogen and 3 min on 56 °C respectively). Immediately after loading, DC were again put in culture for 24 h in DC medium with GM-CSF, and 0.5 µg/ml *E. coli* lipopolysaccharide (LPS, Sigma-Aldrich) was added to induce maturation. The next day, DCm were harvested, counted and resuspended at suitable concentration for further application. Maturation was assessed by flowcytometry as described further.

3.3. Amplification of total cellular mRNA

Total GL261 mRNA was amplified according to the optimized protocol by Harris *et al* (151). Briefly, one microgram of total RNA was used in a 10 µl reverse transcriptase reaction containing 1 µM capswitch primer, 1 µM CDS 64T+ oligo primer, 100 U of Powerscript reverse transcriptase (BD Biosciences Clontech), 1x first strand synthesis buffer, 1 µM dNTPs and 2 mM DTT. The reaction mixture was incubated for 1 h at 42 °C. 2 µl of the reaction product was then diluted into a 100 µl PCR reaction containing 0.4 µM of T7 Capswitch and CDS 64T+ oligo primers, 0.4 µM dNTPs, 1x KlenTaq PCR buffer, and 2 µl Advantage KlenTaq polymerase mix (BD Biosciences Clontech). Amplification was achieved after 20 cycles consisting of 95 °C for 5s, 65 °C for 5 s, 68 °C for 6 min. The amplified cDNA was purified using a PCR purification kit (QIAGEN). Three µg of each cDNA was transcribed *in vitro* using a T7 mMessage mMachine kit (Ambion) according to the manufacturer's instructions. Final RNA was purified using an RNeasy mini column (QIAGEN) following the manufacturer's protocol for RNA cleanup.

3.4. Flowcytometry

Murine DC were stained for H-2K^b, I-A/I-E, CD80, CD86, CD40 and CD11c. Lysed whole blood, splenocytes, dLN and brain-infiltrating cells were analysed for CD4, CD8, CD25, CD62L, Gr-1, CD11b, CD45 and F4/80. For each staining, appropriate isotype stainings were used. For intracellular detection of FoxP3, the protocol guidelines of the FoxP3 staining kit (eBioscience, San Diego, CA, USA) were followed. Cell viability was assessed by propidium iodide (PI) staining according to manufacturer guidelines (BD Pharmingen, Erembodegem, Belgium). Analysis was performed using the Cellquest software on a FACSort flowcytometer (BD Pharmingen) for 2- and 3-color analysis and on a FACSCanto flowcytometer for 4-color analysis. For determination of absolute cell numbers of specific cell populations, relative cell fractions (as percent of total) were multiplied by the total number of viable cells (FSC-SSC gated).

3.5. In vitro assessment of cell function

3.5.1. Mixed lymphocyte reaction

A total of 2 x 10^5 responder splenocytes (isolated from a naïve BALB/C mouse) were plated in flat-bottom 96-well culture plates. C57/BL6 BM-derived DC were used as stimulator cells in a responder:stimulator ratio ranging from 5:1 to 50:1. Phytohemagglutinin (PHA) was used as positive control. Final volume was 200 µl in each well. After 96 h of incubation at 37 °C and 5 % CO_2, cultures were pulsed with 1 µCi [^{3}H]thymidine per well and harvested 18 h later. Triplicate cultures were set up for every condition. Results are expressed as mean counts per min (cpm) ± standard error of the mean (SEM).

3.5.2. Expression of eGFP in DC after electroporation with eGFP-mRNA

Twenty-four h after electroporation, eGFP expression in DC was assessed by flowcytometry or fluorescence microscopy. Untouched cells and mock-electroporated DC were used as controls.

3.5.3. In vitro stimulation experiments

Basic methodology. Mouse T cells were enriched out of total splenocytes from naïve C57BL/6 mice with nylon wool (Kisker-Biotech, Leiden, The Netherlands). T cells underwent three stimulation cycles of 7 days each with DCm-GL261-RNA or DCm-GL261-L. As a control, unstimulated T cells or T cells stimulated with DC loaded with LLC RNA (DCm-LLC-RNA) or unloaded DC (DCm-mock) were used. Responder – stimulator ratio was 10:1 and 20 U/ml rhuIL-2 (Hoffmann-La Roche, Vilvoorde, Belgium) was added on day 1 and 4 of each cycle. Cells were counted with an automatic hemato-counter (Micros 60, Horiba ABX, Montpellier, France). *In vitro proliferation assay.* Two hundred thousand lymphocytes were restimulated *in vitro* with 2 x 10^4 DCm-GL261-L for 96 h in a 96-well plate in a total volume of 200 µl. Read-out was similar as for MLR (see 3.3.1.) *Flowcytometr*y and *in vitro tumor cell viability assay* were performed as described.

3.5.4. In vitro tumor cell viability assay

The viability assay has been performed as described (160). In brief, target tumor cells (5 x 10^3) were co-cultured with effector cells (5 x 10^4) in a total volume of 200 µl in a flat bottomed 96-well cell culture plate (TPP, St. Louis, MO, USA). After 2, 4 or 6 days of co-culture, medium together with non-adherent cells was removed, the wells were carefully rinsed with PBS and 100 µl of a 0.5 mg/ml 3-(4,5-dimethylthiazol-2-yl)-2,5-diphenyltetrazolium bromide (MTT, Sigma) solution in culture medium was added. The plates were wrapped in tinfoil to protect them from light and incubated for 2 h. After incubation, the MTT solution was removed from the wells and 100 µl pure dimethylsulfoxide (Merck, Darmstadt, Germany) was added. After gentle shaking of the plates (400 rpm, 5 min), optical density was measured on 570 and 620 nm using an ELISA reader (Thermo Labsystems, Franklin, MA, USA). The $OD_{570\text{-}620\ nm}$ value was used as measure for cell viability.

3.6. Murine glioma model

3.6.1. Orthotopic glioma challenge

For the orthotopic intracranial model, GL261 cells were harvested, washed, counted and adjusted to 5 x 10^5 in 10 µl of culture medium, unless mentioned otherwise. Mice were anesthetized

intraperitoneally with 6 µl per gram body weight of a 18.75 mg/ml ketamine (Pfizer, Puurs, Belgium) and 0.125 % xylazine hydrochloride (Bayer, Brussels, Belgium) mixture. After shaving of the skull, mice were fixed in a stereotactic frame (Kopf Instruments, CA, USA) and 2 % lidocain hydrochloride (AstraZeneca, Brussels, Belgium) was applied locally for one min. A 1.5 cm longitudinal incision was made and a burr hole was drilled through the skull at 1.0 mm lateral and 1.5 mm posterior from the bregma. Tumor cells were injected over 1.5 min at a depth of 3 mm below the dura mater with a 26 Gauge syringe (Hamilton, Bonaduz, Switzerland). See also Figure 2. After injection, the syringe was left in place for an additional 2 min and then slowly retracted. The site of the burr hole was rinsed with saline and sterile bone wax was used to seal off the burr hole. The incision was closed with stitches and 2 % sodium fusidate (Leo Pharma, Wilrijk, Belgium) was applied. Stereotactic challenge was performed under sterile conditions. Three times per week, mice were weighed and clinical symptoms were scored with a neurological deficit scale adapted from an experimental autoimmune encephalomyelitis model, with grade 0 for healthy mice, grade 1 for slight unilateral paralysis, grade 2 for moderate unilateral paralysis and/or beginning hunchback, grade 3 for severe unilateral or bilateral paralysis and pronounced hunchback and grade 4 for moribund mice (161). Unless mentioned otherwise, mice were sacrificed by cervical dislocation when they showed grade 4 symptoms and brain was prelevated for histological analysis. Mice with a survival longer than 60 days were considered long-term survivors. Rechallenge was performed between day 80 and day 90 and each time, naïve mice of approximately the same age were challenged as controls.

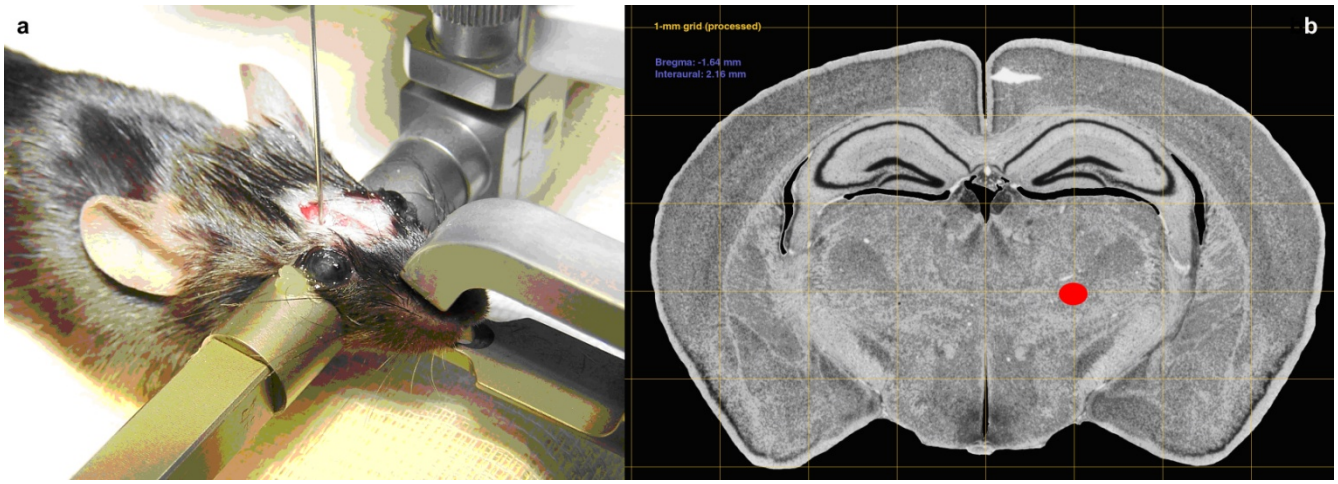

Figure 2. Intracranial challenge with glioma cells under stereotaxic guidance.

(a) Positioning of mouse in stereotaxic frame and intracranial injection of tumor cells with a Hamilton syringe. (b) Coronal brain section of an adult C57/BL6 mouse, cresyl-violet stained. Red ellipse marks position where tumor cells are injected. Printed with permission from Neurogenetics at UT Health Science Center, Memphis, TN (USA) ©1999 RW Williams, design by AG Williams, atlas by T Capra (www.mbl.org) (162).

3.6.2. Subcutaneous tumor challenge

For subcutaneous tumor challenge, GL261 or MC17-51 tumor cells were resuspended at 1 x 10^5 in 50 µl of culture medium. Mice were anesthetized as mentioned above, the skin of the right hind limb was shaved and cells were injected subcutaneously over 1 min with an insulin syringe. After injection, the syringe was left in place for 1 additional min and then slowly retracted. Long (a) and short (b) perpendicular tumor diameters of the tumor were measured three times per week with a caliper. Approximation of the tumor volume was calculated using the following formula: volume = a x $b^2/2$ (144).

3.6.3. Treatment with RNA-loaded DC

Mice were vaccinated with one million CD11c+ DCm on day -14 and -7 before tumor challenge. Vaccinations were given intraperitoneally in a volume of 200 µl PBS. For each vaccination, flowcytometric quality control of the DC was performed. A representative image is depicted in Figure 3.

3.6.4. Functional immune monitoring

Spleen cells and pooled lymph node cells from the inguinal and axillary lymph nodes were used for *ex vivo* restimulation experiments. 2 x 10^5 cells were restimulated with 2 x 10^4 mature DCm-GL261-L. PHA was used as positive control. Mouse IFN-ã ELISPOT was performed with ethanol activated polyvinylidenfluoride 96 well plates (Millipore, Billerica, MA, USA). For coating, the AN18 antibody (15 µg/ml, Mabtech, Stockholm, Sweden) was used. Cells were plated in triplicates with the respective stimuli and incubated for 36 h. For spot detection, the R4-6A2-biotin mAb (1 µg/ml, MABTECH) was used together with streptavidin:ALP (1:1000, Mabtech). Spots were analyzed with an ImmunoScan (Mabtech). Finally, AP-conjugated substrate (Bio-Rad, Nazareth, Belgium) was added until spots emerged. For *ex vivo* proliferation assays, see 3.5.3.

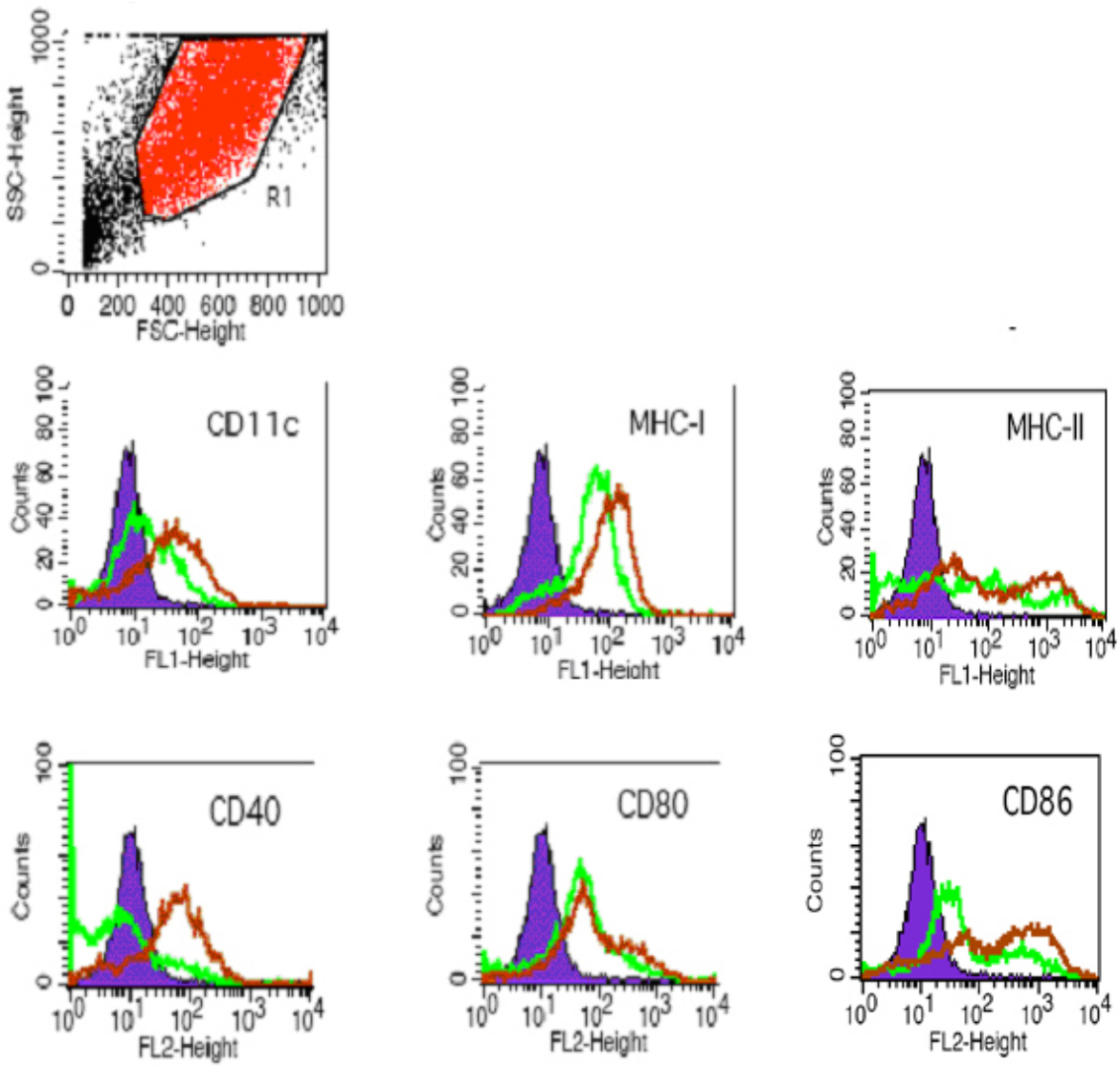

Figure 3. Quality control of murine bone-marrow derived DC. Flowcytometry was performed on immature (green curves) and mature DC (brown curves). Filled histograms represent isotype control stainings. DC were gated on FSC-SSC plot (R1).

3.6.5. In vivo depletion of specific lymphocyte subpopulations

For depletion of CD25+ cells, mice received a single bolus injection (250 µg) of the PC61 mAb (Bioceros, Utrecht, The Netherlands) 21 days before tumor challenge. CD8+ cells were depleted using 200 µg 1 day before and 100 µg 1 day after tumor challenge of the YTS169 anti-CD8 mAb (Bioceros, Utrecht, The Netherlands). Ab were diluted in sterile PBS and all injections were given intraperitoneally. Polyclonal rat IgG (Rockland, Gilbertsville, USA) was used as control.

3.6.6. Isolation of brain-infiltrating cells

Mice were anaesthetized by intraperitoneal injection of 100 µl sodium pentobarbital (Ceva Sante Animale, Brussel, Belgium), both femoral arteries were opened and the animals were perfused through the left cardiac ventricle with 50 ml cold PBS. Brains were removed and cut in small pieces with a scalp in a 50 ml tube in 1 ml of digestion medium. Next, 2 ml of digestion medium was added and the tissue was incubated on 37 °C for 30 min. After incubation, the digested tissue was passed through a cell strainer (BD) and thoroughly washed. The suspension was centrifuged (400 g, 5 min) and the pellet was resuspended in 10 ml of 40 % percoll (Sigma). This suspension was carefully brought on top of 4 ml of 70 % percoll in a 15 ml tube and centrifuged for 25 min at 800 g. After gradient centrifugation, the top myelin and debris layer was removed and the mononuclear cell interphase was recovered and washed two times in PBS. For further functional assays, cells were separated based on the expression of CD11b using CD11b MicroBeads (Miltenyi Biotec, Bergisch Gladbach, Germany). Briefly, cells were counted and centrifuged at 300 g for 10 min. Cells were resuspended in buffer (PBS with 0.5 % FCS and 2 mM EDTA) according to manufacturer guidelines. For 10^7 cells, 10 µl of CD11b MicroBeads were added, mixed and incubated for 15 min at 4 °C. Cells were washed by adding 2 ml of buffer per 10^7 cells and centrifuged at 300 g for 10 min. Cells were resuspended in 500 µl of buffer and magnetic separation was performed with MS or LS columns (depending on the cell number). Both the unlabeled CD11b- fraction and the magnetically labelled CD11b+ cells were collected and washed with PBS. Flowcytometric quality control was performed before further use.

3.7. Imaging

3.7.1. In vitro bioluminescent imaging of living cells

Cells were plated in triplicates in black 96 well plates in 50 µl of culture medium. Medium containing D-luciferin potassium salt (Xenogen, Alameda, CA, USA) was added to a final concentration of 150 µg/l. After 5 min incubation, the cells were imaged for 1 to 5 s in an IVIS 100 system (Xenogen).

3.7.2. In vivo bioluminescence imaging

For all experiments, the IVIS 100 system (Xenogen) was used. Mice were anesthetized just before imaging in an induction chamber with 2 % isoflurane gas in 100 % oxygen at a flow rate of 1 l/min and maintained in the IVIS with a 1.5 % mixture at 0.5 l/min. During the induction phase, mice were injected with D-luciferin (126 mg/kg) dissolved in PBS (15 mg/ml) by intraperitoneal administration. Mice were then immediately placed in prone position in the IVIS and consecutive 10 s to 5 min imaging frames were acquired until the peak in bioluminescent signal was reached. For each frame, the bioluminescent signal was depicted as a pseudocolor image superimposed on a grayscale photographic image. *In vivo* imaging data are reported as the photon flux (p/s) from a 1.35 cm^2 circular region of interest around the head. For subcutaneous measurements, a 3.22 cm^2 circular region of interest was defined.

3.7.3. Ex vivo brain luminescent imaging

Mice were anesthetized as described and injected with 126 mg/kg D-luciferin in the lateral tail vein. Two consecutive imaging frames of 1 min were acquired. Immediately afterwards, the mice were sacrificed by cervical dislocation, decapitated and the brain was dissected. The brain was placed in an acrylic brain matrix (Harvard Apparatus, Holliston, MA, USA) and sliced into 1.0 mm thick coronal sections. Serial sections were imaged for 30 s in the IVIS. From each mouse, the section with the highest emission was stored at -80 °C. *Ex vivo* BLI data are represented as maximum flux (p/s/cm^2/sr) from the most intense luminescent brain slice.

3.7.4. In vitro measurement of luciferase activity

For measurement in GL261 cell cultures, cells were harvested from culture flasks and counted. Four million living cells were pelleted and lysed with 150 µl of Luciferase Cell Culture Lysis Reagent (Promega, Leiden, The Netherlands). Frozen brain slices were cut in halves along the midline, thawed and protein extracts were prepared by homogenization with a rotor-stator homogenizer in 300 µl Luciferase Cell Culture Reagent.

All samples were centrifuged for 15 s at 12,000 g and supernatant was collected. In an opaque 96 well plate, 20 µl of supernatants was plated in triplicate, 50 µl of Luciferase Assay Reagent was added and luciferase activity was determined after 1 s exposure time with a luminometer (Thermo Labsystems, Franklin, MA, USA). Protein content from each sample was measured in triplicate using the Bradford method (163).

3.8. Histology

Brain slides. Prelevated brains from sacrificed animals were long-term fixed in 6 % p-formaldehyde. Fixed brain samples were embedded in paraffin and 10 µm thick serial coronal sections were prepared and mounted on glass slides. All slides were stained with hematoxylin and eosin (HE).

Stereological counting. Tumor volume was determined by stereological counting of serial slides based on the Cavalieri algorithm (164). The interval between the slides was 500 µm and all slides (minimally three) going through the region of interest were used to estimate tumor volume. Stereological tumor area estimations were performed on previously collected samples of which at least three coronal slides of the entire region of interest were available. From each sample, the slice with the largest tumor area was selected. StereoInvestigator software was used (Microbrightfield, Magdenburg, Germany).

Cytospins of brain-infiltrating cells. From each sample, 2 x 10^5 cells were used for cytospin preparation. Cells were pelleted (500 g, 5 min) and resuspended in 2 ml saline. For each cytospin, 500 µl cell suspension was used. Slides were centrifuged at 300 g for 10 min and May Grünwald-Giemsa stained. Cytospins were analysed with a stereomicroscope. For each sample, lymphocytes, macrophages and granulocytes were enumerated per field of view (FOV) on 40 x magnification.

3.9. Statistical analysis

All data are represented as mean ± standard error of the mean (SEM). Survival analysis was performed using the Logrank test. For comparing multiple groups, one-way ANOVA was used. Parametric testing was performed if allowed. For comparison of 2 groups, Student t-test was performed. The Pearsons correlation coefficient was obtained through linear regression analysis. Statistics were calculated with Prism software 4.0a (Graphpad Software Inc., San Diego,CA). In graphs, statistical significances are indicated as follows: $p < 0.05$ (*), $p < 0.01$ (**), $p < 0.001$ (***).

Chapter 4. Immunotherapy against GBM with RNA-loaded DC: proof of concept

4.1. Introduction

Due to the lack of a well characterized TAA profile for GBM, DC-based GBM immunotherapy mostly relies on the use of whole tumor cell preparations as source of tumor antigens. Hence, every immunogenic epitope is theoretically covered, thereby avoiding tumor escape. Methods that take advantage of the entire protein content of the tumor cell to load DC include tumor cell lysates, engulfment of apoptotic or necrotic tumor cell remnants and fusions of DC with tumor cells (48). Alternatively, total tumor RNA or mRNA has been used. Several groups have reported that loading RNA-molecules into DC in the context of cancer immunotherapy is both safe and highly efficient (76-81,151,165,166). Moreover, total mRNA can be amplified *in vitro* (151). This could prove to be very relevant for GBM patients, since the amount of tumor tissue available for tumor cell lysate preparation is often limited. Throughout the years, electroporation has emerged as the method of choice to load DC with RNA-molecules, although very little uniformity exists with regards to electroporation conditions (81,167). This part of the study focuses on both technical issues related to RNA-loading of DC as well as on functional validation of these cells in the context of GBM immunotherapy.

4.2. Specific aims

- To perform an ***in vitro*** **feasibility study** on **loading of DC with foreign RNA (4.3.)**. Expression of DC surface markers, induction of apoptosis, cytokine production, allogeneic stimulatory capacity and reporter gene expression were monitored.
- To investigate whether **DC loaded with tumor-derived RNA** were **functional APC *in vitro***, leading to an antitumor immune response **(4.4.)**. Therefore, T cells were stimulated in vitro by DC loaded with total RNA from glioma cell lines and the cytotoxic effect of stimulated T cells was assessed.
- To evaluate the **efficacy of immunization with RNA-loaded DC in an experimental mouse glioma model (4.5.)**.[1]
- To determine the **specificity of the induced immune response (4.6.)**.[1]

[1] These parts of the study have been published elsewhere in a slightly different format; Maes *et al.* (60).

4.3. Loading DC with foreign RNA-molecules

Out of the wide range of voltage and capacitance settings tested for electroporation of murine BM-derived DC, the best overall results were obtained with an exponential decay pulse of 300 V and 150 µF. Analysis of DC surface marker expression revealed a significant lower expression of B7 costimulatory signals on electroporated DC compared with untouched cells (Figure 4a). The number of dead cells (PI+, Figure 4b) was only slightly higher when analysed 24 h after electroporation, but the yield of electroporated DC was reduced to 71.2 ± 7.92 % of the number of untouched DC (n = 14). The concentration of IL-12p70 in culture supernatant was unchanged between electroporated (190 ± 47.7 pg/ml) and untouched cells (205 ± 61.0 pg/ml) after 24 h pulsing with 1 µg/ml LPS (n = 6). MLR experiments with electroporated and untouched DC as stimulator cells revealed that the capacity to stimulate allogeneic cells was not compromised by electroporation (Figure 4c). Finally, we assessed translation of mRNA into functional proteins by transfecting DC with mRNA encoding EGFP (Figure 4d). The transfection efficiency, determined by the percentage of EGFP+ DC was 72.7 ± 9.32 % (n = 8).

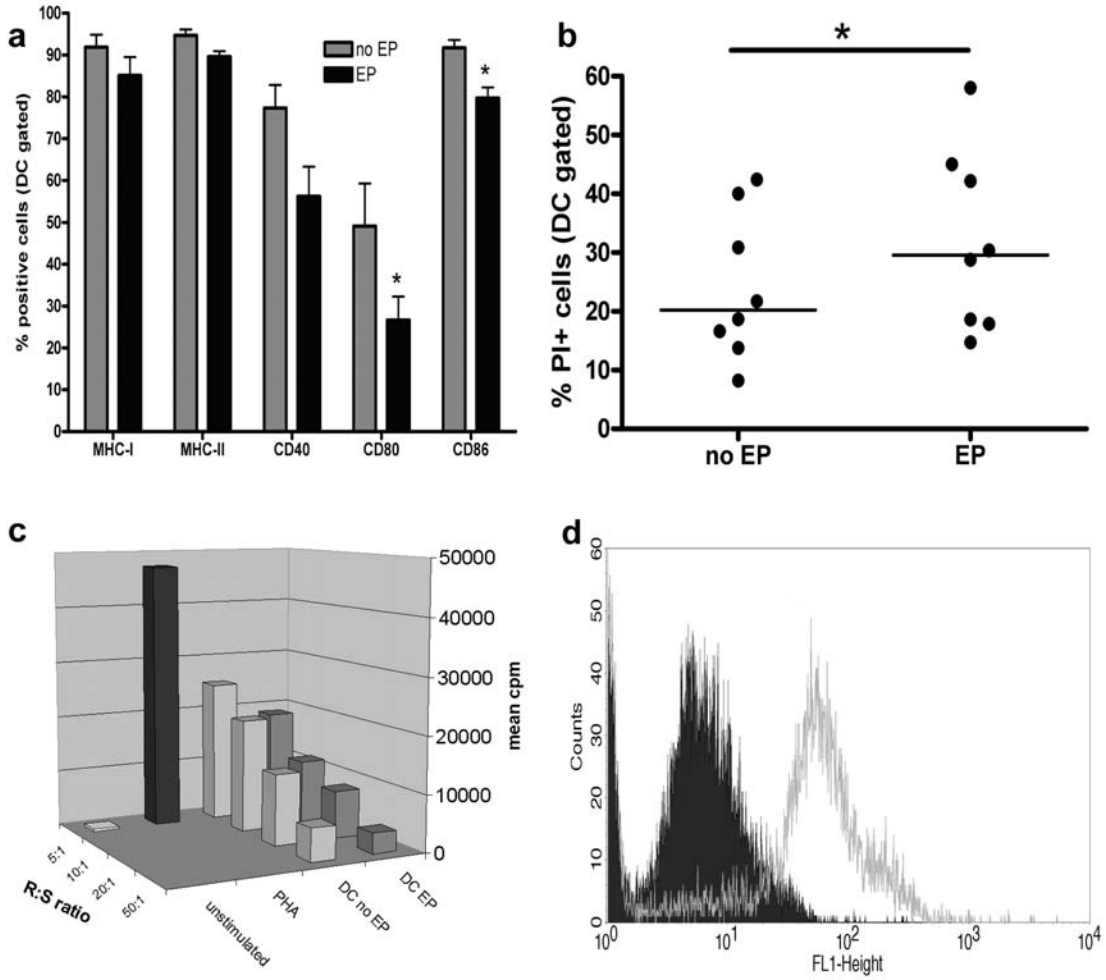

Figure 4. Electroporation of DC with RNA-molecules is feasible without major loss of cell function *in vitro*

Immature DC were left untouched (no EP) or electroporated (EP) and immediately afterwards matured with 1 µg/ml LPS for 24 h. Mature DC (n = 8) were analyzed by flowcytometry for surface marker expression (a) and viability through PI staining (b). The capacity to stimulate allogeneic cells was assessed in an MLR with total splenocytes from naïve BALB/C mice as responder cells. Responder:stimulator ratio (R:S ratio) was either 5:1, 10:1, 20:1 or 50:1. PHA was used as positive control. One representative experiment is shown (n = 3) (c). EGFP reporter gene expression was measured by flowcytometry 24 h after electroporation with 1 µg EGFP-mRNA per million DC (d). Non-electroporated DC were used as control (filled histogram).

4.4. In vitro assessment of tumor RNA-loaded DC as APC

In a murine *in vitro* system, we demonstrated that bone-marrow derived DC, loaded with GL261 tumor antigens in the form of total RNA (DCm-GL261-RNA), were sufficient for the induction of antitumor cytotoxic T cell activity in nylon-wool enriched splenocytes from naïve C57BL/6 mice. As control, unloaded DC (DCm-mock) and DC electroporated with LLC tumor antigens (DCm-LLC-RNA) were used for stimulation of T cells. Flowcytometric characterisation of lymphocytes before and after stimulation revealed pronounced activation on forward and side scatter if the cells were stimulated with DCm, independent of antigen-loading (Figure 5a). This was found to be concomitant with an increase in absolute cell number which was not observed with unstimulated T cells (data not shown). Whereas the percentage of total CD8+ T cells decreased if stimulated with DCm-mock, stimulation with DCm-GL261-RNA restored this population. We observed an increase in CD8+CD25+ fractions between DCm-mock (10.8 ± 0.95 %, $p < 0.05$, $n = 3$) and DCm-GL261-RNA stimulated T cells (26.9 ± 1.68 %, $p < 0.05$) respectively compared with baseline values before stimulation (3.02 ± 0.62 %). Within the CD8+CD25+ T cells, we could distinguish a $CD25^{hi}$ subpopulation, which was clearly upregulated ($p < 0.05$) when DCm-GL261-RNA stimulated T cells (14.8 ± 1.18%) were considered *versus* DCm-mock stimulated T cells (4.02 ± 0.55 %). Functionality of stimulated T cells was addressed after three cycles of *in vitro* stimulation. Therefore, a proliferation assay was performed with DCm-GL261-L as stimulator cells (Figure 5b). Unstimulated and PHA stimulated cells were used as controls. Only T cells that underwent stimulation with DCm-GL261-RNA ($5.65 \pm 1.76 \times 10^3$ cpm, $p < 0.05$, $n = 3$) were able to mount specific proliferation upon restimulation with DCm-GL261-L, whereas baseline T cells (367 ± 64.6 cpm), DCm-LLC-RNA stimulated T cells (530 ± 46.2 cpm) and DCm-mock stimulated T cells (363 ± 38.2 cpm) could not. Co-incubation of GL261 target and effector cells, of which the latter were stimulated by DCm-GL261-RNA (Figure 5c) clearly reduced tumor cell viability (OD 0.47 ± 0.05) compared with untreated target cells (OD 1.37 ± 0.10, $p < 0.001$, $n = 3$). A significant decrease in tumor cell viability was also noted when DCm-mock (OD 0.71 ± 0.12, $p < 0.01$) and DCm-LLC-RNA (OD 0.72 ± 0.05, $p < 0.01$) were used compared with untreated target cells. The immunogenicity of DCm-GL261-L was also tested and induced similar immune responses as compared with stimulation with DCm-GL261-RNA considering the induction of *in vitro* cytotoxicity, T cell phenotype and proliferative capacity (data not shown).

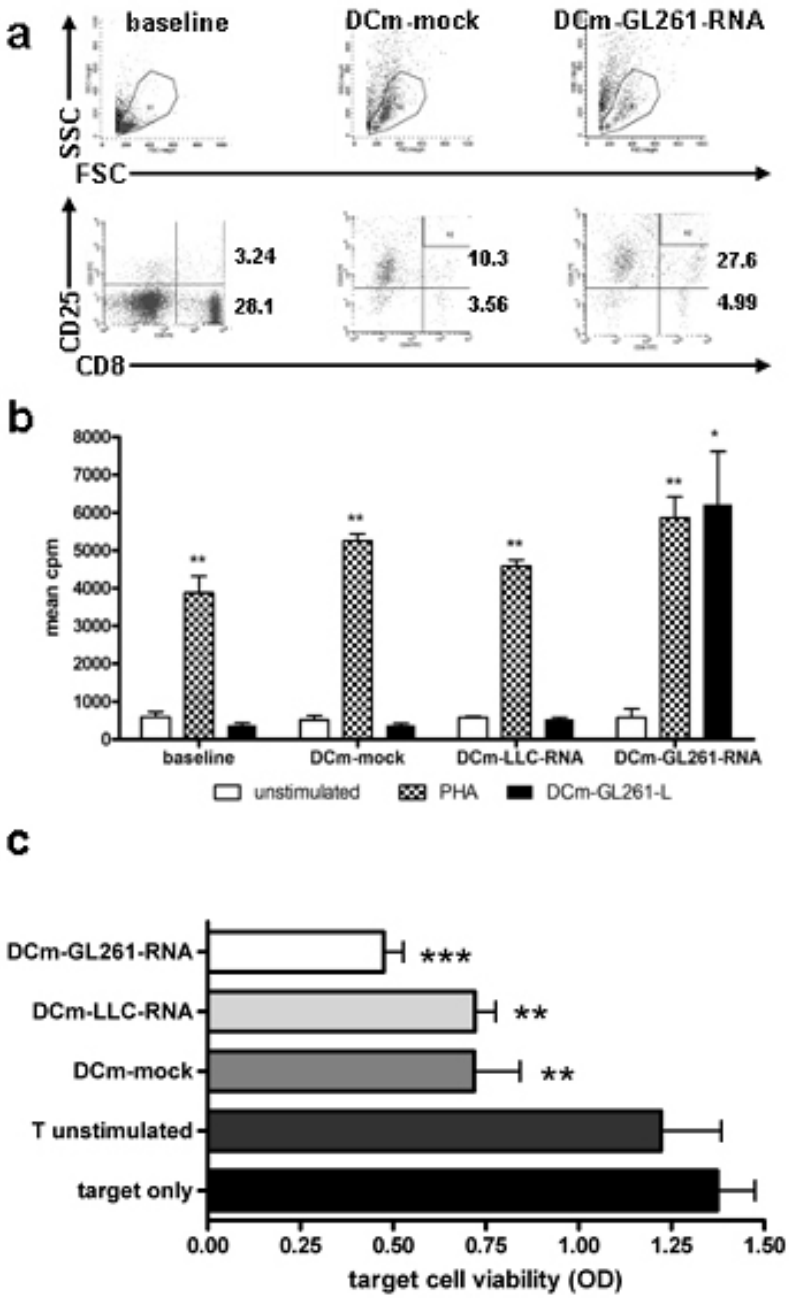

Figure 5. RNA-loaded DC induce a T cell-mediated antitumor immune response *in vitro*

From one representative experiment (n = 3), flowcytometric analysis of T cells prior to stimulation (baseline) and T cells stimulated for two rounds with DCm-mock or DCm-GL261-RNA is shown. Cells were FSC-SSC gated on lymphocytes (R1) and CD25 expression on CD8+ T cells is shown. Quadrants are set based on isotype control stainings. Numbers on dotplots indicate relative cell fractions in respective quadrants. The R2 region is defining CD8+CD25^{hi} cells. (b) Restimulation of primed T cells was performed with DCm-GL261-L. For each group, unstimulated cells and PHA-stimulated cells were used as controls respectively. Responder to stimulator ratio was 10:1. Thymidine incorporation was measured after 4 days of restimulation. Results are represented as mean cpm ± SEM. (c) Stimulated T cells were used as effector cells and co-incubated with GL261 tumor cells in an effector to target ratio of 10:1. Unstimulated T cells were used as control. Tumor cell viability was measured in an MTT assay (OD = optical density) after 2 days of co-culture and compared with target cells without effector cells added. The mean result (± SEM) from 3 independent experiments are shown. Overall ANOVA $p < 0.001$.

In the abovementioned system, we also studied the feasibility of *in vitro* amplification of total mRNA. Therefore, total cellular RNA from the murine GL261 glioma cell line was isolated and subjected to *in vitro* amplification as described by Harris *et al.* (151). The process of *in vitro* total mRNA amplification is depicted in Figure 6a. For one reaction, 1 µg total GL261 RNA was used as input. The yield of amplified total cellular mRNA was 12.4 ± 1.72 µg per µg cDNA. In our hands, loading of DC with amplified cellular GL261 mRNA (cRNA) did not result in a more efficient *in vitro* induction of cytotoxic T cell activity compared with loading with total cellular GL261 RNA within the same experiment (n = 2, Figure 6b).

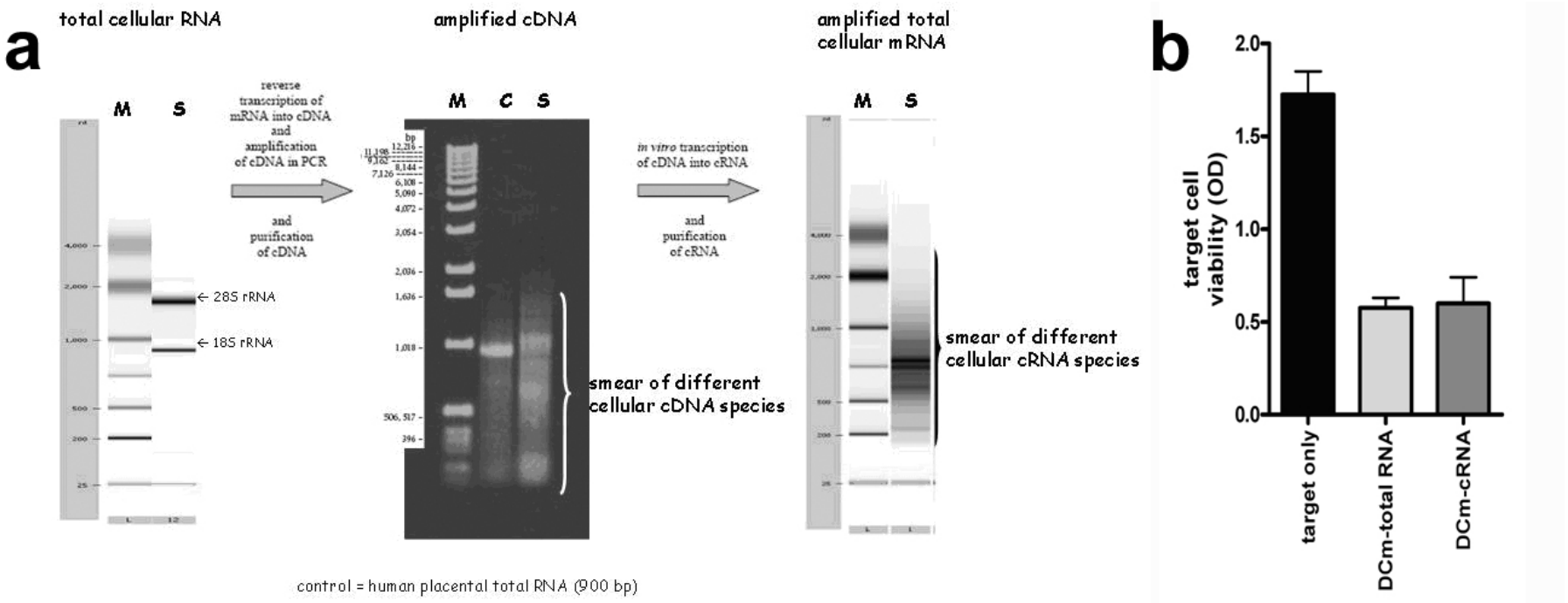

Figure 6. Amplification of total cellular mRNA.

(a) Concept. In the left panel, the gel picture of total cellular RNA isolated from the GL261 murine glioma cell line is shown. In the sample (S), the two thick bands correspond to the large (28S) and small (18S) ribosomal RNA species. RNA integrity was not compromised by the isolation procedure. M = marker. Only mRNA was reverse transcribed into cDNA. In the middle panel, a smear of different cellular cDNA species after amplification and purification is shown. The cDNA was then *in vitro* transcribed into cRNA. In the right panel, a smear of different cellular cRNA species is depicted, i.e. amplified total cellular mRNA. (b) T cells were stimulated with DC loaded with either total GL261 RNA or GL261 cRNA and co-incubated with GL261 target cells in an effector to target ratio of 10:1. Target cell viability was measured in an MTT-assay after 2 days of co-culture.

4.5. Prophylactic vaccination with RNA-loaded DC induces a protective antitumor immune response in vivo

We implemented RNA-loaded DC immunotherapy in an established IC mouse glioma model (168;169). Using a preventive treatment strategy consisting of two vaccinations with DCm-GL261-RNA before tumor challenge (Figure 7a), we observed a significant increase in median survival (Figure 7b) compared with untreated animals (21 *versus* 35 days, $p < 0.001$). Interestingly, vaccination with DCm-mock (26 days, $p < 0.001$), DCm-LLC-RNA (29.5 days, $p < 0.001$) and DCm-splenocyte-RNA (24 days, $p = 0.04$) also shifted median survival significantly as compared with untreated animals. However, when compared with DCm-mock, only GL261 RNA-loading of DC yielded a significant ($p < 0.01$) better survival and protected 12 out of 26 animals (46.2 %) from tumor development. No protection was observed in untreated animals and animals treated with DCm-mock, DCm-LLC-RNA or DCm-splenocyte-RNA. In some experiments, mice responding to DCm-GL261-RNA treatment were followed up to five months after tumor challenge and no relapse was noted. Consistently with overall survival, mapping of the tumor-induced neurologic deficits (Figure 7c) revealed not only a more pronounced clinical manifestation but also an earlier ($p < 0.01$) onset of symptoms in untreated animals (18.0 ± 0.82 days) compared with DCm-GL261-RNA treated animals (29.2 ± 2.21 days). Loss of body weight to less than 80 % of the initial weight coincided with the onset of neurologic deficit (data not shown). Histological analysis on day 14 after tumor challenge showed infiltrating immune cells into the tumor bed in animals that received DCm-GL261-RNA treatment (Figure 7d, left picture), whereas this phenomenon was absent or much less pronounced in untreated mice. Comparison of brain slides of untreated moribund (grade 4) mice and animals responding to DCm-GL261-RNA treatment (grade 0), sacrificed on day 21 after tumor challenge showed the massive presence and total absence of tumor cells respectively (Figure 7d, right pictures).

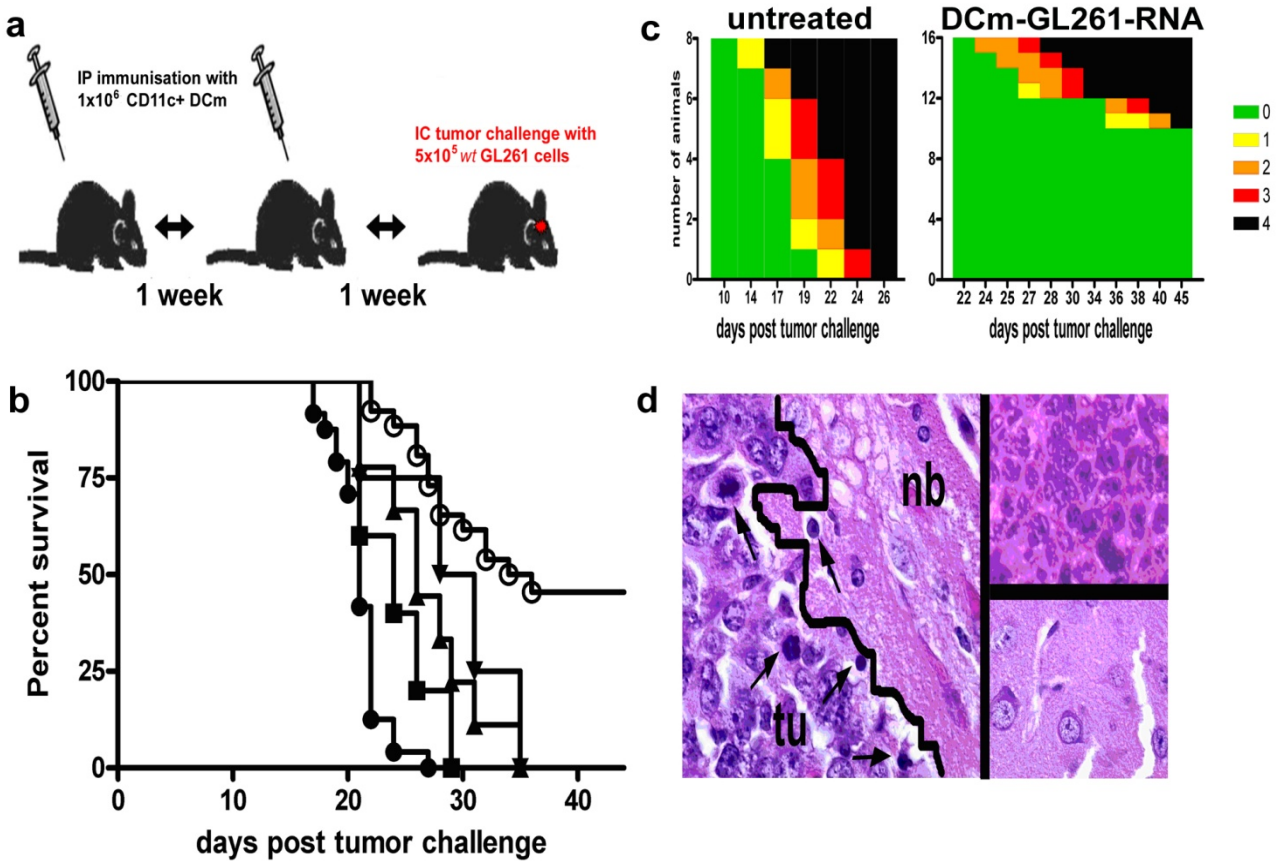

Figure 7. Vaccination with RNA-loaded DC is partially protective against intracranial glioma challenge.

(a) Overview of the DC vaccination model. DCm-GL261-RNA were intraperitoneally injected on day 14 and day 7 before tumor challenge. Tumor challenge consisted of intracranial implantation of 5 x 10^5 GL261 tumor cells under stereotaxic guidance. (b) Survival data represented as Kaplan-Meier graph of pooled experiments. Overall Logrank $p < 0.0001$. Survival curves of animals vaccinated with DCm-GL261-RNA (○, n = 25), DCm-mock (▲, n = 9), DCm-LLC-RNA (▼, n = 4), DCm-splenocyte-RNA (■, n = 5) and untreated animals (●, n = 24) are depicted. (c) The tumor-induced neurological deficit is displayed graphically over time by color-coding symptom severity, both for untreated mice (left graph, n = 8) and DCm-GL261-RNA treated mice (right graph, n = 16). Grade 0 (green) = healthy mice, grade 1 (yellow) = slight unilateral paralysis, grade 2 (orange) = moderate unilateral paralysis and/or beginning hunchback, grade 3 (red) = severe unilateral or bilateral paralysis and pronounced hunchback and grade 5 (black) = moribund and/or dead mice. (d) Histological analysis of HE-stained brain slides. Normal brain parenchyma (nb) adjacent to the tumor bed (tu) with infiltration of immune cells (black arrows) on day 14 after tumor challenge from a DCm-GL261-RNA treated animal (left picture). Untreated mouse with progressive disease (upper right picture) and mouse responding to DCm-GL261-RNA treatment (lower right picture). Representative pictures are shown from tissue slides obtained 21 days after tumor challenge.

4.6. Prophylactic DC vaccination results in a tumor-specific cell-mediated immune response

Specificity of the induced immune response was assessed *in vivo* by subcutaneous challenge with either GL261 glioma or MC17-51 fibrosarcoma tumor cells in mice that were treated with DC loaded with either GL261 or MC17-51 RNA (Figure 8a). In GL261 challenged mice, a delay in the onset of subcutaneous tumor growth was noted in DCm-GL261-RNA treated (28.0 ± 1.27 days) but not DCm-MC17-51-RNA treated (19.0 ± 0.41 days) animals, as compared with untreated mice (21.7 ± 1.26 days). Reciprocally, tumor onset in mice that were challenged with MC17-51 fibrosarcoma cells was delayed compared with untreated mice (11.7 ± 0.67 days) if mice were treated with DCm-MC17-51-RNA (21.7 ± 0.48 days) but not if treatment with DCm-GL261-RNA (11.7 ± 0.42 days) was given.

To study the immune status of the animals that received DC treatment, we investigated whether cells responsive to GL261 antigens could be found within the splenocyte and/or tumor dLN cell pools. Therefore, the number of IFN-ã producing cells upon specific *in vitro* restimulation with DCm-GL261-L was measured in an ELISPOT assay. Baseline values obtained prior to treatment did not reveal a significant number of IFN-ã producing cells (data not shown). Compared with untreated animals, DC treated mice displayed a significantly higher number of both IFN-ã producing splenocytes (317 ± 40.9 *versus* 119 ± 10.9, $p < 0.01$) and dLN cells (320 ± 38.3 *versus* 47.7 ± 11.2, $p < 0.001$), when assessed 14 days after subcutaneous tumor challenge (Figure 8b).

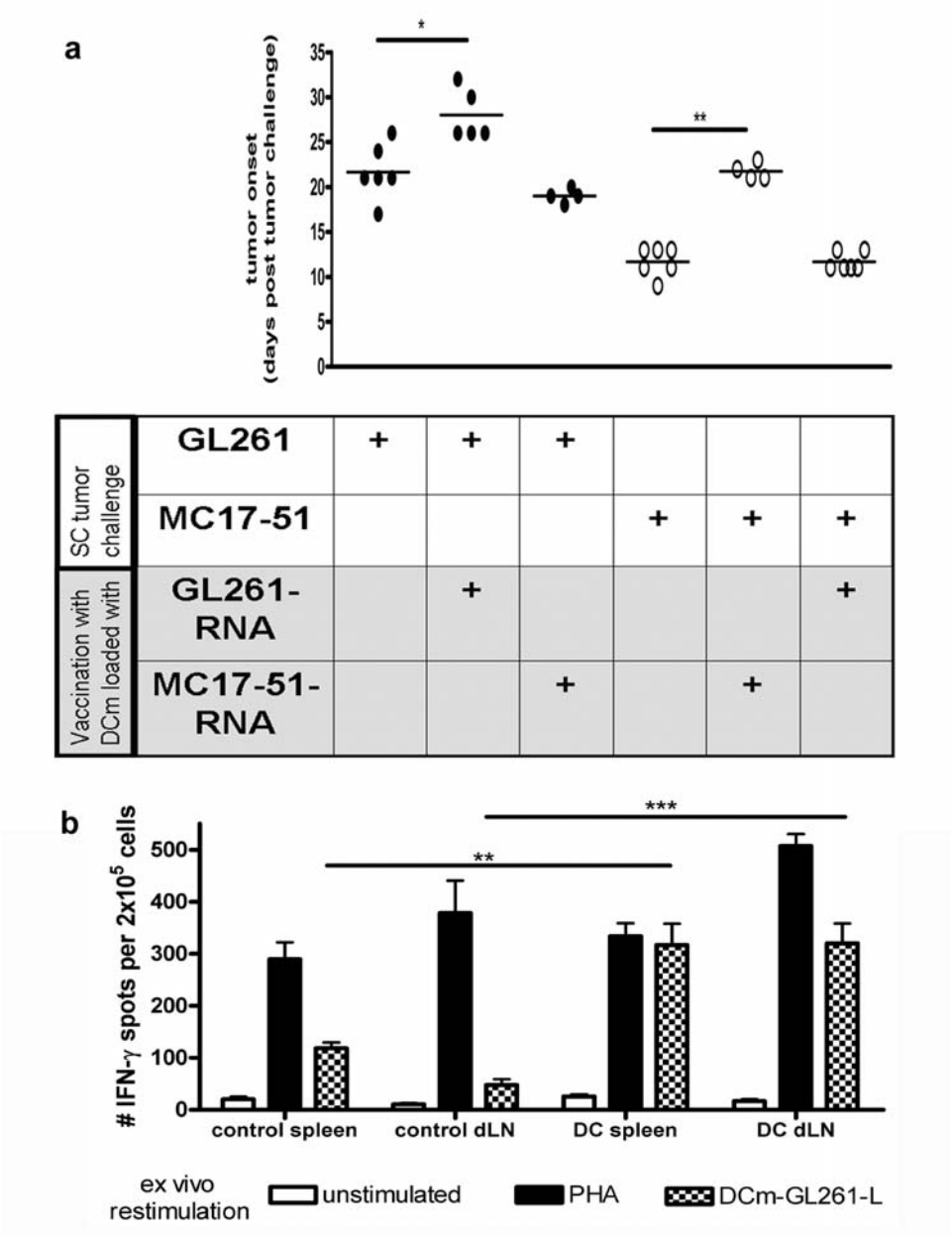

Figure 8. Specificity of DC immunization

(a) Treatment with DCm-GL261-RNA results in a GL261 tumor-specific immune response *in vivo*

Mice were either left untreated or prophylactically treated with DCm-GL261-RNA or DCm-MC17-51-RNA and subsequently subcutaneously challenged with GL261 glioma (●) or MC17-51 fibrosarcoma (○) cells. The growth of subcutaneous tumors was measured with a caliper. For each group, the onset (in days *post* tumor challenge) of a detectable tumor mass is depicted.

(b) *Ex vivo* assessment of specific immunization by treatment with DCm-GL261-RNA

Fourteen days after tumor challenge, pooled splenocytes and dLN cells from either DCm-GL261-RNA vaccinated ("DC", n = 8) or untreated ("control", n = 8) mice were restimulated *ex vivo* for 36 h with DCm-GL261-L or PHA. Cells that were left unstimulated were used as background within the assay. The production of IFN-ã was measured with ELISPOT. Data are represented as mean ± SEM number of IFN-ã spots per 2 x 10^5 cells in triplicate cultures.

4.7. Discussion

In this chapter, we delivered proof that immunotherapy directed against experimental glioma with RNA-loaded DC is technically feasible and scientifically meaningful. We first tried to monitor critical aspects of in vitro DC function and demonstrated that although not unaltered, electroporation does not compromise their main characteristics. These results are in accordance with data published by others (79-81). Initial proof of concept was obtained by eliciting a primary tumor-specific cytotoxic T cell-mediated response from a pool of naive T cells through stimulation with DCm-GL261-RNA. Robust proof of concept could be obtained in the *in vivo* mouse GL261 glioma model, where DCm-GL261-RNA treatment resulted in prolonged median survival and even fully protect nearly half of the mice, in contrast to any of the control conditions. Finally, as indicated further in this dissertation, the brain-infiltrating lymphocytes have a specific cytotoxic activity against GL261 tumor cells but not against LLC tumor cells (see 6.6.1.).

One of the central hallmarks of active immunotherapy is the specificity of the anti-tumoral immune response, which contrasts to non-specific immune stimulations upon administration of cytokines (44). In our *in vitro* cultures, however, DCm-mock- and DCm-LLC-RNA-stimulated T cells were also capable of reducing GL261 tumor cell viability. This background and non-specific reactivity might partly be explained as a consequence of the repetitive rIL-2 additions to the cultures and/or by a so-called autologous MLR phenomenon resulting in aspecific lymphocyte activity as previously described by our group in human *in vitro* stimulation experiments (58,168). The strongest evidence of the in vitro induction of tumor-specific T cells was obtained through T cell proliferation upon restimulation of DCm-GL261-RNA primed T cells with lysate-loaded DC and through analysis of the *ex vivo* specific cytotoxic activity of brain-infiltrating lymphocytes after vaccination of mice (see 6.6.1.). In our *in vivo* model, specificity was demonstrated by challenging DCm-GL261-RNA treated mice with an immunogenic fibrosarcoma cell line which is embryologically unrelated to glial tumors, or *vice versa* by challenging DCm-MC17-51-RNA treated mice with GL261 tumor cells. In both cases the DC-mediated immunity against the target tumor resulted in a delay of growth of the target tumor in sharp contrast to the unchanged growth rate of the non-targeted tumor. Treatment with DCm-LCC-RNA and DCm-splenocyte-RNA also resulted in a prolonged median survival of glioma-bearing mice as compared with untreated mice. A similar finding was observed in the group of mice treated with DCm-mock. We postulate that the induction of a minor immune response upon tumor challenge itself might be boosted in a non-specific manner by administration of activated DC. In none of these control conditions, however,

tumor challenged mice survived, pointing to the specific immunological protective effect of DCm-GL261-RNA treatment.

In clinical practice, DC loaded with total RNA or mRNA have been used for different types of malignancy, including renal cell carcinoma (169), prostate cancer (170), melanoma (171,172), colon cancer (77), pediatric brain tumors (173,174) and malignant glioma (156). The number of patients treated in these pilot studies is very limited and most patients are in an advanced stage of disease, which compromises the drawing of conclusions on objective clinical response and immunological response. In this work, we implemented total RNA-loading of DC in our experimental glioma model and demonstrated its efficiency.

An important advantage of opting for loading DC with RNA as source of tumor Ag is that total cellular mRNA can be amplified *ex vivo* to a virtually unlimited extent. This might be of particular interest for GBM immunotherapy for which the amount of available tumor material is often a limiting factor. Briefly, the commercially available systems for total mRNA amplification encompass the reverse transcription of all polyA+ cellular RNA species into cDNA. Subsequently, the PCR-amplified cDNA species are *in vitro* transcribed into mRNA by the SP6 or T7 bacteriophage RNA polymerase. These methods have been optimized throughout the years, yielding now 100 % of amplified sense cRNA (151). However, this method is labour-intensive and costly when aimed to be performed under good manufacturing practice conditions for clinical use (172,175). Since the portion of mRNA or antigen-encoding RNA species is very small within an eukaryotic cell (less than 10 % of total RNA content), one could assume that either enrichment for mRNA or mRNA amplification would be necessary for DC loading. In our hands, we were able to load DC with total cellular RNA. Moreover, loading with amplified RNA did not result in a more favourable outcome in terms of cytotoxic T cell induction. This is in line with one of the pioneering reports in the field of DC loading with RNA species by Boczkowski *et al*., revealing similar activity between DC loaded with total or polyA+ RNA (76). The above mentioned *in vitro* results are in general accordance with data published by others regarding immunotherapy based on RNA-loaded DC against glioma but also many other types of cancer (155,176,177).

We studied the concept of glioma immunotherapy with *ex vivo* total RNA-loaded DC in an experimental GL261 mouse glioma model (178). We opted for prophylactic treatment since others reported the very aggressive nature of the GL261 model, necessitating additional intervention in curative settings (96,179). Curative treatment with tumor lysate-loaded DC in this model has shown to be ineffective, probably because the immune response is too slow to generate sufficient numbers of immune cells with highly avid recognition of tumor antigens that are able to control

the rapidly growing intracranial tumors. Another presumable explanation for failure of curative DC therapy is the active and potent suppression of activated T cells by a variety of tumor-induced mechanisms. Moreover, this model reflects the clinical therapeutic setting in which DC vaccination is given at a stage of minimal residual disease after (sub)total resection and not at the time of bulky disease (59,63). Vaccination with DCm-GL261-RNA prolonged survival and could fully protect nearly half of the treated animals against subsequent tumor challenge. Since no real "gold standard" treatment is available in this experimental setting, we compared the relative *in vivo* potency of the RNA-loaded DC to DC that were pulsed with tumor lysate. Completely similar to DCm-RNA treatment, prophylactic immunization with lysate-loaded DC resulted in both a significant shift in median survival and protection of half of the treated animals against subsequent tumor challenge (180). Mapping of weight loss and tumor-induced neurologic deficit clearly underscored the survival data. Finally, histological analysis revealed that DCm-GL261-RNA vaccination resulted in infiltration of lymphocytes and non-lymphoid cells, in particular at the interface of the tumor mass with the normal brain parenchyma. These findings are in correlation with the data previously reported by Insug *et al.* (143).

The stimulated status of the immune system of DCm-GL261-RNA vaccinated animals was shown by specific *ex vivo* restimulation of splenocytes and dLN cells. Splenocytes and dLN cells responding to GL261 antigens were retrieved in DCm-GL261-RNA treated animals and only to a significantly lower extent in untreated mice. Similar immunomonitoring has been reported by Grauer *et al.*, using IFN-γ pretreated and irradiated tumor cells for *ex vivo* restimulation instead of tumor antigen-loaded DC (98).

Applying our current treatment, only half of the treated mice could be protected. We hypothesize that immunotherapy modulates a delicate balance between immunogenic antitumor and counteracting tolerogenic and/or suppressive mechanisms involved in the antiglioma immune response. This will be further discussed in Chapter 6.

Chapter 5. Bioluminescent imaging in an experimental mouse model for DC immunotherapy against glioma

5.1. Introduction

In experimental cancer research models, imaging has become of crucial importance. Molecular imaging allows visual representation, characterization and quantification of biological processes at the cellular and subcellular level in intact living organisms (181). Amongst different imaging approaches, *in vivo* BLI is a highly sensitive imaging modality for small rodents that is rapid, easily accessible and affordable. Therefore, BLI represents an ideal tool for the evaluation of (new) antineoplastic therapies in mice or rat models (182-185). BLI relies upon the administration of the appropriate substrate to cultured cells or to an animal harboring cells that express luciferase. The most commonly used enzyme-substrate pair is Fluc and D-luciferin. When oxidized by Fluc, D-luciferin emits photons that are able to traverse living tissues and that can subsequently be captured by a CCD camera. Since the pioneering work by Contag *et al*., this technique has become universally accepted for straightforward and high-throughput evaluation of rodent tumor models, thereby extensively facilitating the study of different types of malignancy in their own micro-environment (186-190). The methylcholantrene-induced GL261 mouse glioma model in B6 mice has been studied extensively and is considered as the gold standard syngeneic model for malignant brain tumors in mice (178). In this model, comparison of BLI with other state-of-the-art imaging methods such as computed tomography, magnetic resonance imaging, positron emission tomography, fluorescence reflectance imaging, intravital microscopy and ultrasound has been addressed in detail (191-196). The application of BLI in experimental glioma has been well documented both in the rat 9L gliosarcoma model and in the U87MG model in humanized SCID mice (197-199). The advantages and disadvantages of BLI in rodent brain were recently summarized by Deroose *et al*. (157).

5.2. Specific aims

- To **validate BLI** as semi-quantitative ***in vivo* real-time tumor monitoring tool** for the GL261 brain tumor model **(5.3.)**.[2]
- To address the **correlation between *in vivo* imaging data and clinical findings (5.4.)**.[2]
- To investigate the **value of BLI in the context of DC-based immunotherapy (5.5.)**.[2]

5.3. Validation of BLI to measure luciferase activity in vivo and correlation between in vivo BLI and stereologically determined tumor dimensions

In order to determine whether the *in vivo* measured BLI signal is an adequate measurement of the luciferase activity in the mouse brain in the GL261 glioma model, we correlated the *in vivo* BLI signal with both *ex vivo* BLI values obtained on brain slices and *in vitro* luminometric measurements. Linear regression analysis (Figure 9a) revealed a strong linear correlation between *in vivo* and *ex vivo* BLI ($r^2 = 0.93$; $p < 0.01$; $n = 5$). From the same animals, the *ex vivo* brain slice with the highest BLI value was used to determine luciferase activity *in vitro*. Therefore, frozen brain slices were cut in halves along the midline and mechanically homogenized. Again, a strong linear correlation was found between *ex vivo* BLI and *in vitro* luciferase measurements ($r^2 = 0.95$; $p < 0.01$; $n = 5$). The linear correlation between *in vivo* BLI and *in vitro* luciferase activity was less pronounced ($r^2 = 0.81$; $p < 0.05$; $n = 5$).

Mice that were initially challenged with a high tumor load (more than 5×10^5 cells) revealed midline crossing of the tumor by day 9 after tumor challenge, as demonstrated both by *ex vivo* BLI and *in vitro* luciferase measurements. The migration of tumor cells across the midline towards the contralateral hemisphere could not be detected by *in vivo* BLI (Figure 9b). *Ex vivo* BLI revealed leakage of tumor cells posterior from the site of injection in mice that received a high challenge dose. Taking into consideration the anatomy of the mouse brain, this could occur through the aqueduct of Sylvius which allows cerebrospinal fluid to move from the third to the fourth ventricle. This phenomenon was not detected on *in vivo* imaging frames prior to *ex vivo* BLI, probably due to masking of this subtle effect by the very bright emitting tumor mass at the site of injection. In our hands, the migration of tumor cells seemed strictly limited to the brain ventricle

[2] These parts of the study have been published elsewhere in a slightly different format; Maes *et al.* (61).

system and did not cause metastatic disease since no *in vivo* BLI signal was detected in the spinal column nor at sites outside the CNS (data not shown).

To confirm that the *in vivo* assessment of luciferase activity in GL261 brain tumors is a well-suited semi-quantitative tool to measure the actual tumor burden, we compared our *in vivo* BLI data of established tumors between 11 and 23 days after tumor challenge with the gold standard method, being stereological counting on histological slides (164). First, a strong linear correlation ($r^2 = 0.95$; $p < 0.001$; $n = 10$) was found between *in vivo* BLI and tumor volume determined by the Cavalieri algorithm on serial coronal slides (Figure 9c, left panel). Although we could note a considerable degree of necrosis in intracranial tumors with a volume exceeding 10^{10} µm³, this had only little influence on the strength of the linear relationship between *in vivo* BLI and tumor volume ($r^2 = 0.99$, $p < 0.001$ for linear correlation for the volumes below 10^{10} µm³ *versus* $r^2 = 0.94$, $p < 0.01$ for the volumes above 10^{10} µm³).

Secondly, we performed a retrospective analysis to determine the tumor area in all brain samples (pooled experiments) of which at least three sections through the tumor mass were available. Regression analysis between the largest tumor area of each sample and *in vivo* BLI (Figure 9c, right panel) again yielded a significant linear correlation ($r^2 = 0.77$; $p < 0.001$; $n = 14$).

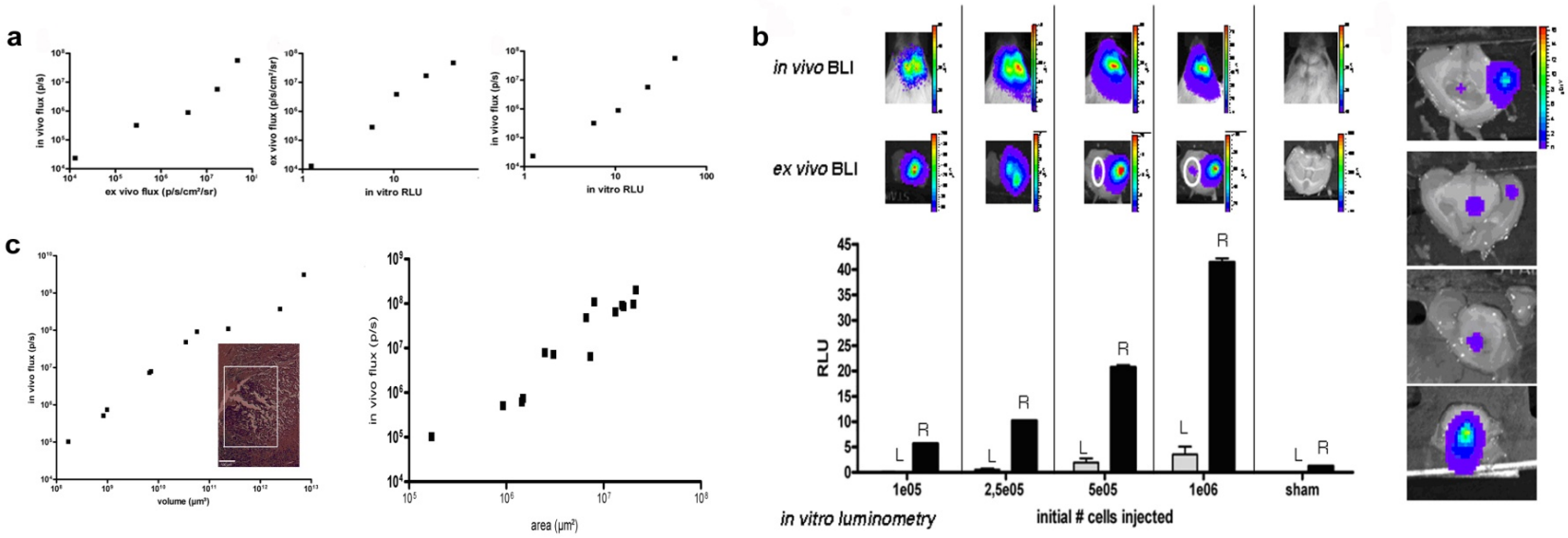

Figure 9. Validation of BLI for *in vivo* luciferase activity and correlation between BLI and stereologically determined tumor dimensions.

(a) Assessment of luciferase activity in GL261 glioma cells with BLI. *In vivo* and *ex vivo* BLI measurements and in vitro luminometric data were correlated. Pearson's correlation coefficients from linear regression analysis were 0.93 ($p < 0.01$; $n = 5$) for *in vivo versus ex vivo* BLI (left panel), 0.95 ($p < 0.01$; $n = 5$) for *ex vivo versus in vitro* RLU (middle panel) and 0.81 ($p < 0.05$; $n = 5$) for *in vivo* BLI *versus in vitro* RLU (right panel).

(b) *Ex vivo* BLI reveals midline crossing of progressing tumors and leakage of tumor cells. Mice initially challenged in the right hemisphere with a high tumor load (more than 5×10^5 GL261 cells) revealed midline crossing of the tumor, 9 days after tumor challenge as demonstrated both by *ex vivo* BLI (signal marked by white ellipse) and *in vitro* luciferase measurements (bar graph). *Ex vivo* BLI revealed leakage of tumor cells posterior from the site of injection in mice challenged with a high tumor load. In the right image frames, *ex vivo* BLI imaging frames on consecutive brain slices from anterior to posterior (top to bottom) are shown from a mouse that received 1×10^6 cells. L,R = left,right hemisphere.

(c) Correlation between *in vivo* BLI measurements and physical dimensions of intracranial GL261 tumors.

Regression analysis showed a strong linear correlation between *in vivo* BLI and tumor volume stereologically determined on serial coronal slides (left panel). HE-staining of massive intracranial tumors randomly obtained between day 11 and 23 after tumor challenge (with tumor volume exceeding 10^{10} µm³) showed substantial necrosis (left panel, inset, white rectangle indicating necrotic area, white bar = 100 µm). Retrospective analysis was performed on brain samples for which at least three different sections through the entire tumor mass were available; regression analysis between the largest tumor area of each sample and *in vivo* BLI (right panel) again yielded a significant linear correlation. All values are represented on a logarithmic scale.

5.4. Monitoring of glioma growth in vivo with BLI and correlation with clinical findings

First, we assessed whether *in vivo* BLI could be applied to monitor subcutaneous GL261 tumor growth. Regression analysis between caliper measured tumor volume and *in vivo* BLI (Figure 10a) showed a moderate linear correlation ($r^2 = 0.65$; $p < 0.01$; $n = 10$). Continued imaging of established subcutaneous tumors with volumes exceeding 1.2×10^3 mm^3 revealed a complete disappearance of *in vivo* BLI signal within the central tumor mass (Figure 10b). On the contrary, tumor cells in the peripheral margins of the tumor were still capable of substrate metabolisation and emission of light. Macroscopic inspection of these large subcutaneous tumor masses revealed a massive central necrotic area (Figure 10c).

To evaluate BLI as *in vivo* monitoring tool for glioma progress *in situ*, we performed a follow-up study in which mice were frequently scanned from the moment of tumor challenge until end-stage disease. Mice were orthotopically challenged with different initial doses of tumor cells, ranging between 1×10^2 and 1×10^6 cells (Figure 10d, amounts lower than 1×10^5 not shown). In all animals that finally developed glioma (except for the mice that received 2.5×10^5 GL261 cells), an initial phase of 10.2 ± 3.25 days was noted characterized by a stable or even decreasing *in vivo* BLI signal (Figure 10d, gray area on graph). This phenomenon was independent of the initial number of tumor cells injected. If *in vivo* BLI values from all experimental groups were compared over time, a higher initial dose of tumor cells did not always correspond to a higher mean peak flux measured later on. Mean peak flux values for each group, measured 14 days after tumor challenge are listed in Table 2, together with the degree of neurological deficit in each group. In our hands, a hundred percent success rate of glioma induction was obtained when mice were intracranially challenged with at least 1×10^5 cells. Challenge with 1×10^4 tumor cells or less was not or at least not always sufficient for induction of glioma, assessed both by *in vivo* BLI and histology (data not shown). Early tumor formation (within the adaptation phase) was histologically compared with established glioma at later timepoint. In virtually all early tumor samples, we noted a pronounced fragmentation of tumor growth in a cluster-like pattern (Figure 10e, upper panel). In contrast, established glioma revealed a central tumor mass clearly delineated from the surrounding brain parenchyma (Figure 9e, lower panel). As control, mice were challenged with 10 µl of cell culture medium (sham) or wt GL261 glioma cells (data not shown).

Next, we tried to link the increasing *in vivo* flux with the development of tumor-induced neurological deficit in diseased animals. Transition in clinical status from grade 0 (healthy) to grade

4 (moribund) corresponded with a mean flux increase of 1.58 ± 0.19 log units, independent of initial tumor load. The onset of clinical deficit showed a clear delay of 5.25 ± 1.13 days compared with the increase in *in vivo* BLI flux.

Initial tumor dose (million cells)	Mean peak flux value (p/s)	Mean peak flux SEM (p/s)	Neurologic deficit				
			Grade 0	Grade 1	Grade 2	Grade 3	Grade 4
sham	4.38×10^4	3.15×10^3	6	0	0	0	0
0.10	2.20×10^6	1.24×10^6	6	0	0	0	0
0.25	5.66×10^6	3.99×10^6	4	1	1	0	0
0.5	5.95×10^6	2.12×10^6	4	2	0	0	0
1	5.19×10^7	3.33×10^7	2	2	1	1	0

Table 2. Follow-up of mice with intracranial glioma challenge: *in vivo* BLI and clinical status

Mice received orthotopic tumor challenge with different doses of tumor cells; respectively 1×10^5, 2.5×10^5, 5×10^5 and 1×10^6. Sham challenged mice received intracranial injection of 10 µl cell culture medium. Mean ± SEM group *in vivo* BLI values are depicted, measured 14 days *post* tumor challenge (n = 6 for each group). For each group, the number of mice exhibiting discrete neurological deficit is shown.

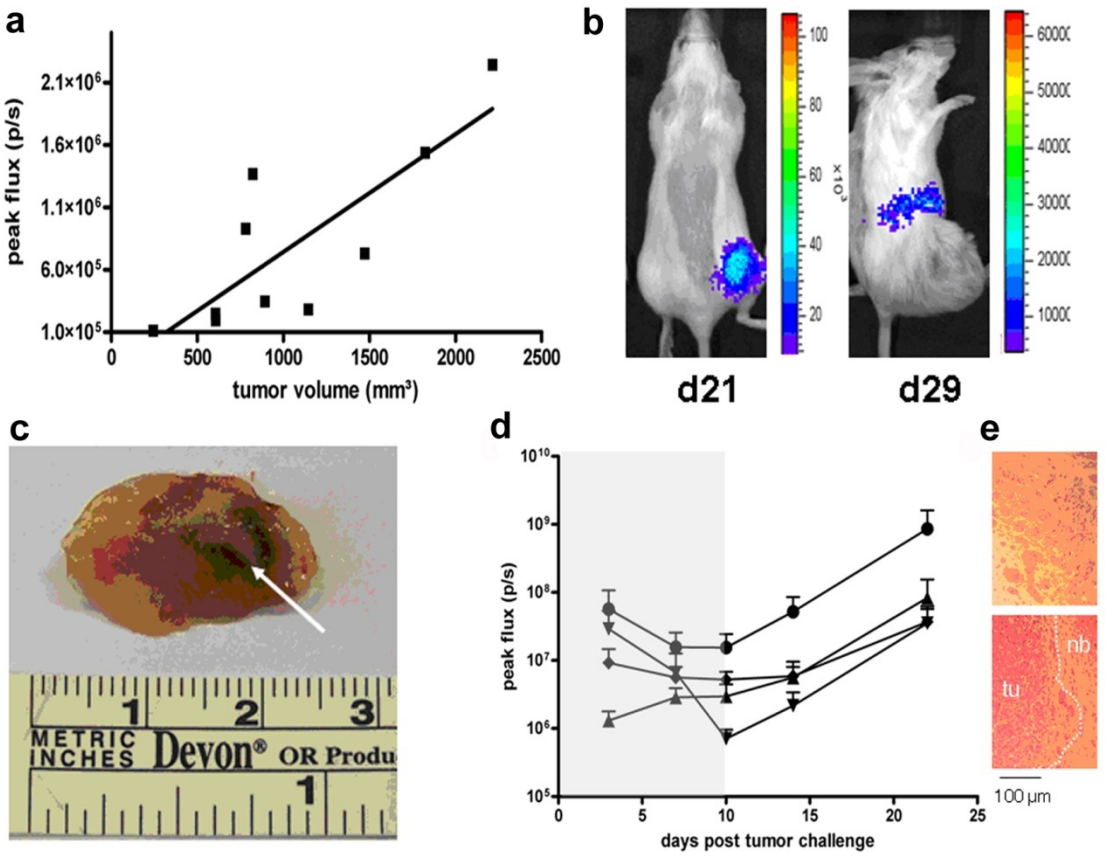

Figure 10. Evaluation of *in vivo* glioma growth and correlation with clinical findings

(a-c) Validation of BLI for a non-orthotopic GL261 glioma model

Caliper measurements of subcutaneous tumor volumes and *in vivo* BLI (a) showed a moderate linear correlation (r^2 = 0.65; $p < 0.01$; n = 10). Upon continued imaging, the *in vivo* BLI signal was completely lost within the central region of subcutaneous tumors with volumes exceeding 1,200 mm³. Tumor cells in the peripheral margins of these tumors were still capable of substrate metabolisation and subsequent emission of light (b, *in vivo* BLI image frames 21 and 29 days *post* tumor challenge respectively). Macroscopic sections of these large subcutaneous tumor masses revealed a massive necrotic area (c, tissue necrosis indicated by arrow).

(d-e) Monitoring of *in vivo* glioma progression with BLI and correlation with clinical findings

Mice received orthotopic tumor challenge with different doses of tumor cells (d), either 1 x 10^5 (▼), 2.5 x 10^5 (▲), 5 x 10^5 (♦) or 1 x 10^6 (●) Fluc transduced GL261 cells. Data are corrected for background light output by subtracting flux values of sham challenged mice from flux values of experimental groups. Sham challenged mice received intracranial injection of 10 µl cell culture medium. Mean group BLI values are depicted for each time point of imaging (n = 6 for each group). In all animals that finally developed glioma within 3 weeks after challenge (except the mice that received 2.5 x 10^5 GL261 cells), an initial tumor adaptation phase of 10.2 ± 3.25 days was noted, characterized by a decreasing or stable *in vivo* BLI signal (filled gray area). Early tumor formation during the adaptation phase is characterized by numerous clustering of tumor cells in the brain parenchyma (e, upper picture, day 4 *post* tumor challenge). Established glioma is noted after the initial adaptation phase (e, lower picture, day 16 *post* tumor challenge) with a clear delineation between tumor (tu) and normal brain parenchyma (nb).

5.5. In vivo BLI measurements are predictive for the response to DC-based immunotherapy

Our final aim in this study was to implement *in vivo* BLI as monitoring tool in an immunotherapy model. For this, prophylactic immunotherapy was performed with murine bone marrow-derived mature DC which were loaded with total GL261 tumor RNA. Whereas implantation of the GL261 tumor cells in untreated control mice revealed a steep and fast increase of the *in vivo* flux over time followed by death within 3 weeks (median survival of 21 days), vaccination with DC revealed different outcomes (Figure 11). A minor fraction (3/10) of the treated mice did not respond to treatment at all and exhibited progressive disease (median survival of 26.5 days, $p = 0.03$ compared with untreated control). Nevertheless, BLI data in 2 of these 3 animals could still be obtained at day 26 *versus* none out of seven untreated mice. Responding mice were either complete responders (4/10) and showed a rapidly decreasing BLI signal that reached background levels by day 10 after tumor challenge. These mice remained in perfectly healthy condition and showed no tumor relapse on *in vivo* BLI up to day 80 after tumor challenge and were hence considered as long-term survivors ($p < 0.01$ compared with untreated control). Interestingly, mice that responded only partially (3/10) to the immunotherapeutic treatment displayed a slow *in vivo* flux decline of 1 log unit after which the signal increased again rapidly. Median survival of the latter subgroup was 47 days ($p < 0.01$ compared with untreated control). Histological analysis of the brain revealed massive tumor burden in control as well as non-responding and partially responding mice. We could not detect any tumor cells in long-term survivors on day 80 after tumor challenge (data not shown).

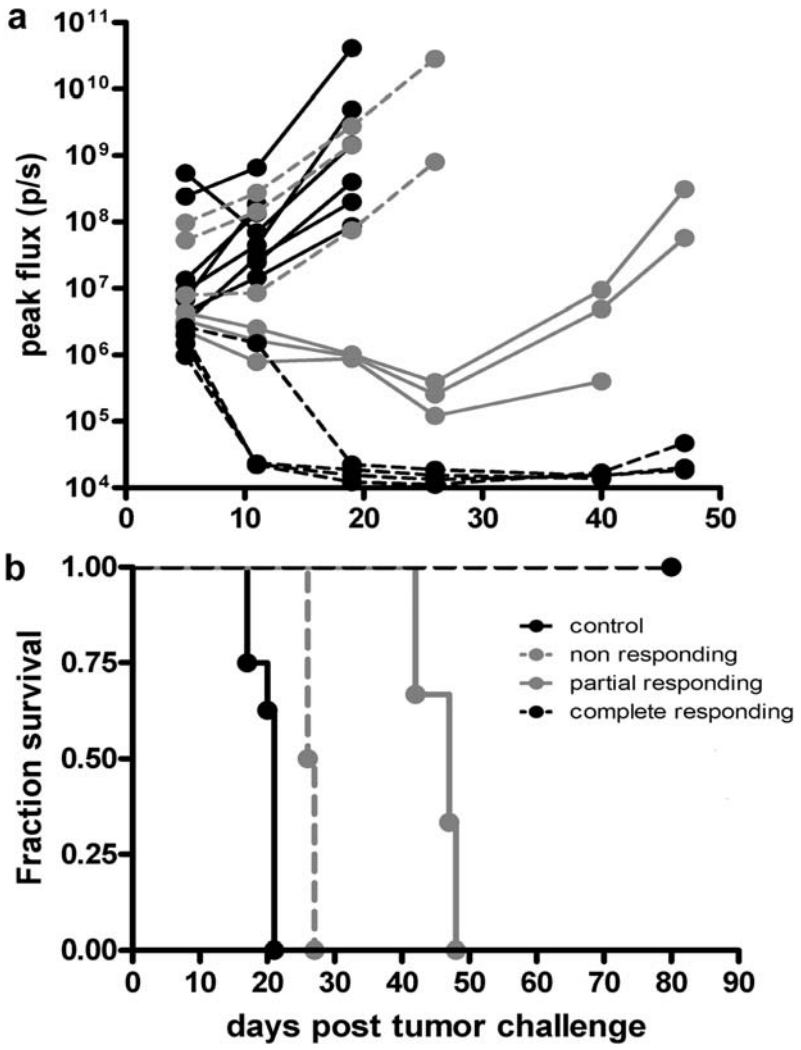

Figure 11. Prediction of response to DC immunotherapy by *in vivo* BLI

In vivo imaging of mice, prophylactically treated with one million DC (loaded with GL261 total RNA) on day 14 and day 7 before tumor challenge, revealed three distinct response patterns; 3/10 mice were unresponsive to treatment (median survival of 26.5 days with $p = 0.03$ compared with untreated control) and displayed a rapid and steep increase of *in vivo* flux (a, dotted grey lines). Two categories of responding mice were observed; 4/10 animals were considered complete responders with long-term survival ($p < 0.01$ compared with untreated control) and displayed a rapid decrease of *in vivo* flux (a, dotted black lines). Partial responders (3/10) were characterized by a temporal decrease of *in vivo* flux with subsequent increase (a, solid grey lines). Median survival of the latter subgroup was 47 days ($p < 0.01$ compared with untreated control). Untreated control mice (a, solid black lines) all died within 3 weeks (median survival of 21 days). Kaplan-Meier survival curves are depicted in panel b. Overall Logrank test p-value = 0.01.

5.6. Discussion

In this study, bioluminescent imaging was established as *in vivo* measuring tool of GL261 glioma load in mice. We further addressed the clinical relevance of *in vivo* generated BLI data, and finally applied this methodology to monitor the response of mice that received immunotherapeutic DC vaccination.

For initial validation of BLI as a semi-quantitative tool to monitor luciferase activity from glioma cells *in vivo*, we compared *in vivo* BLI with *ex vivo* BLI and *in vitro* luciferase measurements. Strong linear correlations were observed between *in vivo* and *ex vivo* BLI values in brain slices on one hand, and *ex vivo* BLI and *in vitro* luminometric data on the other hand. The linear correlation between *in vivo* BLI and *in vitro* luciferase activity was less pronounced. This phenomenon was also observed by Deroose *et al*., who ascribed this effect to experimental error in the procedure of brain extraction (157). Overall, the presented data show that *in vivo* BLI of living mice can be used to detect luciferase activity in GL261 tumor cells in a non-invasive and semi-quantitative way.

From the *ex vivo* BLI and *in vitro* luminometric data, we observed that GL261 tumor cells tend to cross the midline to the contralateral hemisphere, at least when a high initial dose is administered. This might compromise the comparison with the contralateral hemisphere as healthy control within one animal, even at an early time point after tumor challenge. Unexpectedly, leakage of inoculated tumor cells through the ventricular system was noticed if more than 5×10^5 tumor cells were inoculated. This can be due to experimental variability in the stereotactic administration of tumor cells in spite of the standardisation of this procedure. The leakage of tumor cells could partially explain the high variability between *in vivo* BLI measurements in groups of mice initially receiving the same dose of cells. We did not observe formation of metastatic tumors within the spinal cord nor outside the CNS, although GL261 tumors are tumorigenic when subcutaneous challenge is performed (178 and unpublished data).

To obtain a robust validation of *in vivo* BLI as non-invasive and semi-quantitative imaging tool for measurement of the actual tumor burden, we compared this technique with the established gold standard to determine physical dimensions of established tumors on histological slides, namely stereological counting (164). A very strong linear correlation was observed between *in vivo* BLI and tumor volume as computed by the Cavalieri algorithm. When the volume of intracranial tumors exceeded 10^{10} μm^3, pronounced necrotic areas within the tumor mass were noted. Because necrotic cells are no longer capable of light emission, it was expected that this phenomenon would

weaken the strong linearity between *in vivo* BLI and tumor volume but this was not observed in the orthotopic glioma model (153,200). A fairly good linear correlation was also observed between the largest tumor area on coronal sections and the *in vivo* BLI signal from pooled, independent experiments. The linear correlation between tumor area and volume (histologically determined in coronal brain sections) on one hand and *in vivo* BLI values obtained through planar imaging in the horizontal plane on the other hand, is suggestive for a radial growth pattern of the intracranial GL261 tumors. Chemically induced tumors such as the GL261 model only partially mimic the growth characteristics of primary, spontaneously arising tumors in genetically engineered mice and one should definitely keep this in mind when comparing different experimental brain tumor models (140). We also want to point out that BLI is not a genuine quantitative but rather semi-quantitative imaging modality since three-dimensional phenomena are visualized bi-dimensionally and BLI is prone to both attenuation and experimental error. When mice were challenged non-orthotopically and the subcutaneous tumor growth was evaluated both by *in vivo* BLI and through caliper measurements, only a moderate linear correlation was observed. This could be due to the high experimental error of the caliper measurements of tumor diameters together with the rapid and pronounced development of necrosis within subcutaneous tumors. This latter phenomenon was extremely prominent in massive subcutaneous tumors. The more pronounced necrosis observed in subcutaneous tumors compared with intracranial tumors might be partially explained by the relative vessel-poor subcutaneous microenvironment compared with the highly vascularised brain parenchyma (201). Due to the location within the CNS, intracranially challenged animals die from an increased intracranial pressure finally resulting in brain stem impingement. This occurs well before massive necrosis can develop, in sharp contrast to the subcutaneous model, where tumors exceeding even 1,000 mm^3 are not fatal by themselves.

Interestingly, by performing *in vivo* BLI on glioma bearing mice, we discovered that not all of the initially injected GL261 glioma cells adapted equally well to the hostile local environment of the immunocompetent mouse brain. This selective stress on inoculated tumor cells caused the *in vivo* BLI signal to drop early or remain stable until day 10 after tumor challenge. To our belief, this is the first report mentioning a tumor cell adaptation phase which could have important consequences on the outcome of antitumor treatment and in particular on the timing of therapeutic interventions in this model. If the number of inoculated tumor cells was below 1×10^5, too few tumor cells escaped this environmental selection to allow establishment of glial tumors in all of the challenged animals, further supporting the hypothesis of an initial tumor adaptation

phase. Other groups have reported successful induction of intracranial glial tumors using 2 x 10^4 or less GL261 cells, probably due to intrinsic differences in the GL261 tumor cell cultures (148,202). It should be noted that the correlation between *in vivo* BLI and intracranial tumor volume was assessed on samples obtained from well established tumors later than 10 days after challenge. To our view, the typical early cluster-like pattern of GL261 tumor formation complicates stereological determination of tumor volumes but does not impair the use of BLI to monitor tumor burden during the tumor adaptation phase. Therefore, besides the aforementioned considerations on this initial adaptation phase after tumor challenge, BLI is still a well suited monitoring tool to quantify GL261 glioma growth *in vivo*. Long-term follow-up of mice that received different initial tumor challenge doses revealed that mean group *in vivo* flux values are not the most robust parameter to consider. Experimental error during tumor challenge and intrinsic differences between the immunocompetent hosts contribute substantially to this high inter-animal variability.

Our data clearly showed a five day delay between the increase of *in vivo* flux and the onset of neurological impairment. The latter phenomenon is likely due to a gradual increase in intracranial pressure (with only limited compensation mechanisms) finally leading to a rapidly expanding extracellular edema (203). Transition of tumor challenged mice from healthy to the moribund state corresponded with a mean BLI flux increase of 1.5 log units, independent of the initial challenge dose. Therefore we propose that the rate of tumor progression, rather than the initial tumor load is the true causative factor for development of neurological deficit.

In the context of immunotherapeutic interventions, it can be postulated that Fluc itself is not immunogenic, in contrast to other cell markers like green fluorescent protein (GFP). The poor immunogenicity of luciferase has been clearly demonstrated by Hakamata *et al.* in a skin grafting test. The authors noted long-term (> 100 days) acceptance of skin grafts from luciferase-transgenic rats on wild-type rats, whereas this was less than 10 days if grafts from GFP transgenic rats were used (204). Moreover, mice that were challenged with wild-type GL261 cells display a parallel pattern of disease progression to the animals that received luciferase transgenic GL261 cells (data not shown).

Finally, we evaluated the implementation of *in vivo* BLI in our model to monitor the response of mice to prophylactic DC immunotherapy. Our *in vivo* BLI data underscore the relevance of *in vivo* BLI for evaluation of experimental antineoplastic treatments such as DC immunotherapy. Mice that were considered complete responders to therapy displayed an *in vivo* flux rapidly decreasing to background levels. Partial responders showed only temporarily a slow and moderate decrease

of *in vivo* BLI signal and subsequently exhibited progressive fatal disease with a prolonged median survival, compared with non-responding mice. From these data, we conclude that *in vivo* BLI imaging is a predictive monitoring tool for the therapeutic outcome of DC-based immunotherapy in the GL261 glioma model.

Chapter 6. Study of the balance between antitumor immunity and immune suppression in experimental murine glioma

6.1. Introduction

Escape from immunosurveillance is considered as one of the hallmarks of malignant cell growth and several mechanisms leading to immune suppression or immune escape have been described in this perspective (37). On the other hand, it is generally accepted that a patient's immune system can be instructed to recognise and attack several types of malignant lesions – including GBM – more efficiently (205). Results of *in vitro* experiments and animal studies, together with pilot data from clinical trials, are very promising although it is still too early to draw definitive conclusions (57-63).

Orthotopic rodent glioma models are highly useful to address fundamental questions regarding the balance between pro- and anti-immunogenic cellular mechanisms in a standardized way (206-208). Some of these pertinent issues will be addressed in this part of the study.

Regulatory T cells (Treg), a subpopulation of CD4+ T cells that constitutively express the transcription factor FoxP3, the high affinity IL-2 receptor and the B7 ligand cytotoxic T lymphocyte-associated antigen 4 (CTLA-4 or CD154), are required for the maintenance of tolerance throughout the lifetime of an organism and are believed to represent key players in tumor immunology as well (209,210). It has been shown by others that CD4+CD25+FoxP3+ Treg accumulate in murine and human glioma during tumor progression and those cells are potent suppressors of anti-glioma immune responses *in vivo* (98). Hence, Treg are becoming an important target in cancer immunotherapy. Since no unique surface marker has been determined yet for Treg, *in vivo* depletion of this cell population in murine models is mainly based on rather non-specific interventions with mAb targeting CD25 (i.e. the alpha chain of the IL-2 receptor), which can also be expressed on activated lymphocytes. Other reports have shown that Treg depletion can lead to an anti-tumor effect in murine neuroblastoma and glioma models (207,211).

For all cancer patients, preventing tumor relapse is crucial. Unfortunately for GBM, total tumor clearance or long-term control is currently still far beyond reach. Therefore, it is definitely worthwhile to investigate in an experimental setting how immunotherapy can lead to persistent protection against tumor relapse.

Within the field of cancer immunotherapy, innate immune cells such as TAM or MDSC have recently drawn the attention of many researchers. After being neglected for a long time, these cells now claim a more prominent role in the overall picture of tumor immunology and should definitely be taken into account when coming in with immunotherapy (108-111).

6.2. Specific aims

To dissect the mechanisms between immunogenic and immunosuppressive cellular processes in the context of DC immunotherapy for experimental glioma.

- To investigate the **role of CD8+ T lymphocytes** in our model by depleting CD8a+ cells *in vivo* **(6.3)**.[3]
- To **boost antitumor immunity by *in vivo* elimination of CD25+ Treg (6.4)**. [3]
- To study whether DC vaccination and/or Treg depletion could lead to **persistent immunological protection** against intracranial glioma. Therefore, **re-challenge** experiments were performed **(6.5)**. [3]
- To **characterize in detail the brain-infiltrating cells** in tumor-bearing mice **(6.6.)**. [3]

6.3. CD8+ T cells are essential for the endogenous and vaccine-induced antitumor immune response

Since RNA-loaded DC are considered to act primarily through priming of CD8+ T cells, prophylactic DCm-GL261-RNA treatment was combined with depletion of CD8+ T cells at time of tumor challenge to study their *in vivo* role in our model. Survival (Figure 12a) was significantly shortened (median survival of 18 days, $p < 0.001$) in mice in which CD8+ T cells were depleted compared with mice that received tumor challenge only (median survival of 22 days). Treatment with DCm-GL261-RNA induced immunological protection and prolonged median survival to 45 days ($p < 0.001$ compared with untreated mice), whereas CD8+ T cell depletion in DCm-GL261-RNA vaccinated mice shortened median survival (28 days; $p = 0.02$ compared with DCm-GL261-RNA vaccinated

[3] These parts of the study have been published elsewhere in a slightly different format; Maes *et al.* (60).

mice). The median survival of DCm-GL261-RNA treated CD8-depleted mice was significantly longer as compared with untreated CD8-depleted mice (28 days *versus* 18 days, $p < 0.001$). Interestingly, whereas DCm-GL261-RNA treatment was sufficient to protect over 40% of animals from glioma development, the combination of DCm-GL261-RNA treatment with depletion of CD8+ T cells resulted in 100 % mortality. Efficiency of depletion was monitored over time and exceeded 90 % when measured in cervical dLN 8 days after depletion (Figure 12b) and CD8+ T cell numbers returned to normal values by day 15 (data not shown). To exclude a major impact of CD8α+ cell depletion on the prophylactically administered DC, the expression of CD8α on *ex vivo* generated DC was measured by indirect staining with unlabeled anti-CD8 mAb YTS169 followed by GAR:FITC. The expression of CD8α on DC was 9.02 ± 1.25 % (data not shown). Injection of control mice with polyclonal rat IgG at time of tumor challenge did not affect survival or the percentage of systemic CD8+ T cells (data not shown).

6.4. Anti-CD25 treatment is dominant to treatment with DC vaccination

It has been well documented in experimental rodent models that malignancy recruits and expands Treg to decrease endogenous antitumor responses. In our model, FoxP3- expression among CD4+ splenocytes was assessed to investigate the influence of DC treatment on Treg. After two rounds of immunization with DCm-GL261-RNA but prior to tumor challenge, no differences in percentage of CD25+FoxP3+ cells within the CD4+ splenocyte population were noted compared with naïve animals. In contrast, 14 days after tumor challenge, prophylactic DCm-GL261-RNA treatment resulted in a significant increase in splenic Treg compared with naïve animals (11.9 ± 0.32 % *versus* 7.35 ± 0.19 %, $p < 0.01$, $n = 5$). In untreated mice, an increase in Treg upon tumor challenge was also noted compared with naïve mice, although to a lesser extent (9.54 ± 0.31 %, $p < 0.05$, $n = 5$). Hence, these data represented the rationale to perform a series of experiments in which Treg were depleted *in vivo* prior to DCm-GL261-RNA treatment. We observed that independent of treatment with DCm-GL261-RNA, the injection of anti-CD25 (Figure 13) was able to rescue all tumor challenged animals ($p < 0.001$, $n = 7$). Depletion efficiency was monitored in peripheral blood 4 days prior and 10 days after tumor challenge (respectively 17 and 31 days after CD25 depletion). Whereas CD25+ cells were still significantly downregulated 4 days before tumor

challenge in anti-CD25 treated mice or mice that received combined treatment compared with naïve animals, a normalization was noted by day 10 after tumor challenge (Table 3).

Strikingly, whereas the percentage of splenic CD25-expressing CD4+ lymphocytes was 9.37 ± 0.38 % in naïve littermates, it was still significantly decreased in anti-CD25 treated mice (0.80 ± 0.08 %, $p < 0.001$, $n = 5$) 14 days after tumor challenge. However, DCm-GL261-RNA vaccination after CD25 depletion nearly completely rescued the CD25-expressing CD4+ cells (8.09 ± 0.13 %, $p < 0.001$, $n = 5$) compared with anti-CD25 treatment only. Moreover, a substantial fraction (3.35 ± 0.72 %) of the restored CD25+CD4+ splenic T cells by combined treatment expressed the Treg transcription factor FoxP3 compared with 0.65 ± 0.14 % for mice that received anti-CD25 treatment only ($p < 0.001$, $n = 5$). The total number of splenic CD4+ T cells was not significantly different between groups (data not shown). The GL261 glioma cells did not express CD25 themselves (data not shown). Prophylactic injection with polyclonal rat IgG of mice that were subsequently challenged with glioma did not affect survival or the percentage of systemic CD25+ cells (data not shown).

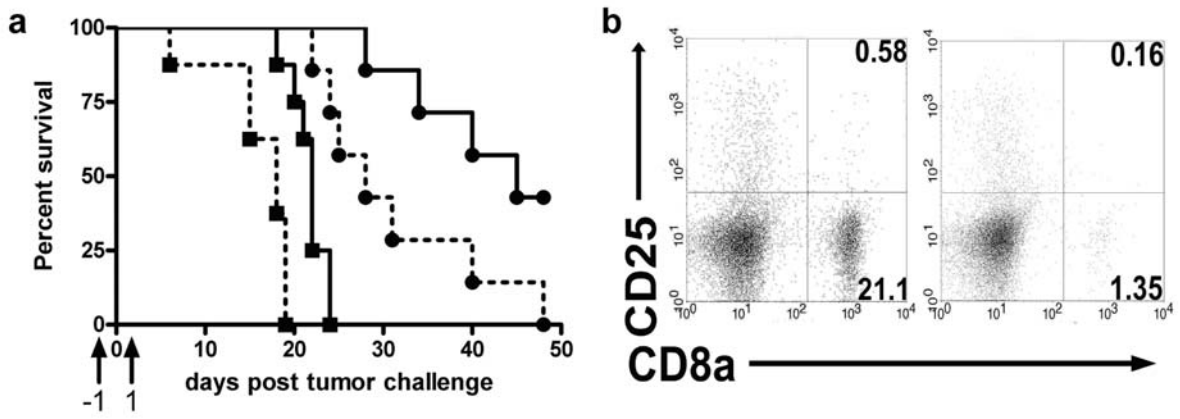

Figure 12. Involvement of CD8+ T cells in the endogenous and vaccine-mediated antitumor immune response

Mice were left untreated or received prophylactic treatment with DCm-GL261-RNA. At time of tumor challenge, CD8a+ T cells were depleted by intraperitoneal injection of the YTS169 anti-CD8α mAb. Animals that were not CD8a-depleted were used as controls (a) Survival data from pooled experiments are shown for untreated mice (■, solid line, n = 8), CD8a-depleted mice (■, dashed line, n = 8), vaccinated mice (●, solid line, n = 7) and mice that received vaccination and were CD8a-depleted (●, dashed line, n = 7). Overall Logrank $p < 0.0001$. Arrows on graph indicate timing of administration of the anti-CD8a mAb. (b) Draining lymph node cells were analysed for CD8α and CD25 expression 7 days after tumor challenge in non-depleted (left) and CD8a-depleted mice (right). Numbers on dotplots indicate relative cell fractions in respective quadrants. A lymphocyte gate was set for the analysis.

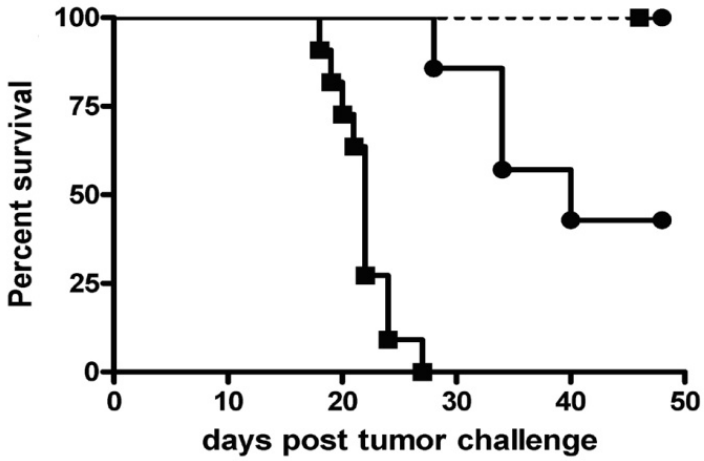

Figure 13. *In vivo* depletion of CD25+ cells is protective against subsequent tumor challenge and is dominant to DC vaccination.

In order to eliminate CD25+ Treg *in vivo*, mice received a single intraperitoneal administration of the anti-CD25 mAb PC61, one week before treatment with DCm-GL261-RNA.Kaplan-Meier graph from pooled experiments depicting survival of untreated mice (■, solid line, n = 11), CD25-depleted mice (■, dashed line, n = 7), DCm-GL261-RNA vaccinated mice (●, solid line, n = 7) and mice treated with CD25 depletion and DCm-GL261-RNA vaccination (●, dashed line, n = 6). Overall Logrank $p < 0.001$.

% CD25+ blood lymphocytes	day 4 before TC	day 10 post TC
naive	2.38 ± 0.13	2.57 ± 0.02
TC	na	1.85 ± 0.05
aCD25 + TC	0.80 ± 0.04 (***)	2.48 ± 0.03
DC + TC	3.68 ± 0.29 (**)	3.41 ± 0.11 (**)
aCD25 + DC + TC	1.26 ± 0.10 (**)	2.58 ± 0.08

Table 3. Monitoring of CD25 on circulating lymphocytes. In blood samples obtained 4 days before and 10 days after tumor challenge, the expression of CD25 was analyzed on lymphocytes. Results are shown as mean ± SEM (for each experimental group, n =5). Percent of CD25-expression was calculated by gating on lymphocytes (na = non applicable).

6.5. DC vaccination but not prophylactic depletion of CD25+ lymphocytes induces long-lasting antitumor immunity

Intracranial re-challenge of long-term survivors after first tumor challenge revealed that initial depletion of CD25+ T cells was not sufficient to maintain immunological protection since the median survival of 19.5 days after re-challenge in these mice was comparable with median survival of untreated animals upon first challenge and since all of these animals also died (Figure 14). On the other hand, anti-CD25 treatment with DCm-GL261-RNA vaccination resulted in protection of 50 % of the animals (3 out of 6) and median survival was significantly prolonged (63.5 days *versus* 21 days for untreated animals, $p < 0.01$). Similarly, 3 out of 7 long-term surviving mice that received only DCm-GL261-RNA vaccination before primary challenge were also protected (median survival of 54 days, $p < 0.001$ compared with untreated mice).

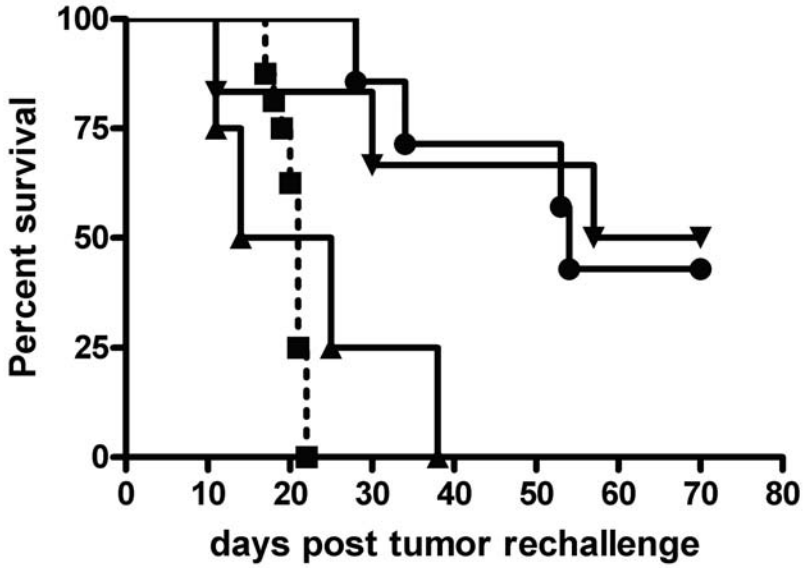

Figure 14. DC vaccination but not anti-CD25 treatment induces persistent immunological protection against intracranial glioma challenge.

Long-term surviving mice after a primary tumor challenge were re-challenged orthotopically with GL261 glioma cells. Kaplan-Meier curve depicts survival of animals that were initially (before primary tumor challenge) treated with anti-CD25 alone (▲, n = 4), vaccination alone (●, n = 7) or anti-CD25 in combination with DCm-GL261-RNA vaccination (▼, n = 6). Untreated control mice are also depicted (■, dashed line, n = 16). Overall Logrank $p < 0.001$.

6.6. Study of brain-infiltrating cells in glioma-bearing animals

6.6.1. Lymphocyte infiltration in the brain of DC and anti-CD25 treated mice, induction of memory T cells and enhancement of CTL activity by anti-CD25 treatment

Brain-infiltrating lymphocytes were analysed by flowcytometry 14 days after tumor challenge. Total lymphocytes (Figure 15a) were significantly increased by anti-CD25 treatment, vaccination and combined treatment compared with untreated tumor challenged animals. Detailed analysis of CD4+ and CD8+ lymphocyte subpopulations was performed (Table 4). Tumor-bearing mice exhibited increased numbers of both CD4+ effector, Treg and CD8+ lymphocytes compared with naïve animals, although not significant. Separate treatment with either anti-CD25 or DCm-GL261-RNA vaccination alone further boosted the influx of all abovementioned subpopulations (except for Treg in anti-CD25 treated mice) with a significant increase in CD25+CD8+ T cells. Combination therapy resulted in a significant upregulation of both CD4+ effector and Treg, but not CD8+ T cells compared with untreated animals. In comparison with anti-CD25 treatment only, combined treatment yielded a significant higher influx of CD4+CD25+Foxp3- and Treg. Compared with vaccination only, solely the CD4+CD25+Foxp3- subpopulation was significantly increased in the combined treatment group.

Analysis of the expression of CD62L (L-selectin) as memory T cell marker on brain-infiltrating lymphocytes (Figures 15b-c) revealed that DCm-GL261-RNA vaccination in combination with anti-CD25 treatment resulted in a significant increase of CD4+CD62L^{lo} cells (4.30 ± 0.66 x 10^5) compared with untreated mice (1.39 ± 0.23 x 10^5, $p < 0.001$, $n = 6$) and mice that received vaccination only (2.09 ± 0.41 x 10^5, $p < 0.01$, $n = 6$). Depletion of CD25+ cells only resulted in a higher influx of CD4+CD62L^{lo} cells (3.08 ± 0.26 x 10^5, $p < 0.05$, $n = 6$) compared with mice that were left untreated. When CD8+CD62L^{lo} cells were considered, a significant increase was noted in mice that received vaccination alone (1.46 ± 0.15 x 10^5, $p < 0.01$, $n = 6$) and combined treatment (1.26 ± 0.17 x 10^5, $p < 0.05$, $n = 6$) compared with untreated mice (4.69 ± 1.43 x 10^4, $n = 6$).

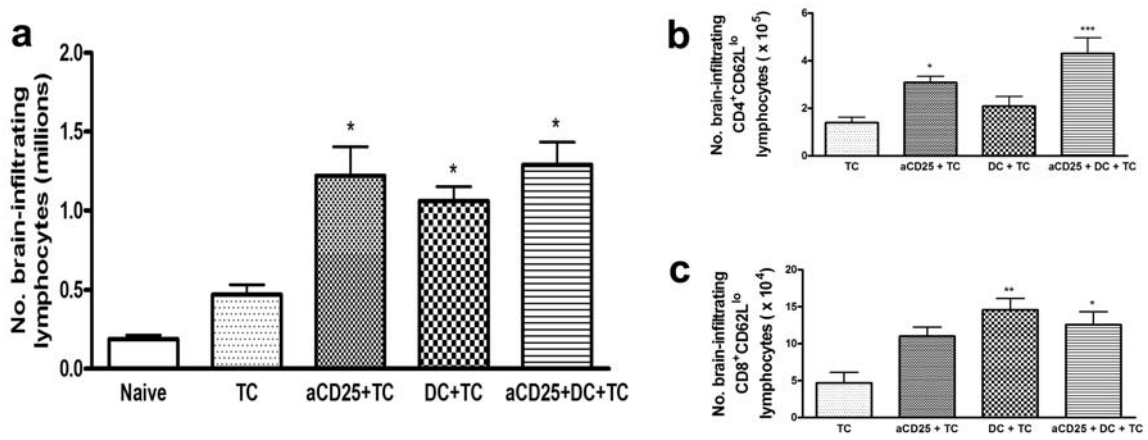

Figure 15. Treatment with DC and/or anti-CD25 mAb leads to infiltration of lymphocytes into the brain and the induction of immunological memory in CD8+ and CD4+ T cells respectively

Fourteen days after tumor challenge, mice were sacrificed and brain-infiltrating lymphocytes were isolated as described. Mice were either left untreated (TC) or received treatment with either anti-CD25 (aCD25 + TC), DCm-GL261-RNA (DC + TC) or combined treatment (aCD25 + DC + TC). As a control, naïve littermates were analysed. Individual data from three independent experiments are pooled and are represented as mean absolute cell numbers ± SEM. For statistical analysis, treatment groups were compared with untreated animals. (a) Absolute numbers of total brain-infiltrating lymphocytes (million cells per mouse). $CD62L^{lo}$ cells were considered as memory T lymphocytes. The expression of CD62L was monitored on both CD4+ (b) and CD8+ lymphocytes (c). Results are represented as mean absolute cell numbers ± SEM. Overall ANOVA $p < 0.01$ for both CD4+ and CD8+ T cells.

	CD4+CD25- ($\times 10^4$)	CD4+CD25+ Foxp3- ($\times 10^4$)	CD4+CD25+ Foxp3+ ($\times 10^3$)	CD8+CD25- ($\times 10^4$)	CD8+CD25+ ($\times 10^3$)
naive (n=6)	9.47 ± 1.21	0.04 ± 0.01	0.22 ± 0.11	10.5 ± 0.97	0.19 ± 0.05
untreated (n=8)	19.5 ± 2.37	2.39 ± 0.70	19.9 ± 7.10	15.4 ± 3.72	5.78 ± 1.32
aCD25 (n=10)	53.4 ± 14.9	6.10 ± 0.92	11.2 ± 2.26	47.6 ± 16.6	18.0 ± 4.52 (*)
DC (n=10)	38.5 ± 4.76	7.02 ± 1.45	28.2 ± 5.66	35.4 ± 5.09	18.2 ± 1.29 (*)
aCD25 + DC (n=9)	61.9 ± 5.22 (*)	*18.2* ± *4.71* (*)	43.9 ± 5.38 (*)	50.0 ± 10.5	12.2 ± 2.09

Table 4. Characterization of brain-infiltrating lymphocytes.

Brain-infiltrating lymphocytes were isolated from naive, untreated, anti-CD25 treated, vaccinated and vaccinated + anti-CD25-treated mice 14 days *post* tumor challenge. Within the CD4+ population, CD25- and CD25+FoxP3- effector cells and CD25+Foxp3+ Treg were assessed. For CD8+ T cells, CD25- and CD25+ cells were discriminated. Significant differences between experimental groups and untreated animals are indicated between brackets. Significant differences between combined treatment and anti-CD25 treatment or vaccination only are highlighted by underlined and italic numbers respectively. Individual data from three independent experiments are pooled and are represented as mean absolute cell numbers ± SEM.

The functionality of the brain-infiltrating cells was addressed *ex vivo* by co-culturing sorted CD11b+ myeloid cells or CD11b- lymphoid cells as effector cells with target tumor cells. After two days of co-culture, GL261 target cell viability (Figure 16) was reduced by co-culture with CD11b- effector cells from anti-CD25 treated (OD 0.07 ± 0.02, $p < 0.001$), vaccinated mice (OD 0.36 ± 0.01, $p < 0.05$) and mice that received combined treatment (OD 0.11 ± 0.03, $p < 0.001$) compared with untreated animals (OD 0.59 ± 0.04). No effect on LLC target cell viability was noted.

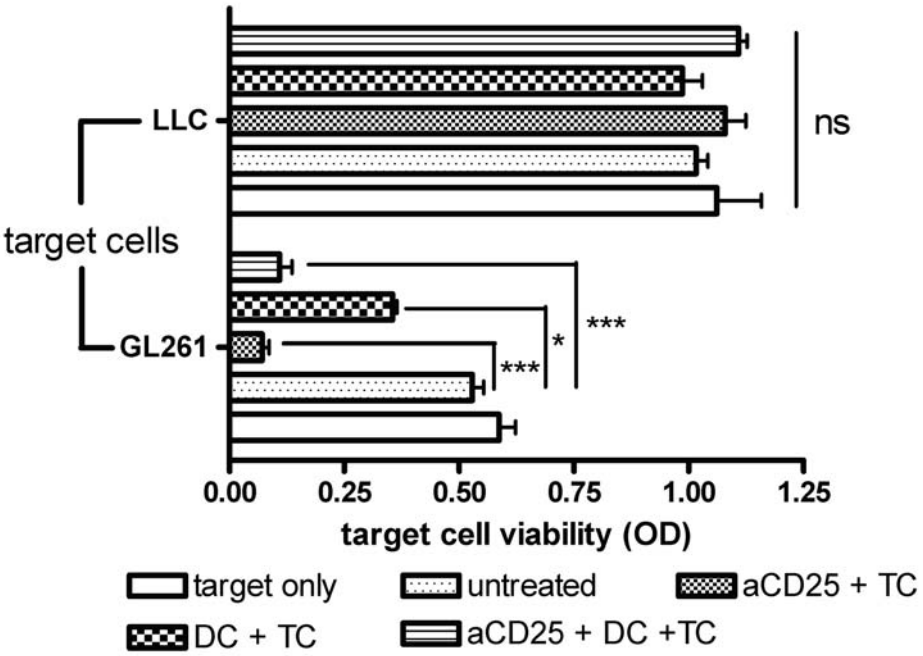

Figure 16. Specific antitumor cytotoxicity of brain-infiltrating lymphocytes by prophylactic DC vaccination and/or *in vivo* depletion of Treg

Sorted CD11b- brain-infiltrating cells were used as effector cells in an *in vitro* tumor cell cytotoxicity assay. Effector and target cells were co-cultured for 48 h at an effector to target ratio of 10:1. As target cells, either GL262 glioma or LLC cells were used. Optical density (OD) is depicted as measurement for target cell viability. Data are from repeated measurements in one assay on pooled samples. For each group, n = 6. ns = not significant.

6.6.2. Anti-CD25 treatment but not DC vaccination leads to myeloid cell infiltration into the brain of tumor-bearing mice

Strikingly, anti-CD25 treatment resulted in a massive increase of brain-infiltrating myeloid cells compared with untreated animals (9.14 ± 2.88 x 10^6 *versus* 1.26 ± 0.36 x 10^6, $p < 0.05$) but this was not observed in DC-treated mice (2.26 ± 1.04 x 10^6) nor mice that receive combined treatment (3.30 ± 0.95 x 10^6). Further characterization of this cell population was performed both with flowcytometry and morphologic analysis on cytospins. The proportion of F4/80^{hi} macrophages among CD45^{hi}CD11b+ myeloid cells (Figure 17a-b) was increased both in mice that were anti-CD25-treated (88.1 ± 2.37 %, $p < 0.05$, $n = 8$) and mice that received combined treatment (91.4 ± 2.58 %, $p < 0.05$, $n = 8$) compared with untreated tumor challenged animals (77.9 ± 1.10 %, $n = 6$). Only in untreated mice, a higher influx (0.31 ± 0.06 x 10^6, $p<0.05$) of Gr-1+CD45^{hi}CD11b+ MDSC was noted compared with naïve animals (0.03 ± 0.01 x 10^6). However, in absolute numbers, only anti-CD25-treatment lead to an increased infiltration of F4/80^{hi}CD45^{hi}CD11b+ macrophages compared with untreated animals (1.83 ± 0.31 x 10^6 *versus* 0.42 ± 0.21 x 10^6, $p < 0.01$). These results were confirmed by cell counting on cytospins (Figure 17c-d) revealing higher macrophage counts in anti-CD25 treated mice (9.47 ± 0.95 cells / FOV, $p < 0.001$, $n = 8$) and mice that receive combined treatment (7.20 ± 0.70 cells / FOV, $p < 0.01$, $n = 8$) compared with untreated mice (2.92 ± 0.38 cells / FOV, $n = 6$). When granulocytes were considered, only anti-CD25 treatment induced a significant higher influx (8.93 ± 1.35 cells / FOV, $p < 0.01$, $n = 8$) compared with untreated mice (4.42 ± 0.61 cells / FOV, $n = 6$). Virtually all granulocytes were identified as neutrophils (data not shown).

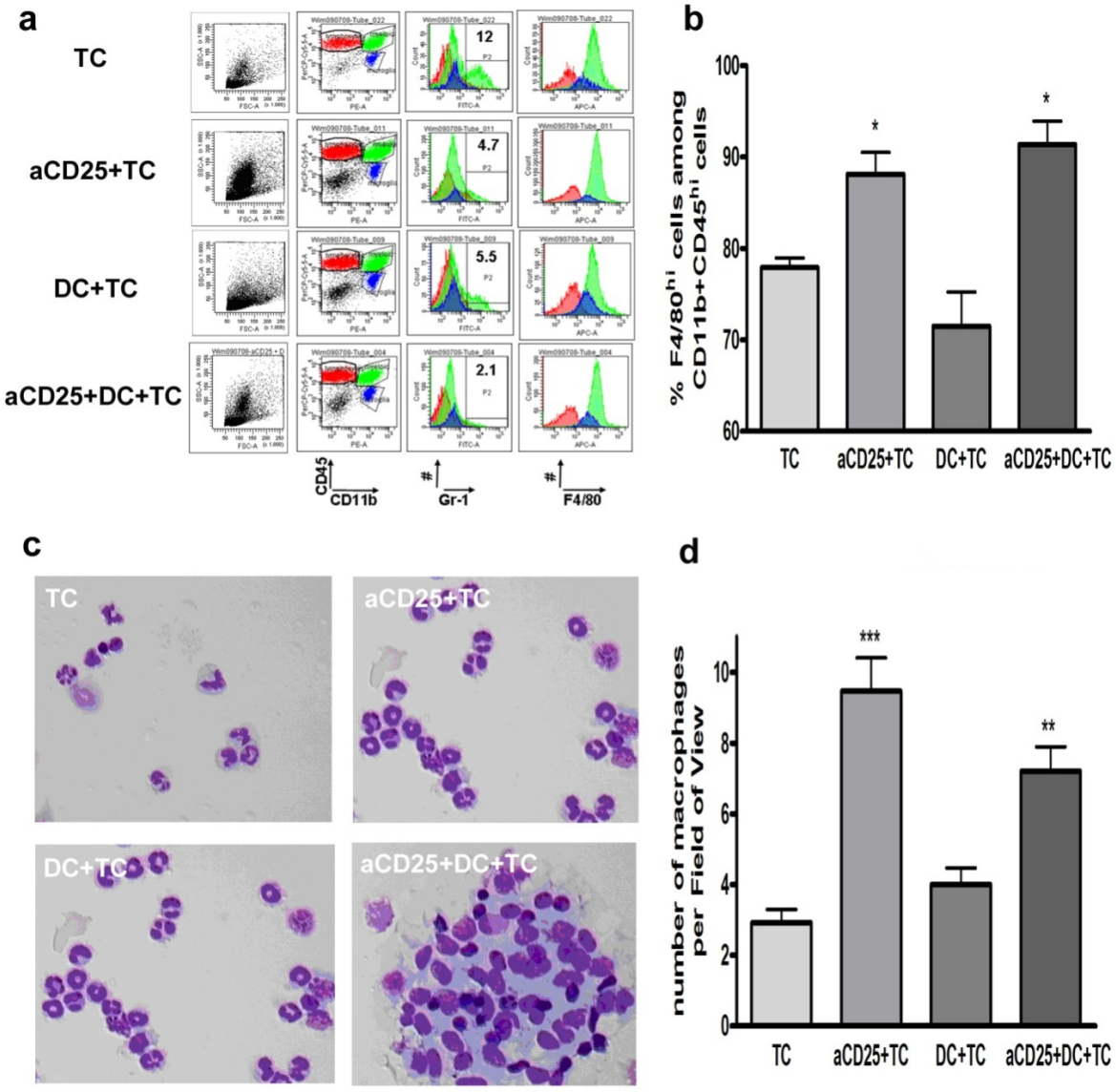

Figure 17. Profiling of infiltrating myeloid cells in glioma bearing mice

(a) Representative FSC-SSC, CD11b-CD45 dotplot images and Gr-1 and F4/80 histograms for each experimental group. Lymphocyte (red), myeloid cell (green) and microglia (blue) subpopulations were identified. (b) Fraction of F4/80^{hi} macrophages within CD45^{hi}CD11b+ myeloid cells.

(c) Representative cytospin images (May-Grünwald Giemsa staining) for each experimental group.

(d) Absolute numbers of macrophages (± SEM) per field of view (FOV). For each individual animal, five counts were taken into account.

6.7. Discussion

In accordance with recently published data by Grauer *et al*. (98), we have shown that CD8+ T cells are involved both in the endogenous and the vaccine-induced antitumor immune response. When CD8+ T cells were depleted at the time of tumor challenge, immunological protection by DC immunization was completely abolished and all animals died. However, the median survival of DCm-GL261-RNA treated CD8-depleted mice was still significantly longer as compared with the untreated CD8-depleted mice. This indicates that DC immunotherapy is not solely acting through CD8+ T cells. Experiments in which both CD4+ and CD8+ T cells were depleted in the context of experimental glioma confirmed that CD4+ T cells are required for both the initiation and effector phase of the immune response, whilst the role of CD8+ T cells was most prominent in the effector phase of the antitumor response (98). Other key players such as NK cells and NK-T cells might be likewise activated by this kind of DC treatment (212-214). In our hands, a minor fraction of the *ex vivo* differentiated DC from bone marrow progenitor cells that were used for immunization, showed low expression of CD8α. Hence, this CD8α+ DC subpopulation is prone to *in vivo* elimination by the injection of anti-CD8α mAb. The functional consequences of this are not clear. The CD8αα homodimer has been regarded as a cell lineage marker rather than a molecule that could contribute to functional differences between ($CD8\alpha^+$) lymphoid and ($CD8\alpha^-$) myeloid DC (215). However, Hong *et al.* recently published that expression of CD8α on BM-derived DC may play a functional role in enhancement of T cell activation (216). In the context of DC vaccination, attempts to increase CD8 T cell activation by boosting co-stimulatory signals, could be highly beneficial to the potency of the final antitumor effect. It might be of special interest to stimulate 4-1BB on CD8+ T cells, an important T cell costimulator receptor that promotes the survival and expansion of activated T cells. This can be achieved through administration of an agonistic mAb or multivalent aptamers with an even superior avidity and specificity to mAb, as recently described by McNamara *et al*. (217).

We noted that a single injection of a CD25-depleting mAb induces a transient decrease of CD4+CD25+FoxP3+ Treg activity, which is sufficient to completely protect animals from subsequent intracranial tumor challenge. This attributes a dominant role to Treg in our experimental glioma model. A direct effect of anti-CD25 on GL261 cells was excluded and this is in accordance with recent findings by Curtin *et al* (95). These authors also demonstrated that the efficiency of Treg depletion in a curative setting is dependent on the tumor burden, since systemic

administration of PC61 had a beneficial effect on survival if applied 15 days after tumor challenge but no longer when given on day 24 post tumor challenge. Other investigators have found that curative DC-based immunotherapy in the GL261 model is efficient only if CD25-expressing Treg are first depleted (207).

The crucial role of Treg in the progression of glioma and other types of cancer and the impact thereof on immunotherapy has been documented extensively both in humans and in experimental rodent models by many groups throughout the last years (218-220). For an excellent review on this subject, we refer to the work of Zou (88). Recent evidence is arising that anti-CD25 treatment with the PC61 mAb does not result in a genuine depletion of Treg but rather a functional inactivation of naive $CD69^{lo}$ Treg with rapid internalization and shedding of the IL-2Rα unit (221). Considerable caution should be taken when CD25 expression on CD4+ T cells is used to monitor Treg kinetics. Hence, in this study, only FoxP3+ cells were considered as the true Treg population. In our experiments, restoration of CD25 expression in CD4+ splenocytes by DC vaccination after initial CD25 depletion was concomitant with an increase in FoxP3 expression. This suggests that DC treatment is capable of inducing Treg cells, besides its beneficial influence on the effector arm of cellular immunity. It remains an open question whether these FoxP3 expressing cells are true functional Treg with *in vivo* suppressive capacity, since all animals that received combined treatment were long-term survivors from primary tumor challenge. The study of Treg infiltration in glioma bearing albino C57BL/6 mice, allowing assessment of tumor progression with *in vivo* BLI, could be of high value to differentiate complete responders to DC treatment from partially and non-responding mice. From re-challenge experiments, we conclude that treatment with DCm-GL261-RNA is capable of inducing immunological memory against the tumor, since animals that initially received combined treatment (consisting of CD25 depletion and DCm-GL261-RNA vaccination) or survived after treatment with DCm-GL261-RNA alone, displayed a prolonged survival and were again partially protected against tumor challenge. To our view, the observed early and also late immunological protection against glioma challenge clearly demonstrates the efficiency of immunization with DC. On the other hand, mice that received anti-CD25 treatment only were not protected upon re-challenge. So either the vaccine-induced FoxP3-expressing CD4+CD25+ cells are non-functional Treg, which is unlikely, or the balance between immunogenicity and tolerance is again sufficiently tilted towards the former at a later time point (day 60). The local inflammatory environment might also downregulate Treg functionality and this can be partially mediated by IL-6 producing DC (222,223). Jouanneau *et al.* reported recently that

lysate-loaded DC are essential for priming but insufficient for maintaining antitumor immune responses in the GL261 model, since late tumor relapses were observed, finally resulting in the complete protection of only 20 percent of treated mice (224). We did not observe late tumor relapses but it should be noted that the DC immunisation procedure or even the DC themselves that were used this study were perhaps suboptimal. Moreover, enhancing the stringency of the experimental system (e.g. by implanting more tumor cells) could reduce the effectiveness of Treg depletion and potentially reveal a more prominent role for DC vaccination. Van Meirvenne *et al*. elegantly demonstrated that *in vivo* depletion of Treg enhanced both the primary and memory CTL response elicited by mRNA-loaded DC in an ovalbumin-specific tumor model (225). Grauer *et al*. recently reported that Treg elimination by anti-CD25 treatment is essential to eradicate established glioma by vaccination with tumor lysate-pulsed DC (99). In our hands, DCm-GL261-RNA vaccination alone was sufficient for the induction of immunological protection and memory in about half of the mice, whilst all of the anti-CD25 treated mice survived but were not longer protected upon re-challenge. Hence, in the aforementioned setting, our data support a combined immunotherapeutic treatment consisting of Treg depletion and DCm-GL261-RNA vaccination for the induction of an optimal antitumor immune response.

Since systemic monitoring of immune reactions within the brain represents an artificial readout that can only partially reflect local events, we opted for genuine *in situ* investigation of brain-infiltrating cells. Taken together, we observed that both CD25 depletion, DCm-GL261-RNA vaccination and combined treatment before challenge with GL261 tumor cells resulted in a pronounced lymphocyte infiltration into the brain. Effector lymphocytes, encompassing both CD4+CD25- and CD4+CD25+FoxP3- and CD8+ T cells were more numerous both after anti-CD25 treatment, vaccination and combined treatment. Combined treatment clearly expanded Treg, which is in concordance with the abovementioned systemic monitoring data. In this regard, time kinetics could provide useful information regarding the expansion and/or reduction in infiltrating lymphocytes but this was beyond the scope of this study. Here, we provide evidence that the CD11b- lymphocyte fraction of the brain-infiltrating cells contained the real cytotoxic effector cells. The function of the latter cells is clearly enhanced by prophylactic Treg depletion.

Mice that were treated with either DCm-GL261-RNA alone or DCm-GL261-RNA together with anti-CD25 treatment clearly displayed a higher number of CD8+CD62L^{lo} lymphocytes, whereas CD4+CD62L^{lo} lymphocytes were rather increased by anti-CD25 and combined treatment. This shift towards induction of immunological memory correlates with the initially vaccinated mice being

partially protected against intracranial re-challenge, even without CD25 depletion. The increase in absolute numbers of infiltrating CD8+ lymphocytes by DCm-GL261-RNA treatment and the concomitant memory-like phenotype of these cells further illustrates their involvement in the vaccine-mediated antitumor immune response, as already evidenced by previously mentioned *in vivo* CD8 co-depletion experiments.

Although we first of all focused on T cells in our model, a pronounced infiltration of myeloid cells was noticed in the brain of glioma-bearing mice, in particular in those animals that received anti-CD25-treatment. Since myeloid cells represent an extremely heterogeneous pool of cells, we attempted to further identify those cells. At present, a vast body of research is dedicated to unravel the role of myeloid cells in the context of tumor immunology. Although terminology is still inadequate, myeloid cells infiltrating the tumor microenvironment are mostly regarded as cells with protumoral activity (102-110). In our model, these infiltrating myeloid cells do not correspond with the phenotype of Gr-1+ MDSC but can rather be classified as F4/80 expressing macrophages and granulocytes. These cells were most prominent in mice that received anti-CD25-treatment and since all of those animals were protected from primary glioma challenge, we argue against the classification of these cells as TAM. Further investigation is therefore required to establish a more complete profile of the infiltrating macrophages in anti-CD25-treated mice that to our view have a beneficial effect on tumor immunity. These cells therefore more likely correspond to so-called 'classic' M1 macrophages that display a MHC^{hi}, $IL\text{-}12^{hi}$, $IL\text{-}23^{hi}$ and $IL\text{-}10^{lo}$ phenotype and are beneficial to tumor immunity through the production of ROS, N-intermediates and inflammatory cytokines (108,109).

It is still unclear how anti-CD25 treatment facilitates the influx of these myeloid cells (which cytokine and chemokine cues might be involved), whether they have the capacity to really establish tumor cell clearance and why their effect lasts only temporarily. Immunization with DC does not result in such a pronounced myeloid cell infiltration which is suggestive for separate mechanisms leading to immunological protection against glioma.

To our view, this is the first report mentioning a possible link between depletion of CD25-expressing lymphocytes through *in vivo* administration of the mAb PC61 and infiltration of myeloid cells into the tumor microenvironment.

Chapter 7. General discussion and future perspectives

Although malignant glioma today still represent a major hurdle in clinical oncology, optimistic voices can be heard on new experimental therapies for this pathology. The basic concept of cancer immunotherapy is not new, but is therefore not less promising. It is only in the last decade that fundamental mechanisms regulating tumor immunity on the one hand and tolerance on the other hand are being unravelled, thereby opening new therapeutic perspectives. It is now becoming clear that manipulating one single aspect of glioma immunology will never represent the magic bullet. Therefore, we favour a combination of different immunotherapeutic strategies, in an attempt to boost innate and adaptive antitumor immunity, while simultaneously reducing immunosuppression.

In the experimental work presented here, we implemented step-by-step the concept of active glioma immunotherapy with RNA-loaded DC. The rationale of loading DC with total RNA from tumoral origin is to provide DC immunotherapy for those glioma patients whose resected tumor material is insufficient to make a lysate for loading DC. Indeed, mRNA can be amplified *in vitro*. Initially, we focused on testing murine DC electroporated with total RNA from a glioma cell line in an experimental *in vitro* design. The data obtained from these *in vitro* stimulation experiments confirmed that DC loaded with tumor antigens as a result of RNA-electroporation, are capable of inducing a T cell mediated antitumor immune response. These results are in correlation with previously published preclinical data from our group and others (58,76). Considering potential translation to a clinical setting, we conclude that it is not worthwile to go through the labour-intensive and costly process of *in vitro* tumor mRNA amplification, except for those patients whose amount of resected tumor material is insufficient. Since *in vitro* systems only partially mimic the complex tumor microenvironment and cell interactions *in vivo*, we endeavoured to validate our findings in an experimental mouse glioma model. After all, it is our ambition that novel insights in glioma immunology eventually find their way to oncologic practice. Prophylactic immunization with DC loaded with glioma-derived RNA was sufficient to protect nearly half of the treated animals from subsequent orthotopic glioma challenge. Why the other mice were not protected is still not completely understood. Longitudinal imaging studies of tumor-bearing mice revealed that within the animals that eventually succumb, a distinct pattern of non-responding and partially responding mice can be identified. We hypothesize that there is a very delicate balance between antitumor immune responses on the one hand (either endogenous or induced or boosted by the

DC vaccine) and natural and tumor-induced immunosuppression on the other hand. In responding mice, it is apparent that treatment with DC shifts this balance towards immunity (away from tolerance), resulting in tumor protection. In contrast, in mice refractory to DC-vaccination, it is likely that DC actually induce or expand immunosuppressive Treg. Moreover, these data provided a rationale to investigate in depth the mode of action of DC-treatment and to implement strategies that are aimed at lowering the detrimental immunosuppression induced by Treg.

Generating an immune response against a complex malignant entity such as GBM with its many escape mechanisms is not at all a straightforward process, not in humans and neither in experimental glioma. In our model, we have shown that active immunization with DC is at least partially effective through the induction of cytotoxic antitumor CD8+ T cells (Figure 18). Other immune effector cells are likely to be involved as well, as demonstrated in many tumor models (37,38). *In vivo* administration of a CD25-targeting mAb, a commonly used Treg depletion tool in mice, had a vast impact in our model. Firstly, prophylactic depletion of Treg enhanced the activity of cytotoxic effector cells and proved to be sufficient for immunological protection against intracranial glioma. However, for long-term immunity to become established, immunization with DC was indispensable. Translated to clinical practice, elimination of Treg by anti-CD25-treatment or other means seems to represent a powerful weapon in the fight against cancer, but is unfortunately not the ultimate tool in cancer immunotherapy after all (226-229). One should also keep in mind that prolonged depletion of Treg is not feasible due to the risk of eliciting autoimmune disease. Pilot data on the use of ONTAK® (a fusion protein of diphtheria toxin and human IL-2) and cyclophosphamide to downregulate Treg in human cancer immunotherapy seem very promising although conflicting data are arising (230-232). Moreover, not only Treg are eliminated by anti-CD25 treatment, but also IL-2-dependent CD4+ helper T cells and proliferating CD8+ lymphocytes can be affected (95). CTLA-4, a negative regulator of endogenous and vaccine-induced antitumor immunity, represents another good selective target in cancer immunotherapy. It has been shown in metastatic melanoma patients that sequential infusions of anti-CTLA-4 mAb after DC-vaccination generate a clinically meaningful antitumor immunity without grade 3 or grade 4 toxicity (233). Secondly, we noted that anti-CD25-treatment but not immunization with DC resulted in an unexpected and pronounced infiltration of myeloid cells, including macrophages and granulocytes (Figure 18). In sharp contrast with current literature on TAM and MDSC, these cells do not seem to hinder tumor rejection in our model, but might on the contrary be genuine tumoricidal innate immune cells. We hypothesize that due to the transient depletion of Treg by

anti-CD25-treatment, the macrophages within the pool of myeloid cells maintain a pro-immune M1-phenotype rather than being transformed in immunosuppressive TAM. Future research will focus on the functional status of these myeloid cell infiltrates *(i)* to define whether they are pro-immune or rather immunosuppressive and *(ii)* to investigate the mechanisms governing transition from one phenotype to the other. It is beyond the scope of this work to clarify the mechanism between anti-CD25-treatment and myeloid cell infiltration, but this certainly represents an intriguing finding, warranting further exploration.

Implementing optical imaging in our experimental glioma model resulted in a more extensive characterization of GL261 glioma behaviour *in vivo*, demonstrating midline crossing and leakage of tumor cells along with the observed initial tumor cell adaptation phase. Together with the distinct response patterns to DC immunotherapy, this kind of information, available in real-time, can be of particular importance to guide therapeutic interventions in this model.

From a clinical point of view, we believe that DC-based immunotherapy should be incorporated in the multimodal treatment for malignant glioma, even for primary tumors. Autologous DC therapy (in which monocyte-derived DC are loaded with total lysate from the patients' own tumor) is under investigation by our research group in a cohort-comparison phase I/II clinical trial for newly diagnosed and relapsed GBM respectively. So far, postoperative adjuvant DC vaccination in more than 150 patients with relapsed HGG yields interesting long-term results with nearly 25 percent two-year survivors after vaccination which compares favourably to any other study in recurrent HGG thusfar (59). For newly diagnosed GBM, we are currently assessing the integration of DC vaccination into the conventional postoperative radiochemotherapy regimen.

In conclusion, we put forward that the most optimal immunological response against experimental malignant glioma – and likely many other tumors – can be achieved by enhancing immunity through active immunization on the one hand and by decreasing immunosuppression on the other hand. Recently, Weiner stated that for cancer immunotherapy in general, the destination is not yet at hand, but in sight (132). No matter how, in the upcoming years, we will witness its real showdown. In the meantime, it is only the continuation of joint research efforts that might shed light on some of the many black boxes in tumor immunology. We, from our part, are determined that the outcome for GBM patients still can be significantly improved, hopefully leading to a meaningful prolongation of life with maintenance of a good quality of life. For some patients at least, translation of the experimental findings of this study, might represent a substantial therapeutic benefit.

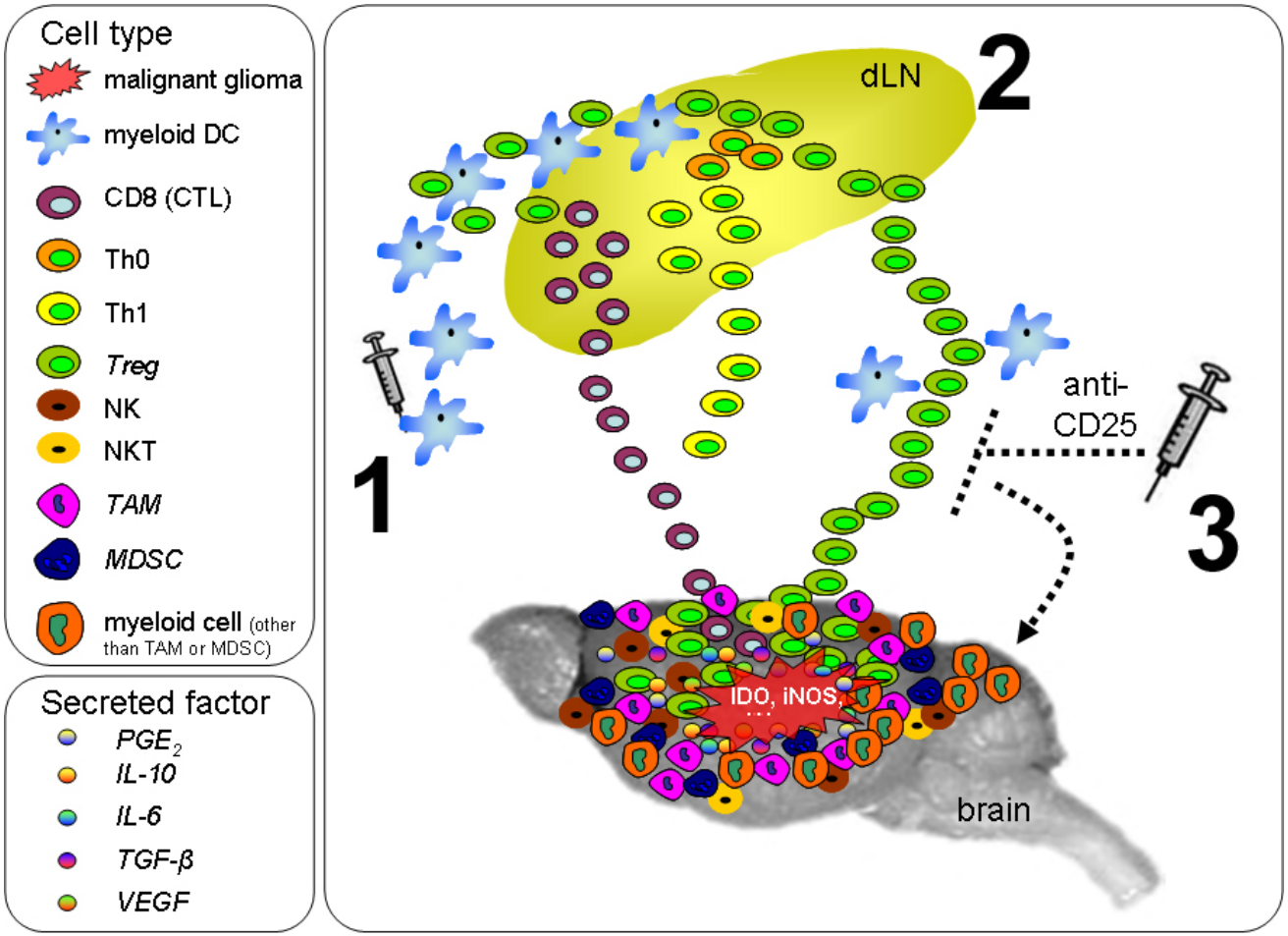

Figure 18. Local immune interactions in the tumor micro-environment of glioma-bearing mice.

(1) RNA-loaded DCm are injected intraperitoneally and migrate to the secondary lymphoid organs (such as dLN). (2) Interactions between DC on the one hand and CD8 and CD4 T cells, NK cells and NKT cells on the other hand result in an antitumor immune response, which is however counteracted by several immunosuppressive mechanisms. Both intrinsic tolerogenic mechanisms, Treg and suppression by innate immune cells such as tumor-associated macrophages (TAM) and myeloid-derived suppressor cells (MDSC) maintain or restore tumor tolerance. Glioma are capable of evading immune surveillance through the secretion of various immunosuppressive factors and cytokines such as PGE_2, IL-10, IL-6, TGF-β and VEGF. Moreover, glioma evade interactions with effector cells and escape NK cell killing and induction of apoptosis. Expression of PD-L1, Gal-1, STAT-3, IDO, iNOS and Arg1 by tumor cells also contribute to immune escape. (3) Treatment with anti-CD25 mAb temporarily lowers Treg activity and leads to a massive infiltration of myeloid cells that do not correspond to TAM nor MDSC.

Summary

Despite advances in surgery, chemo- and radiotherapy for malignant glioma, prognosis for patients with this type of aggressive cancer still remains dismal. Hence, new therapeutic options are absolutely required. We investigated active immunization against malignant glioma based on tumor antigen-loaded dendritic cells (DC) in a preclinical mouse model. In the experimental work presented here, we demonstrate that murine DC can be efficiently loaded with tumor-derived total RNA and that these cells can induce specific antitumor cytotoxic T cells *in vitro*. Moreover, when prophylactically administered *in vivo* in an experimental mouse glioma model, RNA-loaded DC protect against intracranial tumor growth in half of the treated animals. Distinct response patterns to DC immunotherapy were clearly revealed by implementing *in vivo* bioluminescence imaging (BLI) in our model. This induced immune response is tumor-specific and at least partially mediated by CD8+ T cells. To lower the effect of immunosuppressive CD25-expressing regulatory T cells (Treg) that might compromise antitumor immunity, the mice were injected with an anti-CD25 depleting monoclonal antibody. Strikingly, anti-CD25 treatment rescued all of the treated mice from primary glioma challenge. For long-term immunological protection however, anti-CD25 treatment alone was not sufficient and immunization with DC was required. Both treatments resulted in a pronounced lymphocyte infiltration into the brain of tumor-bearing mice. Both CD4+ and CD8+ effector and memory T cells were retrieved locally and anti-CD25 treatment enhanced the cytotoxic activity of effector T cells. Besides effector T cells, counteracting Treg were also expanded by vaccination with DC. Unexpectedly, anti-CD25 treatment but not immunization with DC led to local recruitment of myeloid cells in the brain of tumor-bearing mice. These cells displayed a mixed phenotype of macrophages and granulocytes and could not be classified as Gr-1+ myeloid-derived suppressor cells. To our view, these recruited macrophages do not resemble immunosuppressive tumor-associated macrophages but rather represent M1 macrophages with a pro-immune function. Further investigation with regard to the functionality of these cells and their relationship with Treg is therefore warranted. Taken together, we validated immunotherapy with RNA-loaded DC in an experimental glioma model and dissected some of the major mechanisms governing antitumor immunity and immunosuppression. We strongly emphasize the translational aspect of our research, finally aiming at improving the therapeutic outcome of GBM patients.

Samenvatting

De prognose voor patiënten met maligne glioma blijft bijzonder slecht ondanks aanzienlijke vooruitgang in chirurgische technieken, chemo- en radiotherapie. Er is bijgevolg een absolute nood aan nieuwe therapeutische invalshoeken. In deze studie hebben wij in een experimenteel muismodel het concept onderzocht van aktieve immunisatie tegen maligne glioma op basis van dendritische cellen (DC) die beladen worden met tumorantigenen. De resultaten uit dit experimenteel werk tonen aan dat muis DC op een efficiënte manier kunnen opgeladen worden met totaal RNA van tumorale oorsprong en dat deze DC specifieke antitumorale cytotoxische T cellen kunnen induceren *in vitro.* Het preventief toedienen van deze cellen *in vivo* in een experimenteel muis gliomamodel is bovendien voldoende om de helft van de dieren te beschermen tegen intracraniële tumorgroei. Implementatie van *in vivo* bioluminescentie in ons model maakte het mogelijk om verschillende responstypes ten opzichte van DC vaccinatie te onderscheiden. Deze immuunrespons is tumorspecifiek en op zijn minst deels gemedieerd door CD8+ T cellen. Om het effect van immuunsuppressieve CD25+ regulatoire T cellen (Treg) – die het opwekken van antitumorale immuniteit kunnen belemmeren – tegen te gaan werden de muizen geïnjecteerd met een anti-CD25 depleterend antilichaam. Alle anti-CD25 behandelde dieren bleken beschermd tegen daaropvolgende 'challenge' met glioma tumorcellen. Voor protectie op lange termijn was anti-CD25 behandeling alleen niet voldoende en was immunisatie met DC noodzakelijk. Beide behandelingen resulteerden in een aanzienlijke infiltratie van lymfocyten in de hersenen van dieren met glioma implantatie. Zowel CD4+ als CD8+ effector en geheugencellen waren aanwezig in dit infiltraat en anti-CD25 behandeling verhoogde bovendien de cytotoxische aktiviteit van de effector T cellen. Naast effectorcellen werden ook Treg geëxpandeerd door vaccinatie met DC. Onverwachts resulteerde anti-CD25 behandeling maar niet immunisatie met DC in de lokale aantrekking van myeloïde cellen naar de hersenen van dieren met intracranieel glioma. Deze cellen presenteerden zich als macrofagen en granulocyten en konden niet als Gr-1+ myeloïde suppressor cellen beschouwd worden. Wij menen dat deze gerecruteerde cellen evenmin als tumorgeassocieerde macrofagen kunnen gezien worden maar eerder antitumorale M1 macrofagen zijn. Verder onderzoek naar de functionaliteit van deze cellen en hun verband met Treg is daarom absoluut noodzakelijk. Samengevat hebben wij in deze studie immunotherapie met RNA-beladen DC gevalideerd in een experimenteel glioma model en enkele belangrijke mechanismen ontrafeld inzake antitumorale immuniteit en immuunsuppressie. In het bijzonder

willen we het translationeel aspect van dit onderzoek benadrukken met als finaal doel het verbeteren van de prognose van gliomapatiënten.

List of references

1. Folz BJ, Silver CE, Rinaldo A, Fagan JJ, Pratt LW, Weir N, Seitz D, and Ferlito A. An outline of the history of head and neck oncology. Oral Oncol 2008;44(1):2-9.

2. Kardinal CG and Yarbro JW. A conceptual history of cancer. Semin Oncol 1979;6(4):396-408.

3. Borgstein P and Meijer S. Historical perspective of lymphatic tumour spread and the emergence of the sentinel node concept. Eur J Surg Oncol 1998;24(2):85-89.

4. Wong JH. The development of lymphatic mapping and selective lymphadenectomy: a historical perspective. Cancer Treat Res 2005;127:1-14.

5. Farrell A, Hutchinsin E, Marte B, and McCarthy N. Nature Milestones in Cancer. Nature 2006;45.

6. Raven R. The Theory and Practice of Oncology: historical evolution and present principles. 1990. Parthenon Publishing Group, London.

7. Varmus H. The new era in cancer research. Science 2006;312(5777):1162-1165.

8. Louis DN, Ohgaki H, Wiestler OD, Cavenee WK, Burger PC, Jouvet A, Scheithauer BW, and Kleihues P. The 2007 WHO classification of tumours of the central nervous system. Acta Neuropathol 2007;114(2):97-109.

9. Wrensch M, Minn Y, Chew T, Bondy M, and Berger MS. Epidemiology of primary brain tumors: current concepts and review of the literature. Neuro Oncol 2002;4(4):278-299.

10. Brada M, Hoang-Xuan K, Rampling R, Dietrich PY, Dirix LY, Macdonald D, Heimans JJ, Zonnenberg BA, Bravo-Marques JM, Henriksson R, Stupp R, Yue N, Bruner J, Dugan M, Rao S, and Zaknoen S. Multicenter phase II trial of temozolomide in patients with glioblastoma multiforme at first relapse. Ann Oncol 2001;12(2):259-66.

11. Finlay JL, Boyett JM, Yates AJ, Wisoff JH, Milstein JM, Geyer JR, Bertolone SJ, McGuire P, Cherlow JM, Tefft M, and et al. Randomized phase III trial in childhood high-grade astrocytoma comparing vincristine, lomustine, and prednisone with the eight-drugs-in-1-day regimen. J Clin Oncol 1995;13(1):112-23.

12. Nieder C, Grosu AL, and Molls M. A comparison of treatment results for recurrent malignant gliomas. Cancer Treat Rev 2000;26(6):397-409.

13. Behin A, Hoang-Xuan K, Carpentier AF, and Delattre JY. Primary brain tumours in adults. Lancet 2003;361(9354):323-331.

14. Fleury A, Menegoz F, Grosclaude P, Daures JP, Henry Amar M, Raverdy N, Schaffer P, Poisson M, and Delattre JY. Descriptive epidemiology of cerebral gliomas in France. Cancer 1997;79(6):1195-1202.

15. Relling MV, Rubnitz JE, Rivera GK, Boyett JM, Hancock ML, Felix CA, Kun LE, Walter AW, Evans WE, and Pui CH. High incidence of secondary brain tumours after radiotherapy and antimetabolites. Lancet 1999;354(9172):34-39.

16. Schwartzbaum JA, Fisher JL, Aldape KD, and Wrensch M. Epidemiology and molecular pathology of glioma. Nat Clin Pract Neurol 2006;2(9):494-503.

17. Hardell L, Carlberg M, Soderqvist F, and Hansson MK. Meta-analysis of long-term mobile phone use and the association with brain tumours. Int J Oncol 2008;32(5):1097-1103.

18. Ohgaki H and Kleihues P. Epidemiology and etiology of gliomas. Acta Neuropathol 2005;109(1):93-108.

19. Backlund LM, Nilsson BR, Liu L, Ichimura K, and Collins VP. Mutations in Rb1 pathway-related genes are associated with poor prognosis in anaplastic astrocytomas. Br J Cancer 2005;93(1):124-130.

20. Ichimura K, Schmidt EE, Goike HM, and Collins VP. Human glioblastomas with no alterations of the CDKN2A (p16INK4A, MTS1) and CDK4 genes have frequent mutations of the retinoblastoma gene. Oncogene 1996;13(5):1065-1072.

21. Goode EL, Ulrich CM, and Potter JD. Polymorphisms in DNA repair genes and associations with cancer risk. Cancer Epidemiol Biomarkers Prev 2002;11(12):1513-1530.

22. Ohgaki H, Dessen P, Jourde B, Horstmann S, Nishikawa T, Di Patre PL, Burkhard C, Schuler D, Probst-Hensch NM, Maiorka PC, Baeza N, Pisani P, Yonekawa Y, Yasargil MG, Lutolf UM, and Kleihues P. Genetic pathways to glioblastoma: a population-based study. Cancer Res 2004;64(19):6892-6899.

23. Rich JN, Hans C, Jones B, Iversen ES, McLendon RE, Rasheed BK, Dobra A, Dressman HK, Bigner DD, Nevins JR, and West M. Gene expression profiling and genetic markers in glioblastoma survival. Cancer Res 2005;65(10):4051-4058.

24. Riemenschneider MJ, Buschges R, Wolter M, Reifenberger J, Bostrom J, Kraus JA, Schlegel U, and Reifenberger G. Amplification and overexpression of the MDM4 (MDMX) gene from 1q32 in a subset of malignant gliomas without TP53 mutation or MDM2 amplification. Cancer Res 1999;59(24):6091-6096.

25. Louis DN. Molecular pathology of malignant gliomas. Annu Rev Pathol 2006;1:97-117.

26. Yip S, Iafrate AJ, and Louis DN. Molecular diagnostic testing in malignant gliomas: a practical update on predictive markers. J Neuropathol Exp Neurol 2008;67(1):1-15.

27. Mischel PS and Cloughesy T. Using molecular information to guide brain tumor therapy. Nat Clin Pract Neurol 2006;2(5):232-233.

28. Stupp R, Mason WP, van den Bent MJ, Weller M, Fisher B, Taphoom MJ, Belanger K, Brandes AA, Marosi C, Bogdahn U, Curschmann J, Janzer RC, Ludwin SK, Gorlia T, Allgeier A, Lacombe D, Cairncross JG, Eisenhauer EA, and Mirimanoff RO. Radiotherapy plus concomitant and adjuvant temozolomide for glioblastoma. N Eng J Med 2005;352(10):987-996.

29. Omuro AM and Delattre JY. Editorial: what is new in the treatment of gliomas? Curr Opin Neurol 2007;20(6):704-707.

30. Stummer W, Novotny A, Stepp H, Goetz C, Bise K, and Reulen HJ. Fluorescence-guided resection of glioblastoma multiforme by using 5-aminolevulinic acid-induced porphyrins: a prospective study in 52 consecutive patients. J Neurosurg 2000;93(6):1003-1013.

31. Aghi M and Chiocca EA. Gene therapy for glioblastoma. Neurosurg Focus 2006;20(4):E18.

32. Rainov NG and Ren H. Gene therapy for human malignant brain tumors. Cancer J 2003;9(3):180-188.

33. Aboody KS, Najbauer J, and Danks MK. Stem and progenitor cell-mediated tumor selective gene therapy. Gene Ther 2008;15(10):739-752.

34. Mason WP. Emerging drugs for malignant glioma. Expert Opin Emerg Drugs 2008;13(1):81-94.

35. Vredenburgh JJ, Desjardins A, Herndon JE, Dowell JM, Reardon DA, Quinn JA, Rich JN, Sathornsumetee S, Gururangan S, Wagner M, Bigner DD, Friedman AH, and Friedman HS. Phase II trial of bevacizumab and irinotecan in recurrent malignant glioma. Clin Cancer Res 2007;13(4):1253-1259.

36. Reardon DA, Rich JN, Friedman HS, and Bigner DD. Recent advances in the treatment of malignant astrocytoma. J Clin Oncol 2006;24(8):1253-1265.

37. Zitvogel L, Tesniere A, and Kroemer G. Cancer despite immunosurveillance: immunoselection and immunosubversion. Nat Rev Immunol 2006;6(10):715-727.

38. Finn OJ. Cancer immunology. N Engl J Med 2008;358(25):2704-2715.

39. Carpentier AF and Meng Y. Recent advances in immunotherapy for human glioma. Curr Opin Oncol 2006;18(6):631-636.

40. Tang J, Flomenberg P, Harshyne L, Kenyon L, and Andrews DW. Glioblastoma patients exhibit circulating tumor-specific CD8+ T cells. Clin Cancer Res 2005;11(14):5292-5299.

41. Fenstermaker RA and Ciesielski MJ. Immunotherapeutic strategies for malignant glioma. Cancer Control 2004;11(3):181-191.

42. Bigner DD, Brown M, Coleman RE, Friedman AH, Friedman HS, McLendon RE, Bigner SH, Zhao XG, Wikstrand CJ, Pegram CN, and . Phase I studies of treatment of malignant gliomas and neoplastic meningitis with 131I-radiolabeled monoclonal antibodies anti-tenascin 81C6 and anti-chondroitin proteoglycan sulfate Me1-14 F (ab')2--a preliminary report. J Neurooncol 1995;24(1):109-122.

43. Boskovitz A, Wikstrand CJ, Kuan CT, Zalutsky MR, Reardon DA, and Bigner DD. Monoclonal antibodies for brain tumour treatment. Expert Opin Biol Ther 2004;4(9):1453-1471.

44. Wolff JE, Wagner S, Reinert C, Gnekow A, Kortmann RD, Kuhl J, and Van Gool SW. Maintenance treatment with interferon-gamma and low-dose cyclophosphamide for pediatric high-grade glioma. J Neurooncol 2006;79(3):315-321.

45. Banchereau J and Palucka AK. Dendritic cells as therapeutic vaccines against cancer. Nat Rev Immunol 2005;5(4):296-306.

46. Gabrilovich DI. Dendritic cell vaccines for cancer treatment. Curr Opin Mol Ther 2002;4(5):452-458.

47. Steinman RM and Banchereau J. Taking dendritic cells into medicine. Nature 2007;449(7161):419-426.

48. Tuyaerts S, Aerts JL, Corthals J, Neyns B, Heirman C, Breckpot K, Thielemans K, and Bonehill A. Current approaches in dendritic cell generation and future implications for cancer immunotherapy. Cancer Immunol Immunother 2007;56(10):1513-1537.

49. Gil-Torregrosa BC, Lennon-Dumenil AM, Kessler B, Guermonprez P, Ploegh HL, Fruci D, Endert PV, and Amigorena S. Control of cross-presentation during dendritic cell maturation. Eur J Immunol 2004;34(2):398-407.

50. Bonini C, Lee SP, Riddell SR, and Greenberg PD. Targeting antigen in mature dendritic cells for simultaneous stimulation of CD4+ and CD8+ T cells. J Immunol 2001;166(8):5250-5257.

51. Banchereau J, Briere F, Caux C, Davoust J, Lebecque S, Liu YJ, Pulendran B, and Palucka K. Immunobiology of dendritic cells. Annu Rev Immunol 2000;18:767-811.

52. Steinman RM. Some interfaces of dendritic cell biology. APMIS 2003;111(7-8):675-697.

53. Gilboa E. DC-based cancer vaccines. J Clin Invest 2007;117(5):1195-1203.

54. Guermonprez P, Valladeau J, Zitvogel L, Thery C, and Amigorena S. Antigen presentation and T cell stimulation by dendritic cells. Annu Rev Immunol 2002;20:621-667.

55. Parajuli P and Sloan AE. Dendritic cell-based immunotherapy of malignant gliomas. Cancer Invest 2004;22(3):405-416.

56. Wheeler CJ and Black KL. Dendritic cell vaccines and obstacles to beneficial immunity in glioma patients. Curr Opin Mol Ther 2005;7(1):35-47.

57. De Vleeschouwer S, Van Calenbergh F, Demaerel P, Flamen P, Rutkowski S, Kaempgen E, Wolff JEA, Plets C, Sciot R, and Van Gool SW. Transient local response and persistent tumor control of recurrent malignant glioma treated with combination therapy including dendritic cell therapy. J Neurosurg Spine 2004;100(5 Suppl Pediatrics):492-497.

58. De Vleeschouwer S, Arredouani M, Ade M, Cadot P, Vermassen E, Ceuppens JL, and Van Gool SW. Uptake and presentation of malignant glioma tumor cell lysates by monocyte-derived dendritic cells. Cancer Immunol Immunother 2005;54(4):372-382.

59. De Vleeschouwer S, Fieuws S, Rutkowski S, Van Calenbergh F, Van Loon J, Goffin J, Sciot R, Wilms G, Demaerel P, Warmuth-Metz M, Soerensen N, Wolff JEA, Wagner S, Kaempgen E, and Van Gool SW. Clinical experience of postoperative adjuvant dendritic cell-based immunotherapy in a large group of patients with relapsed glioblastoma multiforme. Clin Cancer Res 2008;14(10):3098-3104.

60. Maes W, Galicia Rosas G, Verbinnen B, Boon L, De Vleeschouwer S, Ceuppens J, and Van Gool S. DC vaccination with anti-CD25 treatment leads to long-term immunity against experimental glioma. Neuro Oncol (in press).

61. Maes W, Deroose C, Reumers V, Krylyshkina O, Gijsbers R, Baekelandt V, Ceuppens J, Debyser Z, and Van Gool SW. In vivo bioluminescence imaging in an experimental mouse model for dendritic cell based immunotherapy against malignant glioma. J Neurooncol 2008;91(2):127-139.

62. Rutkowski S, De Vleeschouwer S, Kaempgen E, Wolff JEA, Kuhl J, Demaerel P, Warmuth-Metz M, Flamen P, Van Calenbergh F, Plets C, Sorensen N, Opitz A, and Van Gool SW. Surgery and adjuvant dendritic cell-based tumour vaccination for patients with relapsed malignant glioma, a feasibility study. Br J Cancer 2004;91(9):1656-1662.

63. De Vleeschouwer S, Rapp M, Sorg RV, Steiger HJ, Stummer W, Van Gool S, and Sabel M. Dendritic cell vaccination in patients with malignant gliomas: current status and future directions. Neurosurgery 2006;59(5):988-999.

64. Prins RM, Shu CJ, Radu CG, Vo DD, Khan-Farooqi H, Soto H, Yang MY, Lin MS, Shelly S, Witte ON, Ribas A, and Liau LM. Anti-tumor activity and trafficking of self, tumor-specific T cells against tumors located in the brain. Cancer Immunol Immunother 2008;57(9):1279-1289.

65. Liu G, Ying H, Zeng G, Wheeler CJ, Black KL, and Yu JS. HER-2, gp100, and MAGE-1 are expressed in human glioblastoma and recognized by cytotoxic T cells. Cancer Res 2004;64(14):4980-4986.

66. Zhang JG, Eguchi J, Kruse CA, Gomez GG, Fakhrai H, Schroter S, Ma W, Hoa N, Minev B, Delgado C, Wepsic HT, Okada H, and Jadus MR. Antigenic profiling of glioma cells to generate allogeneic vaccines or dendritic cell-based therapeutics. Clin Cancer Res 2007;13(2 Pt 1):566-575.

67. Soling A and Rainov NG. Dendritic cell therapy of primary brain tumors. Mol Med 2001;7(10):659-667.

68. Bonehill A, Heirman C, and Thielemans K. Genetic approaches for the induction of a CD4+ T cell response in cancer immunotherapy. J Gene Med 2005;7(6):686-695.

69. Hegmans JP, Gerber PJ, and Lambrecht BN. Exosomes. Methods Mol Biol 2008;484:97-109.

70. de Vries IJ, Lesterhuis WJ, Scharenborg NM, Engelen LP, Ruiter DJ, Gerritsen MJ, Croockewit S, Britten CM, Torensma R, Adema GJ, Figdor CG, and Punt CJ. Maturation of dendritic cells is a prerequisite for inducing immune responses in advanced melanoma patients. Clin Cancer Res 2003;9(14):5091-5100.

71. Banerjee DK, Dhodapkar MV, Matayeva E, Steinman RM, and Dhodapkar KM. Expansion of FOXP3high regulatory T cells by human dendritic cells (DCs) in vitro and after injection of cytokine-matured DCs in myeloma patients. Blood 2006;108(8):2655-2661.

72. Schrama D, Pedersen LO, Keikavoussi P, Andersen MH, Straten PP, Brocker EB, Kampgen E, and Becker JC. Aggregation of antigen-specific T cells at the inoculation site of mature dendritic cells. J Invest Dermatol 2002;119(6):1443-1448.

73. Prins RM, Craft N, Bruhn KW, Khan-Farooqi H, Koya RC, Stripecke R, Miller JF, and Liau LM. The TLR-7 agonist, imiquimod, enhances dendritic cell survival and promotes tumor antigen-specific T cell priming: relation to central nervous system antitumor immunity. J Immunol 2006;176(1):157-164.

74. Aarntzen EH, Figdor CG, Adema GJ, Punt CJ, and de Vries IJ. Dendritic cell vaccination and immune monitoring. Cancer Immunol Immunother 2008;57(10):1559-1568.

75. Melief CJ. Cancer immunotherapy by dendritic cells. Immunity 2008;29(3):372-383.

76. Boczkowski D, Nair SK, Snyder D, and Gilboa E. Dendritic cells pulsed with RNA are potent antigen-presenting cells in vitro and in vivo. J Exp Med 1996;184(2):465-472.

77. Nair SK, Morse M, Boczkowski D, Cumming RI, Vasovic L, Gilboa E, and Lyerly HK. Induction of tumor-specific cytotoxic T lymphocytes in cancer patients by autologous tumor RNA-transfected dendritic cells. Ann Surg 2002;235(4):540-549.

78. Gilboa E and Vieweg J. Cancer immunotherapy with mRNA-transfected dendritic cells. Immunol Rev 2004;199:251-263.

79. Grunebach F, Muller MR, Nencioni A, and Brossart P. Delivery of tumor-derived RNA for the induction of cytotoxic T-lymphocytes. Gene Ther 2003;10(5):367-374.

80. Erdmann M, Dorrie J, Schaft N, Strasser E, Hendelmeier M, Kampgen E, Schuler G, and Schuler-Thurner B. Effective clinical-scale production of dendritic cell vaccines by monocyte elutriation directly in medium, subsequent culture in bags and final antigen loading using peptides or RNA transfection. J Immunother 2007;30(6):663-674.

81. Michiels A, Tuyaerts S, Bonehill A, Corthals J, Breckpot K, Heirman C, Van Meirvenne S, Dullaers M, Allard S, Brasseur F, van der BP, and Thielemans K. Electroporation of immature and mature dendritic cells: implications for dendritic cell-based vaccines. Gene Ther 2005;12(9):772-782.

82. Schaft N, Dorrie J, Thumann P, Beck VE, Muller I, Schultz ES, Kampgen E, Dieckmann D, and Schuler G. Generation of an optimized polyvalent monocyte-derived dendritic cell vaccine by transfecting defined RNAs after rather than before maturation. J Immunol 2005;174(5):3087-3097.

83. Van Tendeloo VF, Ponsaerts P, Lardon F, Nijs G, Lenjou M, Van Broeckhoven C, Van Bockstaele DR, and Berneman Z. Highly efficient gene delivery by mRNA electroporation in human hematopoietic cells: superiority to lipofection and passive pulsing of mRNA and to electroporation of plasmid cDNA for tumor antigen loading of dendritic cells. Blood 2001;98(1):49-56.

84. Wheeler CJ, Black KL, Liu G, Mazer M, Zhang XX, Pepkowitz S, Goldfinger D, Ng H, Irvin D, and Yu JS. Vaccination elicits correlated immune and clinical responses in glioblastoma multiforme patients. Cancer Res 2008;68(14):5955-5964.

85. Ehtesham M, Black KL, and Yu JS. Recent progress in immunotherapy for malignant glioma: treatment strategies and results from clinical trials. Cancer Control 2004;11(3):192-207.

86. Prendergast GC and Jaffee EM. Cancer immunotherapy: immune suppression and tumor growth. 2007;409 pages. Elsevier Academic Press. ISBN:978-0-12-372551-6.

87. Heath WR and Carbone FR. Cross-presentation, dendritic cells, tolerance and immunity. Annu Rev Immunol 2001;19:47-64.

88. Zou W. Regulatory T cells, tumour immunity and immunotherapy. Nat Rev Immunol 2006;6(4):295-307.

89. Suri-Payer E, Amar AZ, Thornton AM, and Shevach EM. CD4+CD25+ T cells inhibit both the induction and effector function of autoreactive T cells and represent a unique lineage of immunoregulatory cells. J Immunol 1998;160(3):1212-1218.

90. Sakaguchi S, Sakaguchi N, Asano M, Itoh M, and Toda M. Immunologic self-tolerance maintained by activated T cells expressing IL-2 receptor a-chains (CD25): Breakdown of a single mechanism of self-tolerance causes various autoimmune diseases. J Immunol 1995;155(3):1151-1164.

91. Maker AV, Attia P, and Rosenberg SA. Analysis of the cellular mechanism of antitumor responses and autoimmunity in patients treated with CTLA-4 blockade. J Immunol 2005;175(11):7746-7754.

92. Shimizu J, Yamazaki S, Takahashi T, Ishida Y, and Sakaguchi S. Stimulation of CD25(+)CD4(+) regulatory T cells through GITR breaks immunological self-tolerance. Nat Immunol 2002;3(2):135-142.

93. Fantini MC, Becker C, Monteleone G, Pallone F, Galle PR, and Neurath MF. Cutting edge: TGF-beta induces a regulatory phenotype in CD4+CD25- T cells through Foxp3 induction and down-regulation of Smad7. J Immunol 2004;172(9):5149-5153.

94. Roncarolo MG, Gregori S, Battaglia M, Bacchetta R, Fleischhauer K, and Levings MK. Interleukin-10-secreting type 1 regulatory T cells in rodents and humans. Immunol Rev 2006;212:28-50.

95. Curtin JF, Candolfi M, Fakhouri TM, Liu C, Alden A, Edwards M, Lowenstein PR, and Castro MG. Treg depletion inhibits efficacy of cancer immunotherapy: implications for clinical trials. PLoS ONE 2008;3(4):e1983-

96. Fecci PE, Sweeney AE, Grossi PM, Nair SK, Learn CA, Mitchell DA, Cui X, Cummings TJ, Bigner DD, Gilboa E, and Sampson JH. Systemic anti-CD25 monoclonal antibody administration safely enhances immunity in murine glioma without eliminating regulatory T cells. Clin Cancer Res 2006;12(14 Pt 1):4294-4305.

97. Fecci PE, Ochiai H, Mitchell DA, Grossi PM, Sweeney AE, Archer GE, Cummings T, Allison JP, Bigner DD, and Sampson JH. Systemic CTLA-4 blockade ameliorates glioma-induced changes to the CD4+ T cell compartment without affecting regulatory T-cell function. Clin Cancer Res 2007;13(7):2158-2167.

98. Grauer OM, Nierkens S, Bennink E, Toonen LW, Boon L, Wesseling P, Sutmuller RP, and Adema GJ. CD4+FoxP3+ regulatory T cells gradually accumulate in gliomas during tumor growth and efficiently suppress antiglioma immune responses in vivo. Int J Cancer 2007;121(1):95-105.

99. Grauer OM, Sutmuller RP, van Maren W, Jacobs JF, Bennink E, Toonen LW, Nierkens S, and Adema GJ. Elimination of regulatory T cells is essential for an effective vaccination with tumor lysate-pulsed dendritic cells in a murine glioma model. Int J Cancer 2008;122(8):1794-1802.

100. Jordan JT, Sun W, Hussain SF, DeAngulo G, Prabhu SS, and Heimberger AB. Preferential migration of regulatory T cells mediated by glioma-secreted chemokines can be blocked with chemotherapy. Cancer Immunol Immunother 2008;57(1):123-131.

101. Shevach EM. CD4+ CD25+ suppressor T cells: more questions than answers. Nat Rev Immunol 2002;2(6):389-400.

102. Friese MA, Steinle A, and Weller M. The innate immune response in the central nervous system and its role in glioma immune surveillance. Onkologie 2004;27(5):487-491.

103. Galarneau H, Villeneuve J, Gowing G, Julien JP, and Vallieres L. Increased glioma growth in mice depleted of macrophages. Cancer Res 2007;67(18):8874-8881.

104. Hussain SF, Yang D, Suki D, Aldape K, Grimm E, and Heimberger AB. The role of human glioma-infiltrating microglia/macrophages in mediating antitumor immune responses. Neuro Oncol 2006;8(3):261-279.

105. Mumm JB and Oft M. Cytokine-based transformation of immune surveillance into tumor-promoting inflammation. Oncogene 2008;27(45):5913-5919.

106. Sica A, Allavena P, and Mantovani A. Cancer related inflammation: the macrophage connection. Cancer Lett 2008;267(2):204-215.

107. Umemura N, Saio M, Suwa T, Kitoh Y, Bai J, Nonaka K, Ouyang GF, Okada M, Balazs M, Adany R, Shibata T, and Takami T. Tumor-infiltrating myeloid-derived suppressor cells are pleiotropic-inflamed monocytes/macrophages that bear M1- and M2-type characteristics. J Leukoc Biol 2008;83(5):1136-1144.

108. Kusmartsev S and Gabrilovich DI. Role of immature myeloid cells in mechanisms of immune evasion in cancer. Cancer Immunol Immunother 2006;55(3):237-245.

109. Gomez GG and Kruse CA. Mechanisms of malignant glioma immune resistance and sources of immunosuppression. Gene Ther Mol Biol 2006;10(a):133-146.

110. Graf MR, Prins RM, Hawkins WT, and Merchant RE. Irradiated tumor cell vaccine for treatment of an established glioma. I. Successful treatment with combined radiotherapy and cellular vaccination. Cancer Immunol Immunother 2002;51(4):179-89.

111. Graf MR, Sauer JT, and Merchant RE. Tumor infiltration by myeloid suppressor cells in response to T cell activation in rat gliomas. J Neurooncol 2005;73(1):29-36.

112. Giglio P and Levin V. Cyclooxygenase-2 inhibitors in glioma therapy. Am J Ther 2004;11(2):141-143.

113. Wobser M, Voigt H, Houben R, Eggert AO, Freiwald M, Kaemmerer U, Kaempgen E, Schrama D, and Becker JC. Dendritic cell based antitumor vaccination: impact of functional indoleamine 2,3-dioxygenase expression. Cancer Immunol Immunother 2006;56(7):1017-1024.

114. Ksendzovsky A, Feinstein D, Zengou R, Sharp A, Polak P, Lichtor T, and Glick RP. Investigation of immunosuppressive mechanisms in a mouse glioma model. J Neurooncol 2009;93(1):107-114.

115. Halder SK, Beauchamp RD, and Datta PK. A specific inhibitor of TGF-beta receptor kinase, SB-431542, as a potent antitumor agent for human cancers. Neoplasia 2005;7(5):509-521.

116. Wick W, Naumann U, and Weller M. Transforming growth factor-beta: a molecular target for the future therapy of glioblastoma. Curr Pharm Des 2006;12(3):341-349.

117. Mocellin S, Panelli MC, Wang E, Nagorsen D, and Marincola FM. The dual role of IL-10. Trends Immunol 2003;24(1):36-43.

118. Johnson BF, Clay TM, Hobeika AC, Lyerly HK, and Morse MA. Vascular endothelial growth factor and immunosuppression in cancer: current knowledge and potential for new therapy. Expert Opin Biol Ther 2007;7(4):449-460.

119. Kikuchi T, Joki T, Akasaki Y, Abe T, and Ohno T. Induction of antitumor immunity using intercellular adhesion molecule 1 (ICAM-1) transfection in mouse glioma cells. Cancer Lett 1999;142(2):201-206.

120. Mehling M, Simon P, Mittelbronn M, Meyermann R, Ferrone S, Weller M, and Wiendl H. WHO grade associated downregulation of MHC class I antigen-processing machinery components in human astrocytomas: does it reflect a potential immune escape mechanism? Acta Neuropathol 2007;114(2):111-119.

121. Wiendl H, Mitsdoerffer M, Hofmeister V, Wischhusen J, Bornemann A, Meyermann R, Weiss EH, Melms A, and Weller M. A functional role of HLA-G expression in human gliomas: an alternative strategy of immune escape. J Immunol 2002;168(9):4772-80.

122. Wintterle S, Schreiner B, Mitsdoerffer M, Schneider D, Chen L, Meyermann R, Weller M, and Wiendl H. Expression of the B7-related molecule B7-H1 by glioma cells: a potential mechanism of immune paralysis. Cancer Res 2003;63(21):7462-7467.

123. Kuipers H, Muskens F, Willart M, Hijdra D, van Assema FB, Coyle AJ, Hoogsteden HC, and Lambrecht BN. Contribution of the PD-1 ligands/PD-1 signaling pathway to dendritic cell-mediated CD4+ T cell activation. Eur J Immunol 2006;36(9):2472-2482.

124. Liu FT and Rabinovich GA. Galectins as modulators of tumour progression. Nat Rev Cancer 2005;5(1):29-41.

125. Wang T, Niu G, Kortylewski M, Burdelya L, Shain K, Zhang S, Bhattacharya R, Gabrilovich D, Heller R, Coppola D, Dalton W, Jove R, Pardoll D, and Yu H. Regulation of the innate and adaptive immune responses by Stat-3 signaling in tumor cells. Nat Med 2004;10(1):48-54.

126. Fujita M, Zhu X, Sasaki K, Ueda R, Low KL, Pollack IF, and Okada H. Inhibition of STAT3 promotes the efficacy of adoptive transfer therapy using type-1 CTLs by modulation of the immunological microenvironment in a murine intracranial glioma. J Immunol 2008;180(4):2089-2098.

127. Muller AJ and Prendergast GC. Marrying immunotherapy with chemotherapy: why say IDO? Cancer Res 2005;65(18):8065-8068.

128. Munn DH and Mellor AL. Indoleamine 2,3-dioxygenase and tumor-induced tolerance. J Clin Invest 2007;117(5):1147-1154.

129. Bronte V and Zanovello P. Regulation of immune responses by L-arginine metabolism. Nat Rev Immunol 2005;5(8):641-654.

130. Peranzoni E, Marigo I, Dolcetti L, Ugel S, Sonda N, Taschin E, Mantelli B, Bronte V, and Zanovello P. Role of arginine metabolism in immunity and immunopathology. Immunobiology 2007;212(9-10):795-812.

131. Wheatley DN. Controlling cancer by restricting arginine availability--arginine-catabolizing enzymes as anticancer agents. Anticancer Drugs 2004;15(9):825-833.

132. Weiner LM. Cancer immunotherapy--the endgame begins. N Engl J Med 2008;358(25):2664-2665.

133. Svane IM, Soot ML, Buus S, and Johnsen HE. Clinical application of dendritic cells in cancer vaccination therapy. APMIS 2003;111(7-8):818-834.

134. Park SD, Kim CH, Kim CK, Park JA, Sohn HJ, Hong YK, and Kim TG. Cross-priming by temozolomide enhances antitumor immunity of dendritic cell vaccination in murine brain tumor model. Vaccine 2007;25(17):3485-3491.

135. Liu G, Black KL, and Yu JS. Sensitization of malignant glioma to chemotherapy through dendritic cell vaccination. Expert Rev Vaccines 2006;5(2):233-247.

136. Andersen MH, Sorensen RB, Schrama D, Svane IM, Becker JC, and Thor SP. Cancer treatment: the combination of vaccination with other therapies. Cancer Immunol Immunother 2008;57(11):1735-1743.

137. Miller RE, Jones J, Le T, Whitmore J, Boiani N, Gliniak B, and Lynch DH. 4-1BB-specific monoclonal antibody promotes the generation of tumor-specific immune responses by direct activation of CD8 T cells in a CD40-dependent manner. J Immunol 2002;169(4):1792-1800.

138. Nair S, Boczkowski D, Moeller B, Dewhirst M, Vieweg J, and Gilboa E. Synergy between tumor immunotherapy and antiangiogenic therapy. Blood 2003;102(3):964-971.

139. Candolfi M, Curtin JF, Nichols WS, Muhammad AG, King GD, Pluhar GE, McNiel EA, Ohlfest JR, Freese AB, Moore PF, Lerner J, Lowenstein PR, and Castro MG. Intracranial glioblastoma models in preclinical neuro-oncology: neuropathological characterization and tumor progression. J Neurooncol 2007;85(2):133-148.

140. Fomchenko EI and Holland EC. Mouse models of brain tumors and their applications in preclinical trials. Clin Cancer Res 2006;12(18):5288-5297.

141. Ni HT, Spellman SR, Jean WC, Hall WA, and Low WC. Immunization with dendritic cells pulsed with tumor extract increases survival of mice bearing intracranial gliomas. J Neurooncol 2001;51(1):1-9.

142. Aoki H, Mizuno M, Natsume A, Tsugawa T, Tsujimura K, Takahashi T, and Yoshida J. Dendritic cells pulsed with tumor extract-cationic liposome complex increase the induction of cytotoxic T lymphocytes in mouse brain tumor. Cancer Immunol Immunother 2001;50(9):463-8.

143. Insug O, Ku G, Ertl HC, and Blaszczyk-Thurin M. A dendritic cell vaccine induces protective immunity to intracranial growth of glioma. Anticancer Res 2002;22(2A):613-321.

144. Saito R, Mizuno M, Nakahara N, Tsuno T, Kumabe T, Yoshimoto T, and Yoshida J. Vaccination with tumor cell lysate-pulsed dendritic cells augments the effect of IFN-beta gene therapy for malignant glioma in an experimental mouse intracranial glioma. Int J Cancer 2004;111(5):777-782.

145. Tsugawa T, Kuwashima N, Sato H, Fellows-Mayle WK, Dusak JE, okada K, Papworth GD, Watkins SC, Gambotto A, Yoshida J, Pollack IF, and Okada H. Sequential delivery of interferon-alpha gene and DCs to intracranial gliomas promotes an effective antitumor response. Gene Ther 2004;11(21):1551-1558.

146. Kuwashima N, Nishimura F, Eguchi J, Sato H, Hatano M, Tsugawa T, Sakaida T, Dusak JE, Fellows-Mayle WK, Papworth GD, Watkins SC, Gambotto A, Pollack IF, Storkus WJ, and Okada H. Delivery of dendritic cells engineered to secrete IFN-alpha into central nervous system tumors enhances the efficacy of peripheral tumor cell vaccines: dependence on apoptotic pathways. J Immunol 2005;175(4):2730-2740.

147. Kjaergaard J, Wang LX, Kuriyama H, Shu S, and Plautz GE. Active immunotherapy for advanced intracranial murine tumors by using dendritic cell-tumor cell fusion vaccines. J Neurosurg 2005;103(1):156-164.

148. Ciesielski MJ, Apfel L, Barone TA, Castro CA, Weiss TC, and Fenstermaker RA. Antitumor effects of a xenogeneic survivin bone marrow derived dendritic cell vaccine against murine GL261 gliomas. Cancer Immunol Immunother 2006;55(12):1491-1503.

149. Pellegatta S, Poliani PL, Corno D, Menghi F, Ghielmetti F, Suarez-Merino B, Caldera V, Nava S, Ravanini M, Facchetti F, Bruzzone MG, and Finocchiaro G. Neurospheres enriched in cancer stem-like cells are highly effective in eliciting a dendritic cell-mediated immune response against malignant gliomas. Cancer Res 2006;66(21):10247-10252.

150. Pellegatta S, Poliani PL, Corno D, Grisoli M, Cusimano M, Ubiali F, Baggi F, Bruzzone MG, and Finocchiaro G. Dendritic cells pulsed with glioma lysates induce immunity against syngeneic intracranial gliomas and increase survival of tumor-bearing mice. Neurol Res 2006;28(5):527-531.

151. Harris J, Monesmith T, Ubben A, Norris M, Freedman JH, and Tcherepanova I. An improved RNA amplification procedure results in increased yield of autologous RNA transfected dendritic cell-based vaccine. Biochim Biophys Acta 2005;1724(1-2):127-136.

152. Ribas A, Butterfield LH, Glaspy JA, and Economou JS. Current developments in cancer vaccines and cellular immunotherapy. J Clin Oncol 2003;21(12):2415-2432.

153. Jenkins DE, Oei Y, Hornig YS, Yu SF, Dusich J, Purchio T, and Contag PR. Bioluminescent imaging (BLI) to improve and refine traditional murine models of tumor growth and metastasis. Clin Exp Metastasis 2003;20(8):733-744.

154. Prendergast GC and Jaffee EM. Cancer immunologists and cancer biologists: why we didn't talk then but need to now. Cancer Res 2007;67(8):3500-3504.

155. Boczkowski D, Nair SK, Nam JH, Lyerly HK, and Gilboa E. Induction of tumor immunity and cytotoxic T lymphocyte responses using dendritic cells transfected with messenger RNA amplified from tumor cells. Cancer Res 2000;60(4):1028-34.

156. Kobayashi T, Yamanaka R, Homma J, Tsuchiya N, Yajima N, Yoshida S, and Tanaka R. Tumor mRNA-loaded dendritic cells elicit tumor-specific CD8(+) cytotoxic T cells in patients with malignant glioma. Cancer Immunol Immunother 2003;52(10):632-637.

157. Deroose CM, Reumers V, Gijsbers R, Bormans G, Debyser Z, Mortelmans L, and Baekelandt V. Noninvasive monitoring of long-term lentiviral vector-mediated gene expression in rodent brain with bioluminescence imaging. Mol Ther 2006;14(3):423-431.

158. Inaba K, Inaba M, Romani N, Aya H, Deguchi M, Ikehara S, Muramatsu S, and Steinman RM. Generation of large numbers of dendritic cells from mouse bone marrow cultures supplemented with granulocyte/macrophage colony-stimulating factor. J Exp Med 1992;176(6):1693-1702.

159. Lutz MB, Kukutsch N, Ogilvie ALJ, Rossner S, Koch F, Romani N, and Schuler G. An advanced culture method for generating large quantities of highly pure dendritic cells from mouse bone marrow. J Immunol Meth 1999;223(1):77-92.

160. De Vleeschouwer S, Spencer L, I, Ceuppens JL, and Van Gool SW. Persistent IL-10 production is required for glioma growth suppressive activity by Th1-directed effector cells after stimulation with tumor lysate-loaded dendritic cells. J Neurooncol 2007;84(2):131-140.

161. Mustafa M, Diener P, Sun JB, Link H, and Olsson T. Immunopharmacologic modulation of experimental allergic encephalomyelitis: low-dose cyclosporin-A treatment causes disease relapse and increased systemic T and B cell-mediated myelin-directed autoimmunity. Scand J Immunol 1993;38(6):499-507.

162. Rosen GD, La Porte NT, Diechtiareff B, Pung CJ, Nissanov J, Gustafson C, Bertrand L, Gefen S, Fan Y, Tretiak OJ, Manly KF, Park MR, Williams AG, Connolly MT, Capra JA, and Williams RW. Informatics center for mouse genomics: the dissection of complex traits of the nervous system. Neuroinformatics 2003;1(4):327-342.

163. Bradford MM. A rapid and sensitive method for the quantitation of microgram quantities of protein utilizing the principle of protein-dye binding. Anal Biochem 1976;72:248-54.

164. Schmitz C and Hof PR. Design-based stereology in neuroscience. Neuroscience 2005;130(4):813-831.

165. Mitchell DA and Nair SK. RNA transfected dendritic cells as cancer vaccines. Curr Opin Mol Ther 2000;2(2):176-81.

166. Ponsaerts P, Van Tendeloo VF, and Berneman ZN. Cancer immunotherapy using RNA-loaded dendritic cells. Clin Exp Immunol 2003;134(3):378-384.

167. Dullaers M, Breckpot K, Van Meirvenne S, Bonehill A, Tuyaerts S, Michiels A, Straetman L, Heirman C, De Greef C, van der BP, and Thielemans K. Side-by-side comparison of lentivirally transduced and mRNA-electroporated dendritic cells: implications for cancer immunotherapy protocols. Mol Ther 2004;10(4):768-779.

168. Prins RM, Odesa SK, and Liau LM. Immunotherapeutic targeting of shared melanoma-associated antigens in a murine glioma model. Cancer Res 2003;63(23):8487-8491.

169. Su Z, Dannull J, Heiser A, Yancey D, Pruitt S, Madden J, Coleman D, Niedzwiecki D, Gilboa E, and Vieweg J. Immunological and clinical responses in metastatic renal cancer patients vaccinated with tumor RNA-transfected dendritic cells. Cancer Res 2003;63(9):2127-2133.

170. Mu LJ, Kyte JA, Kvalheim G, Aamdal S, Dueland S, Hauser M, Hammerstad H, Waehre H, Raabe N, and Gaudernack G. Immunotherapy with allotumour mRNA-transfected dendritic cells in androgen-resistant prostate cancer patients. Br J Cancer 2005;93(7):749-756.

171. Kyte JA, Kvalheim G, Aamdal S, Saeboe-Larssen S, and Gaudernack G. Preclinical full-scale evaluation of dendritic cells transfected with autologous tumor-mRNA for melanoma vaccination. Cancer Gene Ther 2005;12(6):579-591.

172. Markovic SN, Dietz AB, Greiner CW, Maas ML, Butler GW, Padley DJ, Bulur PA, Allred JB, Creagan ET, Ingle JN, Gastineau DA, and Vuk-Pavlovic S. Preparing clinical-grade myeloid dendritic cells by electroporation-mediated transfection of in vitro amplified tumor-derived mRNA and safety testing in stage IV malignant melanoma. J Transl Med 2006;4:35.

173. Caruso DA, Orme LM, Neale AM, Radcliff FJ, Amor GM, Maixner W, Downie P, Hassall TE, Tang ML, and Ashley DM. Results of a phase 1 study utilizing monocyte-derived dendritic cells pulsed with tumor RNA in children and young adults with brain cancer. Neuro Oncol 2004;6(3):236-246.

174. Caruso DA, Orme LM, Amor GM, Neale AM, Radcliff FJ, Downie P, Tang ML, and Ashley DM. Results of a Phase I study utilizing monocyte-derived dendritic cells pulsed with tumor RNA in children with Stage 4 neuroblastoma. Cancer 2005;103(6):1280-1291.

175. Mu LJ, Gaudernack G, Saeboe-Larssen S, Hammerstad H, Tierens A, and Kvalheim G. A protocol for generation of clinical grade mRNA-transfected monocyte-derived dendritic cells for cancer vaccines. Scand J Immunol 2003;58(5):578-586.

176. Heiser A, Maurice MA, Yancey D, Wu NZ, Dahm P, Pruitt S, Boczkowski D, Nair SK, Ballo MS, Gilboa E, and Vieweg J. Induction of polyclonal prostate cancer-specific CTL using dendritic cells transfected with amplified tumor RNA. J Immunol 2001;166(5):2953-2960.

177. Mitchell DA and Nair SK. RNA-transfected dendritic cells in cancer immunotherapy. J Clin Invest 2000;106(9):1065-1069.

178. Szatmari T, Lumniczky K, Desaknai S, Trajcevski S, Hidvegi EJ, Hamada H, and Safrany G. Detailed characterization of the mouse glioma 261 tumor model for experimental glioblastoma therapy. Cancer Sci 2006;97(6):546-553.

179. Lumniczky K, Desaknai S, Mangel L, Szende B, Hamada H, Hidvegi EJ, and Safrany G. Local tumor irradiation augments the antitumor effect of cytokine-producing autologous cancer cell vaccines in a murine glioma model. Cancer Gene Ther 2002;9(1):44-52.

180. Van Gool SW, Maes W, Ardon H., Verschuere T., Van Cauter S., and De Vleeschouwer S. Dendritic cell therapy of high grade gliomas. Brain Pathol 2009 (in press).

181. Massoud TF and Gambhir SS. Molecular imaging in living subjects: seeing fundamental biological processes in a new light. Genes Dev 2003;17(5):545-580.

182. Rehemtulla A, Stegman LD, Cardozo SJ, Gupta S, Hall DE, Contag CH, and Ross BD. Rapid and quantitative assessment of cancer treatment response using in vivo bioluminescence imaging. Neoplasia 2000;2(6):491-495.

183. Shah K, Tang Y, Breakefield X, and Weissleder R. Real-time imaging of TRAIL-induced apoptosis of glioma tumors in vivo. Oncogene 2003;22(44):6865-6872.

184. Soling A, Theiss C, Jungmichel S, and Rainov NG. A dual function fusion protein of Herpes simplex virus type 1 thymidine kinase and firefly luciferase for noninvasive in vivo imaging of gene therapy in malignant glioma. Genet Vaccines Ther 2004;2(1):7.

185. Weissleder R. Scaling down imaging: molecular mapping of cancer in mice. Nat Rev Cancer 2002;2(1):11-18.

186. Contag CH, Jenkins D, Contag PR, and Negrin RS. Use of reporter genes for optical measurements of neoplastic disease in vivo. Neoplasia 2000;2(1-2):41-52.

187. Contag PR, Olomu IN, Stevenson DK, and Contag CH. Bioluminescent indicators in living mammals. Nat Med 1998;4(2):245-247.

188. Edinger M, Cao YA, Hornig YS, Jenkins DE, Verneris MR, Bachmann MH, Negrin RS, and Contag CH. Advancing animal models of neoplasia through in vivo bioluminescence imaging. Eur J Cancer 2002;38(16):2128-2136.

189. Liao CP, Zhong C, Saribekyan G, Bading J, Park R, Conti PS, Moats R, Berns A, Shi W, Zhou Z, Nikitin AY, and Roy-Burman P. Mouse models of prostate adenocarcinoma with the capacity to monitor spontaneous carcinogenesis by bioluminescence or fluorescence. Cancer Res 2007;67(15):7525-7533.

190. Ragel BT, Elam IL, Gillespie DL, Flynn JR, Kelly DA, Mabey D, Feng H, Couldwell WT, and Jensen RL. A novel model of intracranial meningioma in mice using luciferase-expressing meningioma cells. J Neurosurg 2008;108(2):304-310.

191. Contag CH and Ross BD. It's not just about anatomy: in vivo bioluminescence imaging as an eyepiece into biology. J Magn Reson Imaging 2002;16(4):378-387.

192. Deroose CM, De A, Loening AM, Chow PL, Ray P, Chatziioannou AF, and Gambhir SS. Multimodality imaging of tumor xenografts and metastases in mice with combined small-animal PET, small-animal CT, and bioluminescence imaging. J Nucl Med 2007;48(2):295-303.

193. Hollingshead MG, Bonomi CA, Borgel SD, Carter JP, Shoemaker R, Melillo G, and Sausville EA. A potential role for imaging technology in anticancer efficacy evaluations. Eur J Cancer 2004;40(6):890-898.

194. Paroo Z, Bollinger RA, Braasch DA, Richer E, Corey DR, Antich PP, and Mason RP. Validating bioluminescence imaging as a high-throughput, quantitative modality for assessing tumor burden. Mol Imaging 2004;3(2):117-124.

195. Soling A and Rainov NG. Bioluminescence imaging in vivo - application to cancer research. Expert Opin Biol Ther 2003;3(7):1163-1172.

196. Szentirmai O, Baker CH, Lin N, Szucs S, Takahashi M, Kiryu S, Kung AL, Mulligan RC, and Carter BS. Noninvasive bioluminescence imaging of luciferase expressing intracranial U87 xenografts: correlation with magnetic resonance imaging determined tumor volume and longitudinal use in assessing tumor growth and antiangiogenic treatment effect. Neurosurgery 2006;58(2):365-372.

197. Hsu AR, Cai W, Veeravagu A, Mohamedali KA, Chen K, Kim S, Vogel H, Hou LC, Tse V, Rosenblum MG, and Chen X. Multimodality molecular imaging of glioblastoma growth inhibition with vasculature-targeting fusion toxin VEGF121/rGel. J Nucl Med 2007;48(3):445-454.

198. Kemper EM, Leenders W, Kusters B, Lyons S, Buckle T, Heerschap A, Boogerd W, Beijnen JH, and van Tellingen O. Development of luciferase tagged brain tumour models in mice for chemotherapy intervention studies. Eur J Cancer 2006;42(18):3294-3303.

199. Ohlfest JR, Demorest ZL, Motooka Y, Vengco I, Oh S, Chen E, Scappaticci FA, Saplis RJ, Ekker SC, Low WC, Freese AB, and Largaespada DA. Combinatorial antiangiogenic gene therapy by nonviral gene transfer using the sleeping beauty transposon causes tumor regression and improves survival in mice bearing intracranial human glioblastoma. Mol Ther 2005;12(5):778-788.

200. Craft N, Bruhn KW, Nguyen BD, Prins R, Liau LM, Collisson EA, De A, Kolodney MS, Gambhir SS, and Miller JF. Bioluminescent imaging of melanoma in live mice. J Invest Dermatol 2005;125(1):159-165.

201. Blouw B, Song H, Tihan T, Bosze J, Ferrara N, Gerber HP, Johnson RS, and Bergers G. The hypoxic response of tumors is dependent on their microenvironment. Cancer Cell 2003;4(2):133-146.

202. Eyupoglu IY, Hahnen E, Heckel A, Siebzehnrubl FA, Buslei R, Fahlbusch R, and Blumcke I. Malignant glioma-induced neuronal cell death in an organotypic glioma invasion model. Technical note. J Neurosurg 2005;102(4):738-744.

203. Manley GT, Binder DK, Papadopoulos MC, and Verkman AS. New insights into water transport and edema in the central nervous system from phenotype analysis of aquaporin-4 null mice. Neuroscience 2004;129(4):983-991.

204. Hakamata Y, Murakami T, and Kobayashi E. "Firefly rats" as an organ/cellular source for long-term in vivo bioluminescent imaging. Transplantation 2006;81(8):1179-1184.

205. Steinman RM and Mellman I. Immunotherapy: bewitched, bothered, and bewildered no more. Science 2004;305(5681):197-200.

206. El Andaloussi A, Sonabend AM, Han Y, and Lesniak MS. Stimulation of TLR9 with CpG ODN enhances apoptosis of glioma and prolongs the survival of mice with experimental brain tumors. Glia 2006;54(6):526-535.

207. El Andaloussi A, Han Y, and Lesniak MS. Prolongation of survival following depletion of CD4+CD25+ regulatory T cells in mice with experimental brain tumors. J Neurosurg 2006;105(3):430-437.

208. Newcomb EW, Demaria S, Lukyanov Y, Shao Y, Schnee T, Kawashima N, Lan L, Dewyngaert JK, Zagzag D, McBride WH, and Formenti SC. The combination of ionizing radiation and peripheral vaccination produces long-term survival of mice bearing established invasive GL261 gliomas. Clin Cancer Res 2006;12(15):4730-4737.

209. Curiel TJ. Tregs and rethinking cancer immunotherapy. J Clin Invest 2007;117(5):1167-1174.

210. Wei WZ, Morris GP, and Kong YC. Anti-tumor immunity and autoimmunity: a balancing act of regulatory T cells. Cancer Immunol Immunother 2004;53(2):73-78.

211. Onizuka S, Tawara I, Shimizu J, Sakaguchi S, Fujita T, and Nakayama E. Tumor rejection by in vivo administration of anti-CD25 (interleukin-2 receptor alpha) monoclonal antibody. Cancer Res 1999;59(13):3128-3133.

212. Kalinski P, Giermasz A, Nakamura Y, Basse P, Storkus WJ, Kirkwood JM, and Mailliard RB. Helper role of NK cells during the induction of anticancer responses by dendritic cells. Mol Immunol 2005;42(4):535-539.

213. Munz C, Dao T, Ferlazzo G, de Cos MA, Goodman K, and Young JW. Mature myeloid dendritic cell subsets have distinct roles for activation and viability of circulating human natural killer cells. Blood 2005;105(1):266-273.

214. Smyth MJ, Wallace ME, Nutt SL, Yagita H, Godfrey DI, and Hayakawa Y. Sequential activation of NKT cells and NK cells provides effective innate immunotherapy of cancer. J Exp Med 2005;201(12):1973-1985.

215. Traver D, Akashi K, Manz M, Merad M, Miyamoto T, Engleman EG, and Weissman IL. Development of CD8alpha-positive dendritic cells from a common myeloid progenitor. Science 2000;290(5499):2152-2154.

216. Hong L, Webb TJ, and Wilkes DS. Dendritic cell-T cell interactions: CD8 alpha alpha expressed on dendritic cells regulates T cell proliferation. Immunol Lett 2007;108(2):174-178.

217. McNamara JO, Kolonias D, Pastor F, Mittler RS, Chen L, Giangrande PH, Sullenger B, and Gilboa E. Multivalent 4-1BB binding aptamers costimulate CD8+ T cells and inhibit tumor growth in mice. J Clin Invest 2008;118(1):376-386.

218. Gallimore A and Godkin A. Regulatory T cells and tumour immunity - observations in mice and men. Immunology 2008;123(2):157-163.

219. Imai H, Saio M, Nonaka K, Suwa T, Umemura N, Ouyang GF, Nakagawa J, Tomita H, Osada S, Sugiyama Y, Adachi Y, and Takami T. Depletion of CD4+CD25+ regulatory T cells enhances interleukin-2-induced antitumor immunity in a mouse model of colon adenocarcinoma. Cancer Sci 2007;98(3):416-423.

220. Leon K, Garcia K, Carneiro J, and Lage A. How regulatory CD25+CD4+ T cells impinge on tumor immunobiology: the differential response of tumors to therapies. J Immunol 2007;179(9):5659-5668.

221. McNeill A, Spittle E, and Backstrom BT. Partial depletion of CD69low-expressing natural regulatory T cells with the anti-CD25 monoclonal antibody PC61. Scand J Immunol 2007;65(1):63-69.

222. Fehervari Z and Sakaguchi S. Control of Foxp3+ CD25+CD4+ regulatory cell activation and function by dendritic cells. Int Immunol 2004;16(12):1679-1680.

223. Pasare C and Medzhitov R. Toll Pathway-Dependent Blockade of CD4+CD25+ T Cell-Mediated Suppression by Dendritic Cells. Science 2003;299(5609):1033-1036.

224. Jouanneau E, Poujol D, Gulia S, Le M, I, Blay JY, Belin MF, and Puisieux I. Dendritic cells are essential for priming but inefficient for boosting antitumour immune response in an orthotopic murine glioma model. Cancer Immunol Immunother 2005;55(3):254-267.

225. Van Meirvenne S, Dullaers M, Heirman C, Straetman L, Michiels A, and Thielemans K. In vivo depletion of CD4+CD25+ regulatory T cells enhances the antigen-specific primary and memory CTL response elicited by mature mRNA-electroporated dendritic cells. Mol Ther 2005;12(5):922-932.

226. Comes A, Rosso O, Orengo AM, Di Carlo E, Sorrentino C, Meazza R, Piazza T, Valzasina B, Nanni P, Colombo MP, and Ferrini S. CD25+ regulatory T cell depletion augments immunotherapy of micrometastases by an IL-21-secreting cellular vaccine. J Immunol 2006;176(3):1750-1758.

227. Linehan DC and Goedegebuure PS. CD25+ CD4+ regulatory T-cells in cancer. Immunol Res 2005;32(1-3):155-168.

228. Matsushita N, Pilon-Thomas SA, Martin LM, and Riker AI. Comparative methodologies of regulatory T cell depletion in a murine melanoma model. J Immunol Methods 2008;333(1-2):167-179.

229. Nair S, Boczkowski D, Fassnacht M, Pisetsky D, and Gilboa E. Vaccination against the forkhead family transcription factor Foxp3 enhances tumor immunity. Cancer Res 2007;67(1):371-380.

230. Audia S, Nicolas A, Cathelin D, Larmonier N, Ferrand C, Foucher P, Fanton A, Bergoin E, Maynadie M, Arnould L, Bateman A, Lorcerie B, Solary E, Chauffert B, and Bonnotte B. Increase of CD4+ CD25+ regulatory T cells in the peripheral blood of patients with metastatic carcinoma: a Phase I clinical trial using cyclophosphamide and immunotherapy to eliminate CD4+ CD25+ T lymphocytes. Clin Exp Immunol 2007;150(3):523-530.

231. Morse MA, Hobeika AC, Osada T, Serra D, Niedzwiecki D, Lyerly HK, and Clay TM. Depletion of human regulatory T cells specifically enhances antigen-specific immune responses to cancer vaccines. Blood 2008;112(3):610-618.

232. Rasku MA, Clem AL, Telang S, Taft B, Gettings K, Gragg H, Cramer D, Lear SC, McMasters KM, Miller DM, and Chesney J. Transient T cell depletion causes regression of melanoma metastases. J Transl Med 2008;6:12.

233. Hodi FS, Butler M, Oble DA, Seiden MV, Haluska FG, Kruse A, Macrae S, Nelson M, Canning C, Lowy I, Korman A, Lautz D, Russell S, Jaklitsch MT, Ramaiya N, Chen TC, Neuberg D, Allison JP, Mihm MC, and Dranoff G. Immunologic and clinical effects of antibody blockade of cytotoxic T lymphocyte-associated antigen 4 in previously vaccinated cancer patients. Proc Natl Acad Sci U S A 2008;105(8):3005-3010.

Curriculum Vitae

Wim Maes was born in Kortrijk on November 27th, 1979. From 1991, he followed a classical secondary school training (Latin-Mathematics) at the Sint-Amandscollege in Kortrijk. In 1998, he started the professional bachelor training “Biomedical Laboratory Technology” at the Katholieke Hogeschool Sint-Lieven in Gent, from which he graduated magna cum laude in 2001. After obtaining the bachelor degree in “Biomedical Sciences” at the Vrije Universiteit Brussel, he entered the master training in “Biomedical Sciences” at the Katholieke Universiteit Leuven from which he graduated cum laude in 2004. In the same year, he became a research fellow in the Laboratory of Experimental Immunology under the supervision of Professor Van Gool and Professor Ceuppens.

List of publications

Ardon H, Verbinnen B, **Maes W**, Beez T, Van Gool SW, De Vleeschouwer S. Regulatory T cell monitoring using CD127 expression in patients with malignant glioma treated with autologous DC vaccination. (submitted)

Ardon H, Spencer I, Van Gool SW, **Maes W**, Sciot R, Wilms G, et al. The integration of autologous dendritic cell-based immunotherapy in the state-of-art primary treatment for patients with newly diagnosed high grade glioma: a pilot study. (submitted)

Galicia Rosas G, **Maes W**, Verbinnen B, Kasran A, Bullens D, Baumann H, Arredouani M, Ceuppens J. Haptoglobin has a dampening effect on the development of autoimmune inflammation. (submitted)

Van Gool SW, **Maes W**, Ardon H, Verschuere T, Van Cauter S, De Vleeschouwer S. Dendritic cell therapy of high grade gliomas. Brain Pathol (in press)

Maes W, Galicia Rosas G, Verbinnen B, Boon L, De Vleeschouwer S, Ceuppens J et al. DC vaccination with anti-CD25 treatment leads to long-term immunity against experimental glioma. Neuro Oncol (Epub ahead of print)

Maes W, Deroose C, Reumers V, Krylyshkina O, Gijsbers R, Baekelandt V et al. In vivo bioluminescence imaging in an experimental mouse model for dendritic cell based immunotherapy against malignant glioma. J Neurooncol 2009;91(2):127-39.

Van Gool SW, Ardon H, **Maes W**, Spencer I, Vandenbrande K, Stegen G et al. Immunotherapie voor hooggradige gliomen: alive and kicking ? Onco 2008;2(6):232-240.

Coosemans A, Moerman P, Verbist G, **Maes W**, Neven P, Vergote I et al. Wilms' tumor gene 1 (WT1) in endometrial carcinoma. Gynecol Oncol 2008;111(3):502-8.